UNIVERSIDAD DE VALLADOLID

PROGRAMA DE DOCTORADO EN INGENIERÍA QUÍMICA Y AMBIENTAL

UNIVERSIDAD DE LOS ANDES

PROGRAMA DE DOCTORADO EN CIENCIAS DE LA INGENIERÍA

TESIS DOCTORAL:

STUDY OF ALTERNATIVE METABOLIC PATHWAYS FOR THE PRODUCTION OF (*R*)-3-HYDROXYBUTYRIC ACID IN POLYHYDROXYBUTYRATE PRODUCING BACTERIA

Presentada por

Luz Francy Yañez Meneses para optar al grado de

Doctor de la Universidad de Valladolid y

Doctor de la Universidad de los Andes

Dirigida por:

Raúl Muñoz Torre

Felipe Scott Contador

To Enrique Yañez, Ana Meneses,
Rocky & Milo and my Higher-Self

ABSTRACT

Considerable rich literature has accumulated concerning biochemical, physiological, and genetic aspects of polyhydroxybutyrate (PHB) intracellular accumulation in bacteria. The costs of substrates and processing, including the extraction of the polymer accumulated in intracellular granules, still hampers a more widespread use of this family of polymers. The PHB monomeric unit, (*R*)-3-hydroxybutyric acid (R3HBA) has found uses at the biomedical, chemical and supplement industries. The literature shows that two main process engineering and metabolic engineering strategies have been identified aimed at the production of chiral R3HBA: (i) production from the accumulated polymer (polymerization and depolymerization system, PDS); (ii) by bypassing the accumulation of PHB using metabolically engineered bacteria. The later includes the use of thioesterases (thioesterase shortcut system, TSS) that removes CoA from R3HBA-CoA, resulting in the R3HBA release to extracellular medium.

This PhD thesis aims at broadening the understanding of the genetic and operational factors leading to PHB polymerization and R3HBA production in *Azohydromonas lata* DSM 1123, *Cupriavidus necator* H16 and *Methylocystis parvus* OBBP. Results showed that the growth associated PHB production observed in *A. lata* mimics an overflow metabolism, additionally, a successful PHB depolymerization in a two stage chemostat was obtained. The feasibility of producing R3HBA through *in-vivo* depolymerization of the intracellularly accumulated PHB in *M. parvus* was investigated. A PHB to R3HBA conversion of 77.2 ± 0.9% (R3HBA titer of 0.153 ± 0.002 g L^{-1}) can be attained in a mineral medium containing 1.0 g L^{-1} KNO_3 at 30 °C with shaking at 200 rpm and a constant pH of 11 for 72 hours. Nitrogen deprivation, oxygen limitation, the supplementation with exogenous R3HBA and neutral or acidic pHs strongly reduced the excreted R3HBA concentration and yield.

The implementation of the TSS system in *M. parvus* and *C. necator* by the construction of an expression vector containing *tesB* was hampered by inconsistencies in the constructed plasmids pLY01 and pLY02. Finally, the production of R3HBA by redirecting fluxes in the PHB metabolic pathway was investigated in *C. necator*; two mutant strains were constructed using the suicide vector pT18mobsacB: *C. necator* Δ*phaC* and *C. necator* Δ*phaC* Δ*hbd*, both unable to polymerize PHB and the last one incapable to transform R3HBA into acetoacetate. The mutant strains released pyruvate and R3HBA, suggesting that a native thioesterase of *C. necator* may play a role in the release of R3HBA by removing CoA from R3HBA-CoA. A protein homology on the genome of *C. necator* showed an enzyme encoded as WP_037025319.1 with a percent identity of 44 % in comparison with Ycia that may trigger R3HBA release.

The results obtained in this work demonstrated the feasibility of R3HBA production by reducing or eliminating the fluxes of the reactions consuming R3HBA via operational manipulation as described in *M. parvus* and *A. lata* or via gene knock outs in *C. necator*.

RESUMEN

Se ha acumulado una abundante literatura sobre los aspectos bioquímicos, fisiológicos y genéticos de la acumulación intracelular de polihidroxibutirato (PHB) en bacterias. Los costos de los sustratos y procesamiento, incluida la extracción del polímero acumulado en los gránulos intracelulares, dificultan un uso más generalizado de esta familia de polímeros. La unidad monomérica del PHB, ácido (*R*)-3-hidroxibutírico (R3HB), ha encontrado usos en la industria biomédica, química y de suplementos. La literatura muestra que se han identificado dos estrategias principales de ingeniería de procesos e ingeniería metabólica para la producción de R3HB: (i) producción a partir del polímero acumulado (sistema de polimerización y despolimerización, SPD); (ii) evitando la acumulación de PHB utilizando bacterias modificadas metabólicamente. Este último incluye el uso de tioesterasas (sistema acceso-directo con tioesterasas, SADT) que elimina el CoA de R3HB-CoA, lo que da como resultado la liberación extracelular de R3HB.

Esta tesis doctoral tiene como objetivo ampliar la comprensión de los factores genéticos y operativos que conducen a la polimerización de PHB y la producción de R3HB en *Azohydromonas lata* DSM 1123, *Cupriavidus necator* H16 y *Methylocystis parvus* OBBP. Los resultados mostraron que la producción de PHB está asociada con el crecimiento en *A. lata* e imita un metabolismo de desbordamiento; además, se obtuvo una despolimerización exitosa de PHB en un quimiostato de dos etapas. Se estudio la viabilidad de producir R3HB a través de la despolimerización *in-vivo* del PHB acumulado intracelularmente en *M. parvus*. La conversión de PHB a R3HB de 77.2 ± 0.9 % (concentración R3HB de 0.153 ± 0.002 g L^{-1}) se pudo lograr en un medio mineral que contiene 1.0 g L^{-1} KNO_3 a 30 °C con agitación a 200 rpm y un pH constante de 11 por 72 horas. La privación de nitrógeno, limitación de oxígeno, suplementación con R3HB exógeno y los pHs neutros o ácidos redujeron fuertemente la concentración y el rendimiento de R3HB excretado.

La implementación del sistema SADT en *M. parvus* y *C. necator* mediante la construcción de un vector de expresión que contenía *tesB* se vio afectada por inconsistencias en los plásmidos construidos pLY01 y pLY02. Finalmente, se investigó la producción de R3HB mediante la redirección de flujos en la ruta metabólica de PHB en *C. necátor*; se construyeron dos cepas mutantes utilizando el vector suicida pT18mobsacB: *C. necator* Δ*phaC* y *C. necator* Δ*phaC* Δ*hbd*, ambas incapaces de polimerizar PHB y el último incapaz de transformar R3HB en acetoacetato. Las cepas mutantes liberaron piruvato y R3HB, lo que sugiere que una tioesterasa nativa de *C. necator* puede desempeñar un papel en la liberación de R3HB mediante la eliminación de CoA de R3HB-CoA. Una homologación proteica en el genoma de *C. necator* mostró una enzima codificada como WP_037025319.1 con un porcentaje de identidad del 44 % con Ycia, la cual puede desencadenar la liberación de R3HB.

Los resultados obtenidos en este trabajo demostraron la viabilidad de producir R3HB al reducir o eliminar los flujos de las reacciones que consumen R3HB a través de manipulaciones operacionales como se describe en *M. par*vus y *A. lata* o mediante la deleción de genes en *C. necator*.

ACKNOWLEDGMENTS

First, I would like to express sincere gratitude to my supervisors Dr. Felipe Scott and Dr. Raul Muñoz for kindly guiding with research and for their continued support throughout my PhD journey. Thank you for providing me with all the great scientific opportunities, all the resources for my work and for making a stressful move to Chile and Spain easy. Specially, I feel very grateful with Dr. Felipe Scott for being a friend and for encouraging my way.

I wish to thank the Universidad de Los Andes for the provision of a *Fondo de Ayuda a la Investigación* (FAI) grant that facilitated these studies. Thanks to the Universidad de Valladolid for the opportunity of study through the double degree agreement between Universidad de los Andes (Chile) and Universidad de Valladolid (Spain). Additionally, the financial support to my work from the National Agency for Research and Development (ANID Chile), projects ANID/CONICYT Fondecyt Regular 1211434 and ANID/CONICYT Fondecyt Regular 1190521; *Apoyo a la Formación de Redes Internacionales entre Centros de Investigación* REDES190137 (CONICYT-PCI) and the regional government of Castile and Leon and the EU-FEDER program (CLU 2017-09, UIC 315) are also gratefully acknowledgment.

Thanks to all the current and previous members of the G-Tech group lab for being great lab mates and always keeping a friendly and collegial working atmosphere. Special thanks to the VOC and Microalgae group for the enthusiastic welcomed, all the deep scientific and philosophic discussions, Tapas night and for all your support and encouragement. Special thanks to Yadira Rodriguez, a great friend, working with her has been a rewarding experience.

To my family and friends who encouraged me all the way until here. Without them, this would have been much harder. To my parents who taught me about never giving up and always staying by my side. Finally, I want to thank Harvey Hernandez for standing beside me throughout this thesis and specially our journey. His faithful support, love, patience, and advice are greatly appreciated.

CONTENTS

LIST OF APPENDICES

LIST OF TABLES

LIST OF FIGURES

NOTATION AND ABBREVIATIONS

μ	Specific growth rate
D	Dilution rate
v/v	Volume per volume
w/v	Weight per volume
Amp^{R}	*Ampicillin resistance* gene
ATP	Adenosine triphosphate
CDW	Cell dry weight
DO	Dissolved oxygen
E-flask	Erlenmeyer flask
GC	Gas chromatograph
GHG	Greenhouse gases
hbd	R3HBA dehydrogenase gene
HPLC	High performance liquid chromatography
LB	Luria Bertani
mcl	medium-chain-length
NAD^{+}	Nicotinamide adenine dinucleotide
NADP	Nicotinamide adenine dinucleotide phosphate
NFMS	Nitrate free mineral salts medium

NMS	Nitrate mineral salts medium
OD_{600}	Optical density at 600 nm
PCR	Polymerase chain reaction
PDS	Depolymerization system
PHA	Polyhydroxyalkanoate
phaA	β-ketothiolase gene
phaC	PHB synthase gene
PHB	Polyhydroxybutyrate
PHBi	Initial PHB content
PHV	Polyhydroxyvalerate
R3HA	(*R*)-3-hydroxyalkanoic acid
R3HBA	(*R*)-3-hydroxybutyric acid or (*R*)-3-hydroxybutyrate acid
R3HBA-CoA	(*R*)-3-hydroxybutyryl-Coenzyme A
R3HD	(*R*)-3-hydroxydecanoic acid
R3HDD	(*R*)-3-hydroxydodecanoic acid
R3HHx	(*R*)-3-hydroxyhexanoic acid
R3HO	(*R*)-3-hydroxyoctanaoic
TCA cycle	Tricarboxylic acid cycle
TSS	Thioesterase shortcut system

1. INTRODUCTION

Climate change presents a series of unprecedented challenges to natural and human systems (Beaumont et al., 2011; Riahi et al., 2022). Despite the ongoing public debate on the causal role of anthropogenic Greenhouse Gases (GHG) (Carmichael & Brulle, 2017; Howe et al., 2015; van der Linden et al., 2017), the Intergovernmental Panel on Climate Change (IPCC) determined through a near-unanimous scientific consensus that forcing from anthropogenic emissions is the primary driver of climate change (Riahi et al., 2022). With continuous economic development, industrialization, and fossil fuel consumption, GHGs emissions have exceeded the buffering capacity of the atmosphere. A total of 73.2% of the global GHG emissions are emitted by the energy sector, out of which 32.9% is attributed to different stages of global oil production, including its extraction, distribution, and refining (Mohamad Noh, 2017). The sources of agricultural GHG emissions are from land-use change (carbon dioxide, CO_2), enteric fermentation (methane, CH_4), and manure management (nitrous oxide, N_2O) (Vergé et al., 2007). Thus, anthropogenic GHG emission are increasingly threatening the sustainability of natural ecosystem and human societies, raising the earth's temperature and leading to one of the critical environmental issues nowadays, global warming.

Among the most prevailing GHGs is CH_4, which accounts for almost one-quarter of the cumulative radiative forcing of CO_2 and NO_2 combined since 1750 (Etminan et al., 2016). Indeed, CH_4 exhibits a global warming potential 86 times stronger per unit of mass than CO_2 on a 20-year timescale and approximately 28 times more powerful on a 100-year time scale (Edenhofer, 2014). The global CH_4 emissions have been steadily increasing over the past few decades up to April 2020 with a global concentration of 1876.3 ppb (Dlugokencky, 2020), exerting a negative effect on the environment. Today, global CH_4 can be captured from anthropogenic sources (125 Mton per year), wastewater treatment (68 Mton per year), agriculture (145 Mton per year), biomass (16 Mton per year), and natural gas production (92 Mton per year) (IEA, 2020) but the main sources are natural gas and biogas (Ghasemi Ghodrat et al., 2018; Strong et al., 2015). Bioconversion of CH_4 offers a broad range of alternatives that can be valorized as an energy vector or as a feedstock for biotechnological processes for the production of ectoine, biopolymers such a polyhydroxyalkanoates (PHAs),

and single cells protein, among others (Jawaharraj et al., 2020) or for the catalytic production of methanol (Latimer et al., 2018).

Emissions of GHGs are also related to plastic's life cycle. Recent estimates have forecasted to cumulative emissions from plastics production and use reaching 56 Gton of carbon by 2050, being equivalent to 10–13% of the remaining carbon budget to stay below 2 °C (Hamilton et al., 2019). Synthetic polymers, such as polyolefins mainly produced from petroleum-based monomers, are non-biodegradable and non-renewable materials. As a result, plastics accumulate, rather than decompose, in the environment and close to 60% of all plastics produced from 1950 to 2015 can be found in landfills or the natural environment, amounting to approximately 4900 Mton (Geyer et al., 2017). PHAs are a family of thermoplastic polymers of renewable, bio-based and biodegradable polyesters that are expected to reduce the impacts of plastic production and use, including greenhouse gas emissions. One of the most promising biopolymers is polyhydroxybutyrate (PHB), a biogenic short chain PHA, produced by various bacteria as a storage compound under nutrient-deficient conditions when a carbon source is present in excess. PHB can be synthesized from a wide range of carbohydrates and lipids including sucrose (Yamane et al., 1996). The use of CH_4 or H_2:CO_2:O_2 (knallgas) (Brigham, 2019) mixtures could help to mitigate climate change by lowering the emissions of harmful gases and tackling the conversion of CO_2 into useful products.

The PHB monomeric unit, (*R*)-3-hydroxybutyric acid (R3HBA), has found uses as a chiral building block for the synthesis of fine chemicals such as antibiotics, vitamins, aromatics, and pheromones (Chiba & Nakai, 1985; Seebach et al., 2001; Steinbüchel & Valentin, 1995). R3HBA has also been known to exhibit antimicrobial, insecticidal, and antiviral activities (Chen & Wu, 2005; Peypoux et al., 1999; Shiraki et al., 2006). Studies have shown that R3HBA confers partial protection and stability to neurons during glucose deprivation (Holmes, 1985; Massieu et al., 2003). There is also evidence that R3HBA could offer neuroprotection in Parkinson's and Alzheimer's disease (Kashiwaya et al., 2000). Additionally, R3HBA may suppress the effects of hyperglycemia, lactic acidemia and hyperalaninemia in hemorrhagic stress (Katayama et al., 1994). Recently, R3HBA has been

commercialized as a supplement for athletes and people following keto diets, further expanding its uses (Martin, Thomas & Soni, 2021). This monomer can be produced either by *in-vivo* depolymerization of the accumulated PHB, by fermentation for the direct production of (*R*)-3-hydroxyalkanoates (R3HAs) into the culture media and by conversion of purified PHB, although the production of R3HAs from recovered PHAs requires more steps. The advantage of the first alternative lies in the fact that R3HBAs production does not require the extraction of the intracellular PHB.

An efficient method to produce R3HBA is through the tunning of pH values that switch the activity of intracellular PHA depolymerase and R3HBA dehydrogenase. *Azohydromonas lata* (formerly *Alcaligenes latus*) is a Gram-negative facultative autotroph, capable of using knallgas and organic molecules (including sucrose and glucose) for growth and PHB production, having the highest volumetric productivity of PHB accumulation reported up to date (Lee et al., 1997). Interestingly, PHB depolymerization and R3HBA release in *A. lata* has been achieved at pH 4 and 35 °C, with a PHB to R3HBA conversion of 96% in 30 min and a decrease to a yield of 31% at a pH 5 (Lee et al., 1999).

One potential candidate for study the R3HBA production, is the well characterized PHB producer, *Cupriavidus necator* H16 (formerly *Ralstonia eutropha),* which is a Gram-negative bacteria and obligate aerobe. *C. necator* growth and PHB accumulation can be achieved using knallgas, sugars, and organic acids as substrates. PHB accumulation in *C. necator* follows a non-growth associated pattern; *i.e*, the specific PHB productivity decreases as the growth rate increases in chemostat culture. R3HBA production in *C. necator* has only been reported by (Lee at al., 1999) where cells that accumulated polyhydroxybutyrate co-valerate (PHB/V) were incubated in water at pH 7 and other low pH values at 30 °C. Under these conditions, a depolymerization mixture was obtained, consisting of R3HBA (5.8 g L^{-1}) and (*R*)-3-hydroxyvalerate (0.6 g L^{-1}) at pH 7. Other pH values did not improve PHB/V depolymerization, which suggest that the depolymerization mechanisms are not influenced by changes of pH values.

The production of R3HBA from PHB produced from sugar-based bacterial processes is expensive nowadays. The costs of supplying the required carbon and energy source for microbial growth and PHB production are estimated to be between 30 and 50% of the product cost if sugars are used (Choi et al., 1999; Levett et al., 2016).However, there is a group of Gram-negative bacteria, collectively termed methanotrophs, that can grow and synthesize value-added products such as biopolymers, from CH_4. Bacteria in this group are classified according to the pathways used for the assimilation of the formaldehyde produced directly from CH_4 into type I and type II methanotrophs. Type I use the ribulose monophosphate pathway for formaldehyde assimilation, and type II methanotrophs use the serine pathway (Nguyen, et al., 2021). The ability to form biopolymer inclusions as PHB is under growth-essential nutrient deprivation (e.g. nitrogen or phosphorous) and methane availability (Asenjo & Suk, 1986; Hanson & Hanson, 1996). A representative type-II methanotrophs is *Methylocystis parvus* a bacteria that is also capable of nitrogen fixation (del Cerro et al., 2012; Vecherskaya et al., 2009). *M. parvus* shows a higher specific growth rate (μ) compared to other species of the *Methylocystis* genera (Bordel et al., 2019) and the ability to synthesize PHB under nitrogen-limited conditions (Rostkowski et al, 2013) leading to accumulations of more than 50% (Pieja et al., 2011; Wendlandt et al., 2001). Up to date, the operational conditions that control the enzyme activity that allows the release of R3HBA are unknown.

1.1 Hypothesis

From the analysis of literature, two systems can be identified for the production of R3HBA in PHB and non-PHB producing bacteria. In the first system, herein termed polymerization and Depolymerization System (PDS), PHB is accumulated and then depolymerized to R3HBA without -or with a reduced activity of- the R3HBA dehydrogenase enzyme that otherwise would transform R3HBA to acetoacetate. Production of R3HBA in *A. lata* by Lee et al (1999) is a prime example of the PDS system.

Nevertheless, the use of PDS system requires a two-stage fermentation: accumulation of the polymer followed by depolymerization. Thereby the required cultivation times are typically long. Hence, the interest in the last decades has focused on the direct microbial production

of extracellular R3HA monomers without going through these two stages and achieving a straightforward, less energy demanding and time-consuming process.

The alternative pathway is called Thioesterase Shortcut System (TSS), which is characterized by the creation of a bypass without PHB accumulation by the insertion of a thiosterase (TesB or Ycia) enzyme that removes the Coenzyme A (CoA) from (*R*)-3-hydroxybutyryl-Coenzyme A (R3HBA-CoA), thus resulting in a R3HBA monomer release to the extracellular medium (Guevara-Martínez et al., 2019; Liu et al., 2007) and the recycling of CoA. The study of TSS mechanism have been reported only in *E. coli* strain is due to that TesB and Ycia are native thioesterases and needs the insertion of *phaA* (β-ketothiolase) and *phaB* (acetoacetyl coenzyme A reductase) genes for evaluating the role of this thioesterases. High production of R3HBA with TesB by the TSS mechanism has been reported in recombinant *E. coli* harboring genes of *phbA* and *phbB* up to 12 g L^{-1} in a 6 L fermenter (Liu et al., 2007). But interestingly, Guevara-Martinez and co-workers described that *tesB* deletion resulted in R3HBA yield reduction of 10%, whereas for *ycia* was 43%. This system shows the importance of evaluating thioesterases native or non-native within a specific pathway and how it involves the PHB-producing strains to achieve significant R3HBA titers.

At present, there is no evidence of the application of the TSS system in PHB-producing bacteria and the PDS system has not been broadly studied in other PHB-producing bacteria that use gaseous substrates (syngas, knallgas, and methane) that can be valorized. Based on the previous information, this work proposed the application of TSS (TesB) and PDS in *C. necator* H16, *A. lata* DSM 1123 and *M. parvus* for R3HBA production. The hypothesis driving this PhD Thesis is:

"R3HBA can be produced by reducing or eliminating the fluxes of the reactions consuming R3HBA, via operational manipulations or gene knock outs, and simultaneously enhancing the supply of R3HBA from PHB (via PHB depolymerase) or R3HBA-CoA hydrolysis using a heterologous *tesB* gene".

1.2 Objectives

General Objective

To broaden the understanding of the genetic and operational factors leading to PHB polymerization and R3HBA production in *A. lata*, *C. necator* H16 and *M. parvus*.

Specifics Objectives

i) To assess the PHB accumulation and depolymerization yield and productivity via operational manipulations in chemostat cultures of *A. lata* DSM 1123 as a benchmark of R3HBA production.

ii) To study a set of operational conditions allowing the depolymerization of the accumulated PHB in *M. parvus*.

iii) To obtain a characterization of PHB and R3HBA production capabilities of PHB synthase (*phaC*) and R3HBA dehydrogenase (*hbd*) knock out mutants of *C. necator* H16.

iv) To quantify the R3HBA titer, yield and productivity of the parent strains obtained in iii) and of strains with the insertion of *tesB*.

1.3 Organization of this document

Chapter 2 presents a literature review summarizing the most important information supporting this thesis, including the developments leading to the current understanding of the mechanisms of PHB accumulation and depolymerization. Chapter 3 presents the materials and methods used to attain the proposed objectives while Chapter 4 summarizes the results obtained, comparing them with relevant information from the literature. Finally, Chapter 5 outlines the conclusion of this thesis and states future research directions and opportunities.

2. LITERATURE REVIEW

This chapter is organized as follows. Section 2.1 presents the main applications of PHAs and their monomers in several industrial fields and the recent uses as a biomedical target. Section 2.2 summarizes the carbon and energy substrates currently used to produce PHAs and the potential of moving to lignocellulosic substrates, agro-food wastes, sugars and abundant gaseous substrates such as syngas, knallgas, or CH_4. Section 2.3 is a brief analysis concernig the regulation of PHB biosynthesis and the influence of the growth factors for its mobilization. Finally, section 2.4 provides insights about strategies based on operational changes or genetic modifications that have been devised for the production of chiral hydroxyalkanoic acids.

2.1. POTENTIAL USES OF PHAs AND THEIR MONOMERS

PHAs have been extensively investigated to identify possible applications. Homopolymers, random copolymers, and block copolymers can be produced depending on the structure of the polymer chain, which in turn is dictated by the species of bacteria and the substrate used for the accumulation of PHA (Braunegg, G., Bona, R; Koller, 2004). The diversity of applications is wide, including production of biodegradable plastics that are environmentally friendly for use in packaging (Khosravi-Darani & Bucci, 2015; Koller, 2014), fibers (Dietrich et., 2017), biodegradable and biocompatible implants (Misra et al., 2006), drugs and fine chemical (Rathbone et., 2010), and biofuels (Zhang et al., 2009).

As biomedical materials, PHAs have been used in suture materials and repair patches, meniscus restoration devices, cardiovascular patches, orthopedic pins, and cartilage regeneration aids, among others (Volova et al., 2003; Wang, Wu, Chen, &, 2005). Many of these uses are related to the customizable composition and properties of PHAs, which allow them to have favorable mechanical properties, biocompatibility, and to degrade in reasonable times under specific physiological conditions (Hazer et al., 2012; Misra et al., 2006). In particular, medium-chain-length-PHAs (mcl-PHAs), have potential applications in coatings and in medical temporary implants such as scaffoldings for the regeneration of arteries and

nerve axons (Witholt & Kessler, 1999). On the other hand, the use of these polymers has been studied for controlled drug delivery (Shah et al., 2010). The kinetics of drug release can be engineered by altering the degradation rate of the PHA matrix coating. In this regard, mcl-PHAs have been used as drug carriers since their low fusion point and low crystallinity makes them suitable for controlled drug release (Ueda & Tabata, 2003).

Finally, PHA-derived compounds can be used as biofuels after the esterification of PHB of mcl-PHAs with methanol for their conversion to hydroxyalkanoate methyl esters (Zhang. et al., 2009). These hydroxyalkanoate methyl esters can be mixed with gasoline or diesel in ratios of 10 to 30%. In particular, (*R*)-3-hydroxy-methyl-butyrate was reported to have similar or superior properties as a fuel additive (oxygen content, dynamic viscosity, flash point, and boiling point) compared to ethanol (Wang et al., 2010). Using PHA derivatives as biofuels can be viewed as a promising application since mixtures of PHA can be used without a costly separation step (Gao et al., 2011).

The most well-known R3HAs is R3HBA, which can be used as a building block in the synthesis of fine chemicals and pharmaceuticals such as antibiotics (Ren, Grubelnik, Hoerler, Ruth, Hartmann, et al., 2005), bulk chemicals for the polymer industry (such as hydrogenation to 1,3-butanediol), fragrances and insecticides (Matsuyama et al., 2001). R3HBA can be esterified with butanol or ethanol or converted to ethers by reaction with alcohols using the catalytic Williamson ether synthesis (Fuhrmann & Talbiersky, 2005) or dehydrated to crotonic acid, which upon hydrogenation yields butyric acid and *n*-butanol (Schweitzer et al., 2015).

Similarly, (*R*)-3-hydroxypropionic acid (R3HPA), a non-chiral compound, can yield upon chemical modifications to acrylic acid, acrylamide, and acrylonitrile, all with market sizes larger than one billion dollars, and other niche market compounds such as 1,3-propanediol, methyl acrylate and malonic acid (Jers et al., 2019).

More than three decades ago Seebach et al. (1986) reported the synthesis of the macrolide antibiotics pyrenophorin, colletodiol, garamycin A1 and elaiophylidene starting from

R3HBA and malate. R3HBA and its derivatives have also been used as potential drugs. Cao et al. (2014) showed that R3HBA and R3HBA methyl ester inhibit the development of osteoporosis in mice kept under simulated microgravity. Using *in-vivo* studies with mice suffering from Alzheimer's disease, Zhang et al. (2013) showed that intragastric administration of R3HBA methyl ester reduced amyloid-β deposition in mouse brains and improved the performance of the treatment group in the Morris water maze (a standardized test in the study of spatial learning and memory) compared to the control group. In a related study in mice, Tieu et al. (2003) showed that the infusion of R3HBA led to improved mitochondrial respiration and ATP production in mice treated with the neurotoxin 1-methyl-4-phenyl-1,2,3,6-tetrahydropyridine causing a mitochondrial deficit reminiscent of Parkinson disease. Finally, Yamanashi et al. (2017) showed that R3HBA could act as a therapeutic candidate for the treatment of stress-related mood disorders (depression). The mechanism involves an anti-inflammatory effect mediated by a reduction in the levels of the inflammatory cytokines inter-leukine 1β and tumor necrosis factor α in the hippocampus of mice. Recently, other positive effects after a R3HBA administration is the reduction of proliferation of colonic crypt cells and potential suppression of intestinal tumour growth (Dmitrieva-Posocco et al., 2022).

Other potential uses of R3HBA include its use as a chemical chaperone for amelioration of heat-mediated denaturation and oxidative damage by Cu^{2+} and H_2O_2 produced on industrially relevant enzymes such as lipases and lysozymes (Obruca et al., 2016).

Finally, R3HAs can be used as building blocks that can be biologically produced, excreted from cells, and then polymerized or co-polymerized to yield PHAs with tunable mechanical and thermal properties (Wang et al., 2018). Advantages of the *ex-situ* polymerization starting from biomonomers over the conventional approach of biopolymer accumulation inside cells include (Adkins et al., 2012): (i) simplified downstream product recovery of the extracellular biomonomers compared to the intracellular polymers, (ii) the polymerization in controlled chemocatalytic environments allows for polymers with finely tuned properties and high purities, and (iii) higher diversity of plastics thanks to the ability to co-polymerize different monomers. Examples of *in-vitro* synthesis include the production of PHB from R3HBA by

a three-enzyme system that only consumes ATP and the monomer (Jossek et al., 1998). The yield of this system was recently improved by using a thermostable acetyl-CoA synthetase, CoA transferase and PHA synthase (Tajima et al., 2016). A polymer incorporating lactate and R3HBA residues was produced by Tajima et al. (2012), using an engineered PHA synthase capable of lactate polymerization. An excellent revision of the chemosynthesis of copolymers containing different R3HAs monomers and lactate was recently published (Hiroe et al., 2019). However, a general drawback of these systems so far is the consumption of ATP, specifically to drive the activation of acetate to acetyl-CoA, a molecule that needs to be present in the reaction mixture to act as the CoA donor to yield the hydroxyacyl-CoAs required for the polymerization reaction.

2.2. SUBSTRATES TO PRODUCE PHAs AND THEIR MONOMERS

Substrates commonly used for the industrial production of PHAs include corn starch, sucrose obtained from sugar cane and vegetable oils, all edible feedstock requiring arable lands, and agricultural practices that affect both their economy and sustainability (Levett et al., 2016). Commercial PHAs are produced using sucrose in *A. lata* (Biomer Germany, with trade name Biomer™) and *Bacillus* sp. (PHB Industrial S.A. Brazil, Biocycle™); glucose from corn in *C. necator* (Metabolix, Mirela™ and Tianan Biologic Material, Enmat™); or fatty acids using *Pseudomonas putida* (ETH, PHA™) or *C. necator* by Kaneka Corporation and marketed as Kaneka PHBH™ (Bugnicourt et al., 2014; Chen, 2009; Możejko-Ciesielska & Kiewisz, 2016).

Due to the high costs and sustainability concerns associated with the raw materials traditionally used in the production of PHAs, the use of agro-food waste, food industry waste, and other non-food industry residues, have been increasingly studied (Braunegg et al., 2004). For example, several solid residues have been examined such as rice bran (Oh et al., 2015), pea-shells (Kumar et al., 2016), chicory roots (Haas et al., 2015), potato peels, apple pomace, onion peels (Kumar et al., 2016), grape pomace (Follonier et al., 2015), animal farm waste, poultry litter (Bhati & Mallick, 2016) and palm oil (Loo et al., 2005). In the case of food wastes for PHAs production, literature report on the use of spent coffee grounds (Cruz et al.,

2014), food waste composite (Amulya et al., 2015), and used cooking oil (Borrero-de Acuña et al., 2019; Gómez Cardozo et al., 2016).

Finally, non agro-food residues are generated by biodiesel manufacturing: crude glycerol (de Paula et al., 2017); oil cake hydrolysate (Bera et al., 2015), and biodiesel fatty acid by-product from glycerol purification (Cruz et al., 2016). Glycerol can be used for the accumulation of mcl-PHAs and short-chain-length PHAs in *Pseudomonas putida* strains (Poblete-Castro et al., 2014), *C. necator* DSMZ 4058 (Mothes et al., 2007) and *Bacillus megaterium* (Naranjo et al., 2013), among others.

The availability and sustainability issues of conventional substrates have motivated the exploration of alternative feedstocks as sources of carbon and energy for microbial production of chemicals, such as lignocellulose which can be obtained from the "residues" left after the harvest of agricultural products or from dedicated high yield cultivars (poplar, *eucalyptus, miscanthus*) (Loow et al., 2016), thus reducing the environmental burden associated with their production. Reducing even further water and land usage, compounds containing one carbon atom, such as methanol and formate can be obtained from the reduction of CO_2 using electrons harnessed from solar energy (Agarwal et al., 2011; Pérez-Fortes et al., 2016; Yishai et al., 2016).

Among inexpensive substrates that are readily available for reducing the total cost of PHAs production, certain C1 carbon sources, e.g., methane, methanol, and CO_2 have received a great deal of attention due to their contribution to global warming (Khosravi-Darani et al., 2013). Production of PHB from waste methane may help reducing the impact of the greenhouse effect of this gas. Accumulation of PHB, but not other PHAs, has been reported in several *Methylocystis* species using methane and *Methylobacterium* from methanol (Strong et al. (2016). In this regard, Listewnik et al. (2007) estimated a price of 6.35 UK pounds per kg of PHB produced from natural gas in a two-stage plant producing 500 tons PHB per year. Similarly, Levett et al. (2016) estimated a production cost range of 4.1 to 6.8 USD per kg of PHB, with a reduction in the share of the carbon source in the total product cost from 30% when sugar feedstocks are used to 22% for methane. However, these

production costs are high when compared to the estimations made by Posada et al. (2011), who performed a techno-economic evaluation of PHB production from glycerol as energy and carbon source. They reported production costs between 1.9 and 2.5 USD per kg and a substrate share between 5 and 8%. The higher production cost when methane is used as a substrate is greatly influenced by the low overall mass transfer coefficient of methane into the medium. This leads to large reactors and, thereby high investment and operating costs.

Knallgas bacteria, such as *C. necator* H16 and *A. lata*, can use mixtures of hydrogen, carbon dioxide and oxygen for the accumulation of PHB (Reinecke & Steinbüchel, 2009), biofuels (Brigham, 2019) or acetoin (Windhorst & Gescher, 2019). Albeit the production of PHB has been studied thoroughly with cultures of *R. eutropha* or *Ideonella* sp. O-1, accumulating over 60 g L^{-1} of PHB (Tanaka et al., 1995; 2011), no reports of PHAs accumulation aside PHB are available.

2.3. ACCUMULATION AND MOBILIZATION OF PHAs

The model organism for PHB production is *C. necator* a gram-negative, obligate aerobe, capable of autotrophic growth in the presence of hydrogen, CO_2 and oxygen, and heterotrophic growth and PHB production from a wide variety of carbon sources including sugars (chiefly fructose in the wild type organism *C. necator* H16 ATCC 17699) and organic acids (Lu et al., 2016). For example, using glucose in a fed-batch culture of *R. eutropha* NCIMB 11599, a mutant of *R. eutropha* H16 capable of using glucose, a concentration of biomass of 164 g L^{-1} was obtained, with a PHB content of 74% (Kim et al., 1994).

In *C. necator*, synthesis of PHB occurs when excess carbon in the form of acetyl-CoA is condensed via a β-ketothiolase (EC 2.3.1.16) to generate acetoacetyl-CoA, which is then reduced to R3HBA-CoA by a NADPH-dependent acetoacetyl-CoA reductase (EC 1.1.1.36). Finally, the enzyme PHB synthase (EC 3.1.1.75) catalyzes the polymerization of (*R*)-3-hydroxybutyrl-CoA monomers. This pathway is the most widespread route in bacteria for providing R3HBA-CoA monomers (Steinbüchel & Hein, 2001). Production of mcl-PHAs, such as the polymers accumulated in *Pseudomonas* spp., requires precursors derived from

the dissociated fatty acid biosynthesis pathway unless these precursors are supplied through related carbon sources (such as octanoic acid for the synthesis of poly(3-hydroxyoctanoate). For details regarding this pathway, the reviews by Lu et al. (2009) and Suriyamongkol et al. (2007) are highly recommended.

The regulation of PHB biosynthesis is tightly connected to the cellular levels of reduced nicotinamide nucleotides. Lee et al. (1995) found that when *R. eutropha* was cultivated in nitrogen-limited media, the NADPH/NADP and NADH/NAD^+ ratios and the intracellular concentrations of NADH and NADP were higher than those found under nitrogen-sufficient conditions. Moreover, the rate of PHB accumulation was found to increase with both NADH/NAD^+ and NADPH/NADP ratios. This effect was explained through the analysis of citrate synthase activity. Citrate synthase was inhibited by NADPH and NADH, thus funneling the carbon to PHB instead of being directed to the tricarboxylic acid cycle. Similar conclusions were reported by Henderson & Jones (1997).

Although PHB accumulation occurs under unfavorable conditions for growth induced by nutrient limitation of oxygen, nitrogen or phosphorous, with excess carbon (Steinbüchel & Hein, 2001), these conditions impact the productivity of the PHB accumulation phase. Grousseau et al. (2013) showed that sustaining a controlled residual growth rate, by feeding a controlled amount of phosphate along with the carbon source (butyric acid), allows for an improved specific productivity and high yield of PHB. Interestingly, using Metabolic Flux Balances they showed that the maximal specific PHB production rate is defined by the maximum specific rate of NADPH produced. When a low growth rate is allowed in the fed-batch fermentation (for example, feeding a nitrogen source), the NADPH is produced in the Entner-Doudoroff pathway, whereas without biomass production regeneration of NADPH is only possible via isocitrate dehydrogenase.

Another possibility to increase PHB volumetric productivities is to rely on microorganisms where growth and PHB production occur simultaneously. In this regard, *A. lata* consumes glucose, sucrose and acetic acid (Chen et al., 1991), but it does not consume xylose, accumulating PHB during its growth (Yamane et al., 1996). In a fed-batch culture using

sucrose as the carbon source and continuous feeding of ammonia, controlled by the decrease in pH as the culture consumes the source of nitrogen (pH-stat), 143 g L^{-1} of cells with 50% PHB were attained with a PHB productivity of 3.97 g $L^{-1}h^{-1}$, one of the highest ever reported (Yamane et al., 1996). One year later, Wang and Lee (1997) reported even higher productivity (4.94 g $L^{-1}h^{-1}$) and PHB intracellular content in *A. lata* (88%) applying nitrogen limitation in a two-stage fed-batch culture (nitrogen sufficient followed by nitrogen-limited culture).

Assuming that PHAs act as a reserve compound of carbon and energy, without a source of carbon and energy, but in the presence of other growth factors (such as nitrogen or oxygen), PHAs should be depolymerized into their monomers and incorporated into the metabolism, using the degradation products for growth and survival, a process termed PHA mobilization. This behavior has been shown at least in *C. necator* H16 (Juengert et al., 2017; Uchino et., 2007), *A. lata* (Lee et al., 1999), *Legionella pneumophila* (James et al., 1999), *Hydrogenophaga pseudoflava* (Choi et al., 1999) and *Halomonas* sp. KM-1 (Kawata et tal., 2015).

Compared to PHB accumulation, depolymerization of PHB to R3HBA, and its transformation to acetyl-CoA, has been less studied as confirmed by fewer reports in the literature. However, evidence exists indicating that the granules of PHB and other PHAs are supramolecular complexes (called carbonosomes), constituted by a polymer core and a surface layer of at least a dozen proteins (Sznajder et al., 2015), but without a phospholipids membrane (Bresan et al., 2016). The proteins in the carbonosomes include the PHA synthase (PhaC) and PHB depolymerases (PhaZs), which are thought to be constitutively expressed (Brigham et al., 2012; Lawrence et al., 2005).

It has been reported that PHB synthesis and its degradation can happen simultaneously in the model PHB accumulating organism *C. necator* (Doi et al., 1990; Taidi et al., 1995). Doi and co-workers concluded this after cultivating *C. necator* in butyrate as the carbon source under nitrogen-free conditions, thus inducing the accumulation of PHB, and changing the carbon source to pentanoic acid. After the shift in the substrate, the accumulated PHB was gradually

replaced by poly(3-hydroxyvalerate-co-3-hydroxybutyrate) without a net increase of total polymer content in the cells. This indicates that PHB was degraded and replaced by polyhydroxyvalerate (PHV) even in the absence of a nitrogen source. Similarly, Taidi et al. (1995) showed a turnover of PHB after the accumulation of the polymer ceased in a nitrogen-limited batch culture with glucose as the sole carbon and energy source. The turnover was evidenced by the incorporation of radioactivity into the accumulated polymer after feeding labeled glucose (D-[U-^{14}C] glucose). Interestingly, the high-molecular-weight polymer accumulated during the unlabeled glucose phase was replaced by a low-molecular-weight polymer during the labeled glucose experiment. These observations are in agreement with the evidence showing the constitutive expression of PHB synthase and PHB depolymerase in *R. eutropha* (Lawrence et al., 2005; Sznajder et al., 2015). Confirmation of constitutive expression of PHB synthase and depolymerase in other organisms is scarce, except for the study of Kim et al. (1996) who found simultaneous activities of both enzymes during the batch culture of *A. lata* under nitrogen-limited conditions.

Thereby, this leads to the intriguing question of how the synthesis and mobilization of PHAs are regulated and particularly, how a cycle of simultaneous synthesis and degradation is avoided. Considering that the simultaneous polymerization and depolymerization of PHB and its conversion to acetyl-CoA trough R3HBA, acetoacetate and acetoacetyl-CoA requires one NADPH molecule and one ATP molecule and produces only one NADH molecule, the cycle would consume energy for the formation of thioester bonds, thus creating a futile cycle.

To tackle this unsolved issue, Uchino et al. (2007) isolated native PHB granules produced in *R. eutropha* by glycerol gradient centrifugation to preserve the proteins bound to the granule and discovered that in the presence of CoA, these granules produced R3HBA-CoA and small amounts of acetyl-CoA. If NAD^+, but not NADH, is added to the initial reaction mixture, R3HBA-CoA remains undetectable, but the concentration of acetyl-CoA increases five-fold. The authors assumed that in the presence of NAD^+, the intermediately formed R3HBA-CoA is rapidly transformed to acetyl-CoA in NAD^+ dependent reactions. The authors also found, as expected, that the native granules release R3HBA in pH-stat experiments using methods previously described (Gebauer & Jendrossek, 2006). Therefore, it remains unclear which

depolymerization mechanism, hydrolysis or thiolysis, is used *in-vivo* for the mobilization of PHB.

In order to identify the enzymes responsible for the thiolytic cleavage, Uchino et al. (2007) incorporated the PHB synthesis genes *phaCAB* in *E. coli* S17-1 along with the phasin gene *phaP1*, the depolymerase gene *phaZa1* or *phaP1 + phaZa1*. Interestingly, the recombinant strain only produced R3HBA-CoA in the presence of CoA when both *phaP1* and *phaZa1* were present in a *phaCAB* background. Moreover, no significant amounts of acetyl-CoA were detected in this experiment, an indication that downstream enzymes for the use of R3HBA-CoA were absent in *E. coli*.

The study of Uchino et al. (2007), suggests that *in-vivo* intracellular depolymerization of PHB does not represent a futile cycle and an energy waste in the form of thioester bonds. If the main product of PHB polymerization, at least in *R. eutropha*, is R3HBA-CoA instead of R3HBA, then there is no loss of energy for the formation of acetoacetyl-CoA from acetoacetate.

Regarding the regulation of PHB synthesis and degradation, Juengert et al. (2017), found that the degradation of the accumulated PHB in *C. necator* was fast and efficient in the absence of the alarmone (p)ppGpp, and when present, (p)ppGpp directly or indirectly inhibits PHB mobilization. (p)ppGpp is a key signaling molecule, which, when present at high concentrations, induces the stringent response in *E. coli* and other bacterial species. This alarmone accumulates in amino acids starved cells and inhibit the synthesis of ribosomal and transfer RNAs (Srivatsan & Wang, 2008). The results suggest that PHB accumulation under nitrogen-limited conditions is favored by the inhibition of PhaZ1 by (p)ppGpp as shown by the observed PHB accumulation in a triple knockout mutant (Δ*spoT1*+Δ*spoT2*+Δ*phaZa1*), which was unable to produce (p)ppGpp. In contrast, the double knockout mutant Δ*spoT1*+Δ*spoT2* accumulated negligible amounts of PHB. In subsequent work, Juengert et al. (2018) identified that PhaC1 was phosphorylated in multiple phosphosites during the stationary growth phase in nutrient broth medium with gluconate as carbon source, but it was not modified during the exponential and PHB accumulation phases or when grown in a

fructose-mineral medium. On the other hand, PhaZa1 was phosphorylated in Ser35 both during the exponential and stationary growth phases. Mutagenesis of the identified residues showed that PHB accumulation was unaffected for most mutants of PhaC1, except for a mutant with changes to four aminoacid residues. On the other hand, exchanging the phosphorylated residues in PhaZa1 to aspartate (a phosphomimetic[1] residue) produced mutants with a strongly reduced ability to mobilize the accumulated PHB.

Little experimental evidence exists concerning the role of the stringent response on the accumulation of PHA in other organisms. In this regard, Mozejko-Ciesielska et al. (2017) obtained a *relA*/*spot* mutant of *P. putida* KT2440. This mutant, unable to induce the stringent response, was used to assess the accumulation of PHA under nitrogen deprived and optimal nitrogen conditions. Results show that this mutant was able to accumulate mcl-PHAs under both conditions.

2.4. PRODUCTION OF R3HAs FROM PHAs

Two categories of strategies to produce chiral hydroxyalkanoic acids have been identified in native PHB producers bacteria, *ex-vivo* strategies and *in-vivo* strategies using non-genetically modified organisms.

2.4.1. *In-vitro* strategies

Under this approach, the accumulated PHAs are extracted from cells and then subjected to a chemical or enzymatic depolymerization process. The PHA recovery process starts when cells are separated by centrifugation to increase product concentration and to remove the components of the culture media. The concentration step is followed by drying or

[1] Phosphomimetic are amino acid substitutions that mimic a phosphorylated protein, thereby activating (or deactivating) the protein.

lyophilization of the concentrated biomass. The extraction of PHAs from the dried biomass can be performed by solvent extraction, by dissolving the biomass using oxidizing agents or by disrupting cells to liberate the PHAs granules (Kosseva & Rusbandi, 2018). Mechanical cell disruption techniques, such as bead milling and high-pressure homogenization, have been widely used to release intracellular protein and have been adapted for PHAs recovery (Kunasundari & Sudesh, 2011; Tamer, 1998). Tamer and colleagues compared bead milling and high-pressure homogenization for the recovery of PHB accumulated in *A. lata*. They recommended bead milling over high-pressure homogenization as the preferred method for recovering PHB from heat-shocked cells of *A. lata*. Interestingly, since PHB is recovered without solubilizing it, the native amorphous morphology of the polymer was conserved.

The common method for PHAs extraction is the use of solvents due to for its speed and simplicity. Solvents alter cell membrane and then dissolve the polymers. PHAs are recovered by solvent evaporation or precipitation with an anti-solvent (Hänggi, 1990; Liddell, 1999). In the solvents category, the chlorinated hydrocarbons chloroform, 1,2-dichloroethane and methylene chloride are used (Ramsay et al., 1994). Non-chlorinated solvents have been proposed such as ethylene carbonate and 1,2-propylene (Lafferty & Heinzle, 1977) or solvent mixtures of acetone/ethanol/propylene carbonate (Fei et al., 2016). On the other hand, the precipitation of PHAs is generally induced by non-solvent agents such as water, ethanol, and methanol (Ramsay et al., 1994; Mikkili et al., 2014). In summary, solvent extraction is characterized by numerous advantages such as the elimination of endotoxins and low polymer degradation (Liddell, 1999). However, there are limitations in the use of solvents, including their high cost (Poirier et al., 1995), high energy consumption for the separation of miscible solvents and anti-solvents, and risks both for the operator and for the environment that needs to be considered during the process design stage (Gorenflo et al., 2001).

On the other hand, digestion with sodium hypochlorite decomposes the cells allowing high levels of PHA purity to be reached (Hahn et al., 1994; Kim et al., 2003). However, sodium hypochlorite degrades PHB, resulting in a polymer with low molecular weight (Mikkili et al., 2014; Ramsay et al., 1990).

2.4.1.1. Chemical and enzymatic hydrolysis of recovered PHAs

After recovery and purification, the extracted PHAs can be chemically or enzymatically converted into high-purity 3-hydroxyalkanoic acids. Chemical methods for modifying PHB have been reported for the production of (*R*)-methyl 3-hydroxybutanoate and (*R*)-3-hydroxybutanoic acid, these methods involve the use of methanol and sulfuric acid and methanol and *p*-toluenesulfonic acid monohydrate, respectively (Seebach et al., 2003). Another approach, reported by Lee et al. (2000), considers the acidic alcoholysis of PHB, yielding methyl, ethyl and *n*-propyl esters of R3HBA, using 1,2-dichloroethane as solvent with either sulfuric acid or hydrochloric acid as catalyst. De Roo et al. (2002) extended this method to produce mcl-(*R*)-3-hydroxyalkanoic acids (mcl-R3HAs) from the mcl-PHAs accumulated in *P. putida*. After a step of acid methanolysis, the obtained R3HA methyl esters were distilled into fractions and saponified to yield the corresponding (*R*)-3-hydroxycarboxylic acids.

The multistep chemical processes outlined in the previous paragraph can be efficiently catalyzed by PHA depolymerases in a single step. This subject has been recently reviewed (Roohi et al., 2018). Thus, only some selected works will be covered. Several extracellular depolymerases have been identified and characterized (an excellent tool for its classification was presented by Knoll et al., 2009). Extracellular PHA depolymerases degrade denaturized PHA granules whose structure has been altered during the extraction process and are not covered by the native layer of proteins surrounding the granule. One exception is the PHB depolymerase from *Pseudomonas lemoignei,* which is active against native PHB granules (Handrick et al., 2001).

PHB degradation studies by extracellular depolymerases are typically performed using PHB films as substrate, producing R3HBA as the hydrolysis product (Polyák et al., 2018), thus limiting the access of enzymes to its substrate. In order to achieve high R3HBA titers, a high initial concentration of PHB should be used. However, due to its water-insoluble nature, only low PHB concentrations can be suspended in water. For example, 24 g L^{-1} of 3RHBA were produced from 25 g L^{-1} of suspended PHB powder using an extracellular PHB depolymerase

from *Pseudomonas* sp. DS1001a (Li et al., 2016). Similarly to with chemical hydrolysis methods, enzymatic hydrolysis requires the separation and partial purification of the PHA accumulated in cells and this contributes to increase the overall costs of R3Has production. These disadvantages could be eliminated in processes where R3HAs are produced directly from the PHAs accumulated by the cells using their own intracellular enzymes for the depolymerization process.

2.4.2. *In-vivo* strategies

2.4.2.1. Hydroxy-acids production by *in-vivo* depolymerization of PHAs: the polymerization-depolymerization system

In-vivo depolymerization of accumulated PHAs to R3HAs has been reported to occur with high yields in *A. lata* (Lee et al., 1999) and *Pseudomonas putida* GPo1 (Ren, Grubelnik, Hoerler, Ruth, Hartmann, et al., 2005). The depolymerization process has been shown to be highly dependent on pH. Lee et al. (1999), in a pioneering work, achieved the depolymerization of PHB to R3HBA in *A. lata* cells grown in a mineral medium with sucrose as the carbon and energy source. The depolymerization process was carried out at different initial pHs in water, after washing the cells, at 37 °C and without shaking to minimize oxygen transfer. Exceedingly high R3HBA yields and productivities, as high as 96% in 30 minutes were found at pH 4, but not at higher pH values. This result was explained in terms of the effects of pH on PHB depolymerase and Hbd activities. The highest activity of PHB depolymerase was achieved at pHs 3 and 4, at which the monomer production rate was also the highest. Interestingly, no activity of Hbd was detected at pH 4 in *A. lata*, therefore it was argued that no R3HBA was degraded to acetoacetate. At pH 5, the attained depolymerization yield was 31% and decreased towards neutral pHs. From the work of Lee et al. (1999), it is not possible to ascertain whether these lower yields are due to the consumption of the released R3HBA or a decrease in the amount of PHB depolymerized. Presumably the latter is true since the depolymerization assays were performed without shaking, thus restricting the ability of cells to regenerate NADH into NAD^+, a cofactor of Hbd.

Following the high depolymerization yields obtained at low pHs, the authors assayed the *in-vivo* depolymerization in *Ralstonia eutropha* NCIMB 11599, *Pseudomonas oleovorans* ATCC 29347 and *Pseudomonas aeruginosa* PAO1 (DSM 1707) at pH values below 7. The depolymerization yields and productivities were close to 20% for *C. necator* and below 10% for *Pseudomonas* species.

Ren et al. (2005) showed that for *P. putida* GPo1, the PHB depolymerization rate was higher at pH 11 in citrate buffer, which helps to control the pH drop caused by the accumulation of R3HAs. The released monomers corresponded to (*R*)-3-hydroxyoctanaoic (R3HO) acid and (*R*)-3-hydroxyhexanoic acid (R3HHx), in a proportion closely matching the ratio of monomers in the copolymer accumulated under continuous cultivation with octanoic acid as carbon and energy source. The depolymerization was performed for 6 hours, thus decreasing the volumetric productivity compared to the work of Lee et al. (1999). A second factor decreasing the volumetric productivity was the low initial PHA concentration used. However, this work showed that R3HAs different than R3HBA could be obtained with high yields by using the correct pH during the depolymerization process. This work was further extended by Ruth et al. (2007) showing that applying the same depolymerization process at pH 10 to PHAs accumulated in *P. putida* GPo1, grown under continuous cultivation with either octanoic, undecanoic or 10-undecenoic acid, led to the production of R3HO, R3HHx, (*R*)-3-hydroxy-10-undecenoic acid, (*R*)-3-hydroxy-8-nonenoic acid, (*R*)-3-hydroxy-6-heptenoic acid, (*R*)-3-hydroxyundecanoic acid, (*R*)-3-hydroxynonanoic acid and (*R*)-3-hydroxyheptanoic acid.

Recently, Anis et al. (2018) studied the *in-vivo* depolymerization of PHAs accumulated in *P. putida* Bet001 after 48 hours of batch culture with lauric acid as the carbon source and under nitrogen-limited conditions. The depolymerization was performed for 48 hours in 0.2 M Tris–HCl buffer, pH 9 and 30 °C. Unlike the report of Lee et al. (1999) using *Pseudomonas aeruginosa* PAO1 (DSM 1707), *P. putida* Bet001 produced R3HO, R3HHx, (*R*)-3-hydroxydecanoic acid (R3HD) and (*R*)-3-hydroxydodecanoic acid (R3HDD) with very different yields, the highest depolymerization yield being achieved for R3HD. It is not clear if this difference in yields was due to a channeling of R3HO, R3HHx and R3HDD toward

cell metabolism or if they have yet to be hydrolyzed from the granules and thus, reflects an affinity of the PHA depolymerases.

The experiments performed by Lee et al. (1999), Ren et al. (2005) and Ruth et al. (2007) used either water or phosphate buffer as depolymerization media at a pH initially set at a given value. However, the release of R3HAs resulted in a decrease in the initial pH, potentially affecting process efficiency. This factor was recognized by Wang et al. (2007), leading to the design and application of a pH-stat process. In this system, the pH is controlled at a setpoint by the automatic addition of an alkaline solution (NaOH). Interestingly, the amount of NaOH added in time (the flow of the alkaline solution), if recorded, allows the estimation of the release rate of acids (hydroxy acids and protons). Using a pH-stat apparatus coupled to a dissolved oxygen meter, Wang et al. (2007) investigated the behavior of the wild type *P. putida* GPo1 strain and a PHA depolymerase negative mutant. Results showed that the rate of acid production (not necessarily hydroxy acids) of the mutant strain was only 27 % of the rate obtained with the wild type. Analysis of the supernatants revealed that the acids released by the wild type were R3HO and R3HHx. On the other hand, no detectable amounts of these compounds were found in the supernatants of the depolymerase mutant. Moreover, oxygen consumption measurements indicated a low respiratory activity for the wild type and a high respiration rate for the mutant. Finally, they also found that the acid production rate of the mutant, but not of the wild type, could be enhanced by aeration. These results support the hypothesis that the high depolymerase activity allowed the wild type strain to compensate for the high external pH. On the other hand, in the PHA depolymerase deficient mutant this could only be performed by the production of protons in aerobic conditions.

Although the results obtained by Wang et al. (2007) supported this hypothesis for the depolymerization of PHAs to R3HAs at high pHs, the compensatory mechanism of pH involved in it does not explain the behavior recorded in *A. lata* at low pH values. Thus, the only conclusion applicable for both species is that the depolymerization process in *A. lata* and *P. putida* GPO1 the depolymerization process is enhanced at a certain pH and simultaneously the consumption of the released monomers is impaired.

Process engineering strategies for R3HAs production are nearly nonexistent with except for the work of Ren et al. (2007), who coupled a chemostat culture of *P. putida* GPo1 (nitrogen-limited, D=0.1 h^{-1}, octanoic acid as the sole carbon source) to a second continuous depolymerization stirred tank reactor. The depolymerization tank was operated as a pH-stat at a pH of 10 and its discharge was sent to a plug-flow reactor with a residence time of 6 hours. This continuous system does not require the separation of cells or the exchange of the culture media to water or buffer. Only a simple pH shift was enough to achieve a depolymerization yield of 90%, however, the volumetric productivity was not different from previously reported works using batch depolymerization (Ren, Grubelnik, Hoerler, Ruth, Hartmann, et al., 2005). Clearly, the volumetric productivity could be improved by increasing the concentration of PHA produced in the chemostat.

A different strategy for the *in-vivo* production of R3HBA has been reported using several strains of *Halomonas*. Using *Halomonas* sp. KM-1, 15.2 g L^{-1} of R3HBA could be obtained under microaerobic conditions from 16.4 g L^{-1} of PHB that was accumulated under aerobic conditions using glycerol as the sole carbon and energy source. The initial concentration of the nitrogen source was 12.5 g L^{-1} (sodium nitrate), hence the limiting nutrient was presumably different from nitrogen, although this was not clarified (Kawata et al., 2012). These conditions, when applied to cultures grown in glucose (Kawata et al., 2014), did not result in any R3HBA secretion. The glucose concentration decreased from 20% to 6% during the first 36 hours of culture and then remained constant. Thus, in this experiment, a nitrogen shortage was suspected.

When extra nitrate was pulse fed at 24, 36 and 48 h to a culture of *Halomonas* sp. KM-1 with 20% (w/v) glucose, then 40.3 g L^{-1} R3HBA were secreted with a productivity of 0.48 g $L^{-1}h^{-1}$ after a shift from aerobic cultivation for 60 h to microaerobic cultivation for 24 hours. No R3HBA was secreted when no extra nitrate was supplemented (Kawata et al., 2014) indicating that a regulatory mechanism was controlling the activity of the PHB depolymerase, presumably related to the stringent response. Glucose concentration during the depolymerization phase under microaerobic conditions was zero and a decrease in total cell concentration was observed. This behavior is consistent with the depolymerization of the

accumulated PHB with only partial use of the released R3HBA for growth (the calculations show that 79% of the depolymerized PHB was recovered as R3HBA, equivalent to 55 % of the maximum recovery if all the accumulated PHB is transformed to R3HBA). This can be ascribed to the microaerobic conditions applied which limited the use of acetyl-CoA for growth and the regeneration of NAD^+ from NADH. Since NAD^+ is the cofactor used by Hbd, this could explain the high titers of R3HBA. Unfortunately, no nitrate concentrations during the growth or depolymerization phase were reported to ascertain whether it is consumed or not during the microaerobic cultivation. Moreover, PHB was not completely mobilized. Since no information regarding the pH of the culture (or its control) was presented, presumably the lack of complete depolymerization was caused by a decrease in pH.

A new species of *Halomonas*, *Halomonas* sp. OITC1261 was isolated by Yokaryo et al. (2017). Unlike *Halomonas* sp. KM-1, *Halomonas* sp. OITC1261 produces R3HBA under aerobic conditions and, apparently, without the need to supplement with extra nitrogen source once the carbon source is exhausted to promote PHB depolymerization. In fact, the data presented by Yokaryo et al. (2017) showed that R3HBA is produced concomitantly with PHB after approximately 10 hours of cell growth. Presumably, PHB and R3HBA started to accumulate after the exhaustion of the nitrogen source, which could also explain the increase in the dissolved oxygen concentration. It is not clear whether the production of R3HBA occurs through PHB *in-vivo* depolymerization or proceeds directly from (*R*)-3-hydroxybutyryl-CoA or acetoacetate.

2.4.2.2. Production of R3HAs in genetically modified microorganisms

- Mutants of native PHA producers

The exploration of alternative pathways for the production of R3HAs emerges from the recognition of two characteristics found in native PHA producers: (i) depolymerization products can be metabolized [for example, R3HBA is converted to acetoacetate by the Hbd enzyme (Tokiwa & Ugwu, 2007)] and (ii) producing R3HA is a two-stage process where PHA is accumulated and then depolymerized in a subsequent step often requires a change in

media or process conditions. A process for the isolation of *hbd* null mutants was described more than 40 years ago (Lafferty & Heinzle, 1977), including UV mutagenesis, followed by the destruction using antibiotics of the bacteria capable of R3HBA assimilation and the selection of *hbd* null mutants by spread plating of the individuals surviving the treatment with bactericidal.

Ugwu et al. (2008) reported the production of R3HBA in *C. necator* through the acetoacetate pathway induced by random mutation using UV radiation. The mutants achieved a titer of 0.150 g L^{-1} of R3HBA in a 5 L fermenter after 48 hours of cultivation using either glucose or sucrose as carbon source. The concentration of R3HBA was increased by feeding lithium acetoacetate to resting cells of the mutant strain, reaching 0.84 g L^{-1} of R3HBA. The results were interpreted as indicative of a disruption in the *phbB* gene (coding for acetoacetyl-CoA reductase), making this strain unable of PHB accumulation. Ugwu et al. (2008) reasoned that the excess of acetoacetyl-CoA produced under conditions allowing for PHB accumulation was channeled towards R3HBA via acetoacetate.

Using UV mutagenesis, Ugwu et al. (2011) obtained an R3HBA-producing mutant of *A. lata*. When cells of this mutant were resuspended in phosphate buffer containing glucose (1 % v/w), ethylacetoacetate (2% v/v) or (*R,S*)-1,3-butanediol (3 % v/v), the resting cells produced R3HBA at concentrations of 6.5, 7.3 and 8.7 g L^{-1}, respectively.

- Recombinant *E. coli* strain: An approximation of thioesterase shortcut system

An alternative process to produce R3HBA is the use of recombinant methods to express PHA related genes in well-characterized non-PHA producing and fast-growing microorganisms such as *E. coli* (Chen et al., 2013). Lee and co-workers modified *E. coli* strains by inserting two plasmid systems containing the $phaA_{Re}$, $phbB_{Re}$, and $phbC_{Re}$ genes and the $phaZ1_{Re}$ depolymerase from *Ralstonia eutropha* (Lee & Lee, 2003). This design achieved an R3HBA concentration of 9.6 g L^{-1} in 51 hours of fermentation using glucose as a carbon source. Similarly, Shiraki et al. (2006) engineered *E. coli* and *R. eutropha* to express the same enzymes leading to the production of PHB but different depolymerases. The strains compared

were an *R. eutropha* null mutant for *hbd* and a recombinant *E. coli* strain harboring the synthetic PHB operon of *R. eutropha* and an extracellular depolymerase of *Paucimonas lemoignei*. The production of R3HBA by the *hbd* null mutant of *R. eutropha* was found to be dependent on the supply of oxygen, achieving a R3HBA concentration of 3.13 g L^{-1} under anaerobic conditions and concentrations in the range of 0.41–1.04 g L^{-1} under aerobic culture conditions. Presumably, the accumulated PHB was depolymerized under aerobic conditions to a molecule different than R3HBA, such as R3HBA-CoA, or the produced R3HBA was metabolized using pathways not using Hbd. In fact, Shiraki et al. (2006) verified that no *hbd* was expressed and no Hbd was found in the supernatant fraction of cells grown under PHB accumulation conditions. However, it was not verified whether the mutant could grow in R3HBA. On the other hand, the recombinant *E. coli* harboring the PHB operon and the *P. lemoignei* depolymerase reached a concentration of approximately 7.3 g L^{-1} of R3HBA after 100 hours. Since *E. coli* is not a native PHB producer, presumably there were no alternative pathways for R3HBA production or consumption different from the inserted genes (Shiraki et al., 2006).

Alternatively, there are pathways that can be constructed without accumulation and depolymerization of PHB. For example, R3HBA-CoA can be directly hydrolyzed into R3HBA using TesB, a class II thioesterase enzyme that catalyzes the hydrolysis of the CoA moiety from acyl-CoAs (Naggert et al., 1991). Liu et al. (2007) used *E. coli* BW25113 as host for the expression of *phbA* and *phbB* genes from *R. eutropha* and *tesB* from *E. coli*. This strain produced 3.98 g L^{-1} R3HBA in a shake flask culture using 11.4 g L^{-1} of glucose. When using a fed-batch strategy, 12.2 g L^{-1} R3HBA were accumulated in 24 hours. The productivity achieved in this system (0.51 g L^{-1} h^{-1}) is among the highest reported so far for the direct production of R3HBA. Previous to this work, it was well established that TesB was capable of releasing CoA from acyl CoA of C_6-C_{18} carbon length, as well as 3-hydroxyacyl-CoA esters, to their corresponding free fatty acids (Naggert et al., 1991), but not from short-chain length hydroxyacyl-CoA. In this regard, Zheng et al. (2004) reported the production of R3HD from fructose by a recombinant *E. coli*. The recombinant strain contains the *phaG* gene from *P. putida* encoding for (*R*)-3-hydroxydecanoyl-acyl carrier protein-coenzyme A transacylase. PhaG links fatty acid de novo biosynthesis and PHA production by catalyzing

the conversion between (*R*)-3-hydroxydecanoyl-acyl carrier protein and (*R*)-3-hydroxydecanoyl-CoA (Rehm et al., 1998). When the *E. coli* strain containing only PhaG was cultured in shake flasks with 20 g L^{-1} fructose, 0.64 g L^{-1} of R3HD, and 2.11 g L^{-1} of biomass were obtained. The R3HD titer was increased to 1.02 g L^{-1} when a plasmid expressing *tesB* was also inserted into the strain along with *phaG*, suggesting that the activity of TesB in the strain containing only *phaG* was insufficient for efficient hydrolysis of the produced (*R*)-3- hydroxydecanoyl-CoA.

Other authors have studied the production of R3HBA using the native *E. coli* acyl-CoA thioesterases (*fadM*, *tesA*, *tesB*, *ybgC*, *ydiI*, and *yciA*) that also are active with acetyl-CoA as substrate. Interestingly, Guevara-Martínez et al. (2019) working with the recombinant strain *E. coli* AF1000 carrying β-ketothiolase (*t3*) and acetoacetyl-CoA reductase (*rx*) from *Halomonas boliviensis* and overexpressing the glucose-6-phosphate dehydrogenase gene (*zwf*) showed that the deletion of *tesA* or *fadM* resulted in minor decreases in R3HBA production, while deletion of *tesB* and *yciA* decreased the R3HBA titer by 11 and 33 %, respectively. These results suggest that YciA, and not TesB, is the acyl-CoA thioesterase largely responsible for R3HBA production from R3HBA-CoA in *E. coli*.

In the same way, the implementation of the thioesterase shortcut system (TSS) has been shown in other microorganisms. A mutant of *Saccharomyces cerevisiae* strain was modified by the insertion of acetil-CoA C-acetyltransferase (Erg10p from *S. cerevisiae* BY4741), acetoacetyl-CoA reductase (Acr from *C. acetobutylicum* ATCC 824) and TesB (*E. coli* K-12 MG1655). The *S. ceverisiae* mutant was studied in fed-batch cultures using ethanol as a substrate and 12 g L^{-1} of (S)-3-hydroxybutyric acid (S3HBA) was obtained in 200 hours (Yun et al., 2015). In addition, the use of photosynthetic organisms for R3HAs also has been explored. A mutant of *Synechocystis* sp. with the insertion of *phaA*, *phaB1* and *tesB* genes produced a R3HBA titer of 1.84 g L^{-1} in 10 days in photoautotrophic culture (Wang et al., 2018).

3. MATERIALS AND METHODS

3.1. MATERIALS

3.1.1. Chemicals

All chemicals used in this work were of laboratory or reagent grade purity and were from established suppliers, such as Sigma-Aldrich (St. Louis, MO, USA), Thermo Scientific (Waltham, MA, USA) and PanReac AppliChem (Spain).

3.1.2. Bacterial strains

Overview of the bacterial strains used in the course of this work, their genotype and source are described in the Table 1.

Table 1. Genotype and source of bacterial strains

Name	**Genotype**	**Source**
Azohydromonas lata DSM 1123 (strain H-1)	Wild type strain isolate	DSMZ (Germany)
Methylocystis parvus OBBP	Wild type strain isolate	Biopolis S.L. (Valencia, Spain)
Cupriavidus necator H16 DSM 428	Wild type strain isolate	DSMZ (Germany)
C. necator H16 PHB-4 DSM 541	*C. necator* H16 mutant with PhaC truncated protein	DSMZ (Germany)
C. necator Δ*phaC*	*C. necator* H16 knock out for *phaC* gene	This work
C. necator Δ*phaC* Δ*hbd*	*C. necator* H16 knock out for *phaC-hbd* gene	This work

3.1.3. Growth media

Table 2 shows the composition of the growth media used for the mutant and wild type strains.

Table 2. Growth media for the bacterial strains

Name	Components in gram per liter	Bacteria	Reference
AL1	1.5 KH_2PO_4, 9 $Na_2HPO_4 \times 12\ H_2O$, 0.2 $MgSO_4 \times 7\ H_2O$, 0.01 $CaCl_2 \times 2\ H_2O$, 0.1 citric acid and 1 mL of trace element solution: 20 $FeSO_4 \times 7\ H_2O$, 0.3 H_3BO_4, 0.2 $CoCl_2 \times 6\ H_2O$, 0.03 $ZnSO_4 \times 7\ H_2O$, 0.03 $MnCl_2 \times 4\ H_2O$, 0.03 $(NH_4)_6Mo_7O_{24} \times 4\ H_2O$, 0.03 $NiSO_4 \times 7\ H_2O$ and 0.01 $CuSO_4 \times 5\ H_2O$	*A. lata* DSM 1123	Wang & Lee, 1997
NMS	1 KNO_3, 1.1 $MgSO_4 \times 7\ H_2O$, 0.8 $Na_2HPO_4 \times 12\ H_2O$, 0.26 KH_2PO_4 and 0.2 $CaCl_2 \times 2\ H_2O$ and 1 mL of trace element solution: 0.3 $Na_2MoO_4 \times 2\ H_2O$, 0.3 $Na_2EDTA \times 2\ H_2O$, 1 $CuSO_4 \times 5H_2O$, 0.5 $FeSO_4 \times 7\ H_2O$, 0.4 $ZnSO_4 \times 7\ H_2O$, 0.03 $CoCl_2$, 0.02 $MnCl_2 \times 4\ H_2O$, 0.015 H_3BO_3, 0.01 $NiCl_2 \times 6\ H_2O$ and 0.38 Fe-EDTA	*M. parvus* OBBP	Rodríguez et al., 2022
NFMS	Identical to NMS medium except without KNO_3	*M. parvus* OBBP	Rodríguez et al., 2022
RE1	20 fructose, 1 $(NH_4)2SO_4$, 1.5 KH_2PO_4, 6.7 $Na_2HPO_4 \times 7\ H_2O$, 0.2 $MgSO_4 \times 7\ H_2O$, 1 mL of trace element solution: 10 $FeSO_4 \times 7\ H_2O$, 2.25 $ZnSO_4 \times 7\ H_2O$, 1 $CuSO_4 \times 5\ H_2O$, 0.58 $MnCl_2 \times 4H_2O$, 2 $CaCl_2 \times 2H_2O$, 0.14 $Na_2B_4O_7 \times 10\ H_2O$, 0.16 H_3BO_3 and 35% HCl 10 mL	*C. necator* H16 DSM 428, *C. necator* 541, *C. necator* Δ*phaC*, *C. necator* Δ*phaC* Δ*hbd*	Adapted from Kim et al., 1994
SOC/ SOB	20 Tryptone, 5 yeast extract, 0.5 NaCl, 10 mL of 250 mM solution of KCl and 2 M $MgCl_2$. For SOC is identical to SOB medium except with 1 M glucose solution	*E. coli* DH5α and *E. coli* S17-1	Hanahan, 1983
Luria Bertani (LB)	10 Tryptone, 5 yeast extract, 10 NaCl	*E. coli* and *C. necator* strains	Bertani, 1951

3.1.4. Primers

All primers used in this work (Table 3 and Table II-1, APPENDIX II) were designed in SnapGene® and ordered to IDT (USA) via Fermelo, Chile. Primers were received as lyophilized pellets and the stock solutions were prepared at 100 μM in Mili-Q water, DNAase free water and were stored at −20 °C. Then, primer working stocks were prepared as 10 μM concentrated solutions with double-distilled water and stored at −20 °C.

Table 3. Primers and their sequences used for the construction of gene knock outs

Primers	**Sequence 5'-3'**
pT18mobsacB-MCS_deleted_fwd_phac	cgcatgggcgatgccaagctcaagcttggcactggccgtc
pT18mobsacB-MCS_deleted_rev_phac	gcgctgatgatggcgatcacgtaatcatgtcatagctgtttcctgtgtg
phaC1_upstream_fwd	aacagctatgacatgattacgtgatcgccatcatcagcgc
phaC1_upstream_rev	cgccggcactcatgcaagcggatttgattgtctctctgccgtc
phaC1_downstream_fwd	ggcagagagacaatcaaatccgcttgcatgagtgccggcg
phaC1_downstream_rev	gacggccagtgccaagcttgagcttggcatcgcccatgcg
pT18mobSac_MCS_deleted_fwd_hbd	gctgattgcgcggctcaacgcaagcttggcactggccgtc
pT18mobSac_MCS_deleted_rev_hbd	gcaggcaggctgacctgcgggtaatcatgtcatagctgtttcctgtgtg
hbdH1_downstream_fwd	aacagctatgacatgattacccgcaggtcagcctgcctgc
hbdH1_downstream_rev	ttctctcgacggaggcttacggagcaaacgatgcaacgacgca
hbdH1_upstream_fwd	gtcgttgcatcgtttgctccgtaagcctccgtcgagagaaagga
hbdH1_upstream_rev	gacggccagtgccaagcttgcgttgagccgcgcaatcagc

3.1.5. *E. coli* strains and plasmids

Three vector backbones, acquired from Addgene, were used for the genetic modifications. pBBR1MCS-2, a low copy vector was used for the expression of *tesB (E. coli* K12) in *C. necator* H16. pAWP89 vector was used for the expression of *tesB* in *M. parvus* OBBP. The pT18mobsacB suicide vector was used for the construction and knock-out of *phaC1*, *hbd* by matting with *E. coli* S17-1 in *C. necator* H16. The *E. coli* strains DH5α or S17-1 were used for the bacterial transformation with the plasmids constructed. Table 4 gives an overview of the most important features of the plasmids, *E. coli* and mutant strains used or constructed in the course of this work.

Table 4. Vector backbones and their relevant genotype

Strains and plasmids	**Relevant genotype**	**Source**
E. coli DH5α	F^-, *endA1*, *hsdR17*, (rk^-, mk^+), *supE44*, *thi-1*, λ^-, *recA1*, *gyrA96*, *ΔlacU169* (*Φ80 lacZ ΔM15*)	NEB
E. coli S17-1 DSM 9079	*thi pro hsdR hsdM* $^+$*recA RP4-2-Tc*::*Mu*::*Tn7 λpir*	DSMZ (Germany)
pBBR1MCS-2	*lacPOZ*, *mobRP4*, *Kanamycin resistance* (km^R)	Addgene
pAWP89	*IncP*, *dTomato* by the tac promoter, km^R	Addgene
pBAD24-sfGFPx2	super folder (sf) *GFP*, *Ampicilin resistance* (Amp^R)	Addgene
pT18*mobsac*B	pMB1 *mob sacB*; Suc^S, Tetraciclina (Tc^R)	Addgene
pL51	pT18mobsacB-*ΔphaC* plasmid with phaC upstream and downstream	This work
pL52	from pL51 with hbd upstream and downstream, pT18mobsacB-*ΔphaC-Δhbd*	This work

3.2. METHODS

3.2.1. Preliminary depolymerization and viability assay in PHB accumulated cells of *A. lata* DSM 1123

Flask cultures of *A. lata* DSM 1123 were carried out for PHB accumulation in a shaking incubator with 1.0 L Erlenmeyer Flask (E-flask) containing 200 mL of AL1 medium with 10 g L^{-1} glucose and 0.5 g L^{-1} of (NH_4) SO_4 at 30°C and 200 rpm for 20 hours. Then, the cells were washed with phosphate buffer and were resuspended in phosphate buffer 50 mM to test the depolymerization at three pHs, 4, 5 and 7. A hot plate stirrer was adapted with a thermoregulated bath at 30°C that containing inside a beaker of 100 mL with 20 mL of PHB accumulated cell suspension at pH of 4, 5 or 7 (two biological replicates) for depolymerization. The pH was controlled by addition of NaOH solution (4 M) to provide a pH constant condition. PHB and R3HBA were measured at the end of the experiment.

To test the viability of the cells at the end of the depolymerization phase, 100 ul of cells suspension were spread on Petri dishes with AL1 agar (AL1 media with 12 g L^{-1}) and incubated at 30 °C for 3 days. The growth was measured by colony counting.

3.2.2. Bioreactor experiments with *A. lata*

3.2.2.1. Chemostat cultivation

Chemostats experiments were performed in a 3.6 L (total volume, 2.3 L working volume) fermenter (Labfors 5, Infors-HT, Basel, Switzerland) equipped with pH, dissolved oxygen (DO) and temperature controllers. Temperature was maintained at 30 °C and water evaporated from the broth was condensed using a water-cooled condenser. DO was controlled above 40% of oxygen saturation in air (except for the oxygen-limited cultures where 1 vvm air and 250 rpm were used) by varying the stirring speed between 300 and 600 rpm and the gas mixture between air and pure oxygen in a cascade control at 2 vvm. Gas

flows were controlled by mass flow controllers and refer to normal conditions. The pH was maintained at 6.8 by the addition of a 2 M NaOH solution. The culture medium was the mineral salt medium AL2 (Wang & Lee, 1997) with 10 g L^{-1} glucose as the carbon and energy source.

Nitrogen-limited, oxygen-limited and glucose-limited chemostats were performed by altering the inlet medium composition or the oxygen transfer rate. The nitrogen-limited feeding medium contained 0.5 g L^{-1} ammonium sulfate while 3 g L^{-1} was used for the glucose and oxygen-limited conditions. Dilution rates ranging from 0.05 to 0.4 h^{-1} were applied under each nutrient limitation condition. Changes between dilution rates were randomized. Cultures were sampled after achieving steady-state (at least after 4 residence times) and checking for signs of contamination using optical microscopy and Raman spectroscopy.

3.2.2.2. Two-stage chemostat for *in-vivo* depolymerization and R3HBA production

A bioreactor was built using a 200 mL Schott flask equipped with a temperature control system, a pH control system, a U-tube for level control and agitation provided by a magnetic stirrer. This bioreactor was connected to the discharge of a nitrogen-limited chemostat culture operated at a D=0.2 h^{-1} and pH 6.8. The depolymerization reactor was operated at pH 4 with a 30 min residence time for 300 min.

3.2.3. Optimization of PHB depolymerization in *M. parvus*

The experiments were performed batch wise using PHB containing *M. parvus* biomass in 125 mL serum bottles (working volume of 45 mL) crimp sealed (three biological replicates). The bottles were incubated at 30 °C (except Test 3) and 230 rpm in an orbital shaker.

Test 1: Influence of the presence of nitrate and O_2 and pH

The assays were performed with NMS and NFMS media at both pH 4 and pH 11 in triplicate for 48 hours. All cultures were inoculated with 10 mL of concentrated *M. parvus* culture previously grown in NFMS for 10 days (1.3 gTSS L^{-1} with 51.4% of PHB) and were incubated for two days under an O_2:CH_4 headspace (66.7:33.3%) and a He:CH_4 atmosphere (66.7:33.3%). A control test at pH 7 under a O_2: CH_4 headspace (66.7:33.3%) and NMS medium was also carried out. Culture samples were collected periodically for the quantification of the R3HBA concentration. Cell dry weights (CDW), total nitrogen, PHAs and pH were determined at the beginning and end of the experiment.

Test 2: Optimization of pH during PHB depolymerization

PHB depolymerization under an O_2:CH_4 atmosphere (66.7:33.3 %) was assessed in triplicate at pH 10, pH 11 and pH 12 with NMS medium as above described for 48 hours. The pH of the cultures was monitored three times per day and manually adjusted using 5 M NaOH, while the concentration of extracellular R3HBA was quantified once per day. The biomass concentration (estimated as CDW) and PHB cells content were determined at the beginning and the end of the experiment.

Test 3: Influence of temperature on the kinetic of PHB depolymerization

PHB depolymerization at pH 11 on NMS medium was assessed in triplicate at 25 and 35 °C for 3 hours using fresh *M. parvus* with a concentration and PHB cell content of 4.17 gCDW L^{-1} and 44.7 %. The determination of extracellular R3HBA concentration was conducted at 15, 30, 60, 120 and 180 min. At the end of the experiment, cell viability was evaluated using the pellets obtained after centrifugation of the biomass from depolymerized cells. Cell viability tests were performed at 25 °C in 2.2 L serum bottles with a working volume of 0.4 L of both NMS and NFMS medium. The bottles were capped with aluminum caps and chlorobutyl rubber stoppers under and O_2:CH_4 atmosphere (66.7:33.3 %) and

incubated as above described until complete CH_4 depletion. CDW, CH_4, O_2 and CO_2 concentrations were periodically measured.

Test 4: Influence of the initial R3HBA concentration and aeration rate

The influence of the oxygen mass transfer rate on PHB depolymerization and R3HBA yield was investigated in E-flasks incubated at 200 rpm and 30 °C in an orbital shaker for 72 hours. The lowest oxygen mass transfer rate was achieved in 100 mL E-flasks containing 100 mL of medium, while the highest oxygen transfer rate was reached in 250 mL E-flasks containing 50 mL of cultivation broth. An intermediate condition was tested in 100 mL E-flasks containing 50 mL of cultivation broth. The initial biomass concentration and PHB content of the cell suspension was 0.51 ± 0.005 gCDW L^{-1} and 31.9 ± 1.9% PHB, respectively. The experiments were conducted in duplicate.

The potential inhibitory effect of extracellular R3HBA over PHB depolymerization was investigated using R3HBA produced in-house following the procedure described by Lee et al. (1999). Then, *M. parvus* cells containing PHB were washed and resuspended in NMS medium at pH 11 supplemented with R3HBA at concentrations of 0, 120, 330 and 650 mg L^{-1}. Cell incubation was performed in 100 mL E-flasks containing 50 mL of cell suspension with the corresponding R3HBA concentration at 30 °C and 200 rpm in an orbital shaker. Culture samples were collected at 0, 3, 6, 48 and 72 hours for R3HBA and crotonic acid quantification. The biomass and PHB cell content were monitored at the beginning and the end of experiments.

- R3HBA production by *A. lata* DSM 1123

A. lata DSM 1123 was cultivated from a frozen stock culture in a nutrient agar plate. A single colony was picked and used to inoculate a 500 mL E-flask with 100 mL of AL1 medium. This culture served as the inoculum for a batch bioreactor cultivation of this bacterium in a Labfors 5 bioreactor (Infors HT, Switzerland). The bioreactor was operated with 1 L of AL2

(Wang & Lee, 1997) medium containing an initial glucose concentration of 30 g L^{-1} and an initial ammonium sulfate concentration of 2 g L^{-1}. Dissolved oxygen was maintained above 40 % saturation by varying the stirring speed up to 700 rpm at 1 vvm air. When necessary, pure oxygen was automatically mixed with the inlet air flow under a cascade control. After 24 hours of cultivation, approximately 12.0 gCDWL^{-1} of biomass were retrieved containing a PHB cell content of 75%. Cells were collected by centrifugation, washed twice with distilled water and resuspended in water at a concentration of approximately 120 gCDW L^{-1}. PHB depolymerization was started by adjusting the pH to 4 with HCl and lasted for one hour. The pH was controlled at 4 using 2 M NaOH. Following the purification procedure outlined in Lee et al. (1999), a solution containing 34.2 g L^{-1} of sodium (*R*)-3-hydroxybutyrate was obtained for the study of inhibitory effect of extracellular R3HBA.

3.2.4. Biomass quantification and culture supernatant collection and analysis

For the estimation of biomass concentration, aliquots of culture were centrifuged (2470 RCF, 10 min) to separate a cell-free supernatant and a biomass pellet. The pellet was washed twice with Type II water, dried and used to determine the cell dry weight concentration. Culture supernatants were obtained by centrifuging broth samples in Eppendorf tubes at 17000 RCF for 1 min at 4 °C and used immediately or stored at −20 °C. Glucose concentration was determined in culture supernatants and feed media using an enzymatic assay (D-glucose assay kit GOPOD, Megazyme, Ireland) according to the manufacturer's instructions or High-Performance Liquid Chromatography (HPLC) analysis (see analytical methods). The concentration of NH_4^+ was determined using an ammonium-ion electrode (EW-27504-00, Cole-Parmer, USA).

3.2.5. Raman spectroscopy

Raman analyses of dry biomass harvested from the cultures, washed twice with Type II water and dried at 70 °C on a Raman grade CaF_2 supports (Crystan, UK) were performed using a Horiba XploRA™ PLUS Raman microscope with a ×50 objective lens. A diode laser of 532 nm was used, and the collected Raman radiation was dispersed with a 1200 lines

(750 nm) grating. All spectra were obtained in the spectral window of 600-1800 cm^{-1} using 60 seconds of acquisition time and 2 accumulations. The Raman spectra were baseline corrected and normalized using the LabSpec 6 suite. The analysis of the characteristic frequencies and intensities was performed using previously reported Raman spectra (Samek et al., 2016) and the spectra of pure PHB (sc-255438, Santa Cruz Biotechnology).

3.2.6. Analytical procedures

CH_4, CO_2 and O_2 gas concentrations were measured in a gas chromatograph (GC) coupled with a Thermal Conductivity Detector (Bruker 430 GC-TCD, Bruker Corporation, USA) following the method described by Estrada et al. (2014). The optical density of the cultures samples was measured by spectrophotometry at 600 nm (UV-2550, Shimadzu, Japan). CDW and pH were analyzed according to Rodríguez et al. (2020). PHB was quantified via Gas Chromatography-Mass Spectrometry (GC–MS) (Rodríguez et al., 2020) or GC-FID (Scott et al., 2021). The concentration of R3HBA was determined using a commercial R3HBA Assay Kit (Megazyme, Ireland) according to manufacturer's protocol or using HPLC with a UV–Vis detector at 210 nm and a refractive index detector (Prominence, Shimadzu) according to Scott et al. (2021). Citrate, succinate, pyruvate, acetate, glucose, malate and crotonic acids (Sigma-Aldrich catalog number, 113018) were quantified using the HPLC-UV-IR method described by Scott et al. (2021). The organic acids standard was purchased from Biorad (catalog number, 125–0586).

3.2.7. Vector construction for *tesB* expression

For the construction of the expression vector for *C. necator* H16, *tesB* was amplified from the synthesized pUC57 plasmid with *tesB* gene fragment (*E. coli* K12) no codon optimized. The RBS and linker sequences used were tested and described by (Lu et al., 2012). The terminator fragment was amplified from the pBAD24-sfGFPx2 plasmid (450 pb) following the plasmid construction strategy described by (Crépin et al, 2016). The fragments were assembled in pBBR1MCS2 plasmid using Gibson Assembly.

The construction of the expression vector for *M. parvus* was assembled in pAWP89 plasmid by the insertion of a promoter and terminator fragments (Section 0, APPENDIX II) from the PHB synthesis of *M. parvus* and *tesB* gene (*E. coli* K12). These were taken from the synthesized pUC57-kan plasmid containing these fragments. All plasmid assemblies were achieved by one-step isothermal DNA assembly protocol (Gibson et al., 2009).

Briefly, the assembly reaction was carried out by mixing the insert(s) and vector backbone with 5 µL Gibson Assembly® Master Mix (New England Biolabs, Ipswich, MA, USA) and Mili-Q and DNase free water to a total reaction volume of 10 µL. The amount of each insert to be used was calculated following the next equation, where the units of vector and insert amount are in nanograms, vector and insert length in kb.

$$\begin{pmatrix}\text{Insert}\\ \text{amount}\end{pmatrix} = \left(\frac{\text{Vector amount}}{\text{Vector length}}\right)\begin{pmatrix}\text{Insert}\\ \text{length}\end{pmatrix}\begin{pmatrix}\text{Molar ratio}\\ \text{insert : vector}\end{pmatrix}$$

Around 50-100 ng of vector backbone were used and a molar insert-vector ratio of 3:1 was used for the assembly of up to three or four fragments (including the vector). The Gibson assembly reaction was incubated for 1 hour at 50 °C. Then, the reactions were stored at 20 °C for subsequent transformations.

3.2.8. Gene knock-out via pT18mobsacB for *C. necator* H16

Two homologous templates which were about 500 bp upstream and downstream of *phaC* or *hbd* were amplified from *C. necator* H16 by colony PCR. The fragments were cloned in the pT18mobsacB plasmid backbone (pL51 and pL52) via Gibson assembly (Gibson et al., 2009) and transformed into *E. coli* S17-1 by electroporation, then identified and transferred to *C. necator* H16 via conjugation. Single colonies were cultured in LB without NaCl but with 15 mg L^{-1} gentamicin and 20 mg L^{-1} tetracycline at 30 °C. A pair of primers with one bound to the genome and another to the plasmid was used for colony PCR to identify strains with the knockout plasmid integrated. Then confirmed colonies were incubated for the second recombination in LB without NaCl and tetracycline, but with 50 g L^{-1} sucrose and 15 mg L^{-1}

gentamicin at 30 °C for 72 hours or until visible colonies appear. Then, colony PCR was used for the screening of the *C. necator* colony knock out for *phaC* or *hbd* using the primers listed in Table 3.

3.2.9. Standard polymerase chain reaction

The mixture used for the standard PCR reaction in this work was the GoTaq Green mastermix polymerase from Promega®. The thermostable Phusion™ High-Fidelity DNA polymerase from Thermo Fisher scientific was used for Gibson PCRs applications. Once prepared, the reaction mixture was placed in a PCR thermocycler and a PCR program was run on the machine following the technical specification of the PCR master mix manufacturer. Time and temperature required for each step of the program were carefully adapted to allow for the successful amplification of the desired target fragment. For Phusion High-Fidelity DNA polymerase the denaturation temperature was set to 98 °C and the initial denaturation was carried out for 30 seconds for all plasmid-based templates. The elongation time was calculated based on the desired fragment length. After completion of the PCR, the amplified sequences were recovered using agarose gel electrophoresis and subsequent gel extraction and purification with GeneJET extraction kit (Thermo Fisher scientific).

3.2.10. Colony PCR

Colony PCR was used to amplify the desired target sequence from a bacterial colony without previous purification of the DNA from the bacterial cells. Here, colony PCRs were mostly carried out to assess the transformation status of positive colony indicator after transformation.

A bacterial colony was picked from an agar plate using the tip of a sterile white 10 µL pipette tip, before resuspending it in 10 µL double distilled water. Next, 1 µL of the suspension were transferred into a PCR tube and were incubated at 95 °C for 5 min at 90 °C. After incubation, 1 µL of the suspension was added to PCR mastermix.

3.2.11. Agarose gel electrophoresis

Agarose gel electrophoresis was carried out to separate DNA fragments and vectors according to their respective sizes in an electric field using 1% agarose gels (w/v). All gels were supplemented with GelRed® Nucleic Acid Gel Stain and prepared with TAE 1X. Samples were mixed with Gel loading purple dye (New England Biolabs, Ipswich, MA, USA) and 1-3 µL were loaded into the pockets. In addition, 0.5 µL of 1 kb DNA ladder (Bionner, Korea) were loaded into one well on the gel to estimate the size and quantity of individual fragments and plasmids. A voltage of 90 V was applied for the electrophoreses. After 40 min, the electrophoresis was stopped, and the agarose gel was recovered to visualize DNA fragments under ultraviolet light in Firereader V6 transilluminator.

3.2.12. Preparation of electrocompetent *E. coli* cells

To create electrocompetent *E. coli* cells, the S17-1 strain was streaked out on LB agar plate. One picked colony was inoculated in a 50 mL sterile E-flask (working volume 20 mL of LB-medium) at 37 °C and 200 rpm overnight. After growth for 14 hours, a calculated enough volume for 1:50 dilution of pre-culture was used for inoculating a 500 mL sterile E-flask (working volume of 100 mL) at 37 °C and 200 rpm until reach ingan optical density (OD_{600}) of 0.35-0.40 after about 3-4 hours of growth time. Next, the main culture was chilled into two 50 mL centrifuge tubes which had been pre-cooled on ice for 5 min. After 10 min on ice, the cells were harvested by 5 min centrifugation at 4000g and room temperature. The supernatant was decanted and the pellets were resuspended in 50 mL chilled double distilled water (4 °C). The tubes were centrifuged at the same condition mentioned above. The same procedure was repeated once more with 20 mL and the pellet was resuspended a final volume of 1 mL of ice-cold 10% glycerol. The suspension OD_{600} was measured and aliquoted in fraction of 50 µL in chilled tubes to be frozen at −80°C.

3.2.13. Transformation of *E. coli* cells

For the transformation of electrocompetent *E. coli* cells with newly constructed plasmids, a 50 µL aliquot of electrocompetent cells was thawed on ice. Once completed thawed, 1-2 µL of Gibson assembly reaction mixture containing the constructed plasmid, were added to the cells. A 0.2 mm pre-cooled electroporation cuvette with cells mixture was placed in an electroporator from Bio-rad and a pulse of 2-5 kV was sent through the cuvette. Immediately after electroporation, 900 µL of SOC medium were added and carefully resuspending by pipetting was undertaken. The cells solution was recovered and transferred into a sterile 1.5 mL microcentrifuge tube and then incubated for 1 hour at 37 °C and 200 rpm.

After incubation, 100 and 900 µL fractions were taken from the transformed cells solution and were placed on individual LB-agar plates supplemented with the respective antibiotic, lactose (1 g L^{-1}) and X- gal (20 µg L^{-1}) for blue-white screening of bacterial colonies. The plates were incubated at 37 °C for 24-48 hours. White colonies were checked using colony PCR. The transformation of chemocompetent *E. coli* DH5α cells was followed by the technical specifications of NEB BioLabs and cultured by the instructions above mentioned.

3.2.14. Characterization of *C. necator* H16 and mutant strains

Glycerol stocks of *C. necator* H16, *C. necator* Δ*phaC*, *C. necator* Δ*phaC* Δ*hbd* and *C. necator* 541 were streaked on a LB agar petri dish without NaCl and incubated at 30 °C. After 24-48 hours one colony was used to inoculate a pre-seed 100 mL E-flask with 20 mL of RE1 mineral medium and incubated for 15-20 hours at 30°C and 250 rpm. This seed culture was used to inoculate a 500 mL E-flask with 100 mL RE1 and incubated for 48 hours. Culture samples were collected periodically for the quantification of biomass, fructose, R3HBA, pyruvate and PHB. Three biological replicates were performed for each strain.

For *C. necator* H16 a depolymerization test was assayed in order to see the R3HBA production at different pHs conditions as described by Lee et al. (1999). At the end of the

48 hours of culture, accumulated PHB cell of *C. necator* H16 were washed two times with mineral RE1 medium (without fructose) and resuspended in E-flasks of 100 mL with a working volume of 20 mL with mineral medium (without fructose) at 3, 4, 7 and 10 pHs. The depolymerization cultures were incubated at 30°C and 250 rpm for 24 hours. CDW, PHB, R3HBA and pH were determined at the beginning and end of the experiment.

3.2.15. Calculations

i). Chemostat cultures

Each chemostat culture is presented as a single data point corresponding to the mean of two or three analytical determinations, along with its standard deviation. Therefore, each data point at a given dilution rate is a biological replicate. Percentages are mass-based and CDW refer to residual (active or PHB free) biomass.

The analysis of the chemostat cultures was carried out using the standard definitions of specific uptake rates and specific productivities following equations reported in Table 5, where D is the dilution rate (h^{-1}), F the PHB fraction (gPHB g total CDW^{-1}), X_T is the total CDW biomass concentration (g L^{-1}), S_o and S the inlet and outlet glucose concentration, C_{AS} the ammonium sulfate concentration (g L^{-1}) and V the reactor volume. Error propagation was performed using standard formulas based on standard deviations and its respective defining equation, where $\|\mathbf{v}\|$ is the Euclidean norm of vector $\mathbf{v}$. The following formulas allow the calculation of an error that is latter plotted as an error bar.

Table 5. Equations defining specific uptakes and production rates

Description	Equation and experimental error propagated
Glucose uptake rate [g gCDW^{-1} h^{-1}]	$\frac{1000}{180} D \frac{S_o - S}{(1-F)X_T}$ $\text{Error} = \frac{50}{9} D \left\| \frac{\Delta S_o}{(1-F)X_T}, \ \frac{\Delta S}{(1-F)X_T}, \ \frac{(S_o - S)\Delta F}{(1-F)^2 X_T}, \ \frac{(S_o - S)\Delta X_T}{(F-1){X_T}^2} \right\|$
Ammonium uptake rate [mmol gCDW^{-1} h^{-1}]	$\frac{1000 \cdot 2}{132.14} D \frac{3 - C_{AS}}{(1-F)X_T}$ $\text{Error} = 6.40738 \, D \left\| \frac{(C_{AS} - 3)\Delta X_T}{(F-1){X_T}^2}, \ \frac{(C_{AS} - 3)\Delta F}{(1-F)^2 X_T}, \ \frac{\Delta C_{AS}}{(F-1)X_T} \right\|$
PHB production rate [g gCDW^{-1} h^{-1}]	$\frac{1000}{104} D \frac{F}{1-F}$ $\text{Error} = \frac{125}{13} \left\| \frac{D \, \Delta F}{(1-F)^2} \right\|$
PHB free or residual biomass [g L^{-1}]	$(1-F)X_T$ $\text{Error} = \|(1-F)\Delta X_T, \ X_T \Delta F\|$

ii). PHB depolymerization and R3HBA yields calculation used in *M. parvus* experiments

The R3HBA molar yield (Y_{R3HBA}) was calculated as the ratio of the moles of R3HBA excreted and the moles of PHB consumed, considering that PHB hydrolysis consumes one mol of water per mol of R3HBA produced. Then PHB depolymerization percentage conversion (C_{PHB}) and Y_{R3HBA} were calculated the following Eq. 1 and 2.

$$C_{PHB} = \frac{X_{PHB}^i - X_{PHB}^f}{X_{PHB}^i} \times 100 \qquad \text{Eq. 1}$$

$$Y_{R3HBA} = \left(\frac{104.1 - 18.01}{104.1}\right) \frac{X_{R3HBA}^f - X_{R3HBA}^i}{X_{PHB}^i - X_{PHB}^f} \times 100 \qquad \text{Eq. 2}$$

Where X_{PHB}^{i} and X_{PHB}^{f} correspond to the initial and final PHB concentrations (g L^{-1}) respectively, and X_{R3HBA}^{i} and X_{R3HBA}^{f} represent the initial and final concentrations of R3HBA (g L^{-1}) respectively. A similar calculation was used for the crotonic acid yield (Y_{crot}). The conversion of PHB to R3HBA can be calculated by Eq.3.

$$C_{PHB,\ R3HBA} = 0.01\ Y_{R3HBA} \cdot C_{PHB} \qquad \text{Eq. 3}$$

Finally, the specific R3HBA release rate per gram of initial intracellular PHB (q_{R3HBA}) was calculated as follows:

$$q_{R3HBA} = \frac{m}{X_{PHB}^{i}} \qquad \text{Eq. 4}$$

Where m is the slope of the line whose independent and dependent variables are the depolymerization time and R3HBA concentration (mg L^{-1}) respectively.

4. RESULTS AND DISCUSSIONS

4.1. EFFECTS OF NUTRIENT LIMITATION AND DILUTION RATE ON PHB AND BIOMASS PRODUCTION IN *A. lata*

Part of the results presented in this section, were published in the following paper "Two internal bottlenecks cause the overflow metabolism leading to poly(3-hydroxybutyrate) production in *Azohydromonas lata* DSM1123" with DOI: https://10.1016/j.jece.2021.105665

A. lata DSM 1123 was grown in chemostat culture at dilution rates ranging from 0.05 to 0.4 h^{-1} with mineral medium and glucose as the sole carbon and energy source. Panels A-F in Figure 1 show culture parameters and their relationship with the dilution rate under nitrogen, oxygen or glucose limiting conditions.

4.1.1. Nitrogen limited-chemostat culture

The PHB content under nitrogen limitation slightly decreases from an average of 75 % at a D=0.05 h^{-1} to 65% at the maximum D=0.4 h^{-1} (Figure 1, panel A), a slight decrease in sharp contrast to nitrogen-limited chemostats of *C. necator*, where a linear decrease from a PHB content of 80% to less than 10% was reported as the dilution rate increases from 0.025 to 0.4 h^{-1} (Henderson & Jones, 1997). The glucose and ammonium sulfate concentration in the chemostat runs (Figure 1, panels C and D) is consistent with an ammonium limited condition: glucose was present at every dilution rate and the titer of ammonium sulfate was negligible at D < 0.2 h^{-1}. As the growth rate increases, the overall PHB yield on glucose decreases from 0.41 ± 0.02 (D=0.05 h^{-1}) to 0.30 ± 0.03 gPHB g $glucose^{-1}$ (D=0.4 h^{-1}).

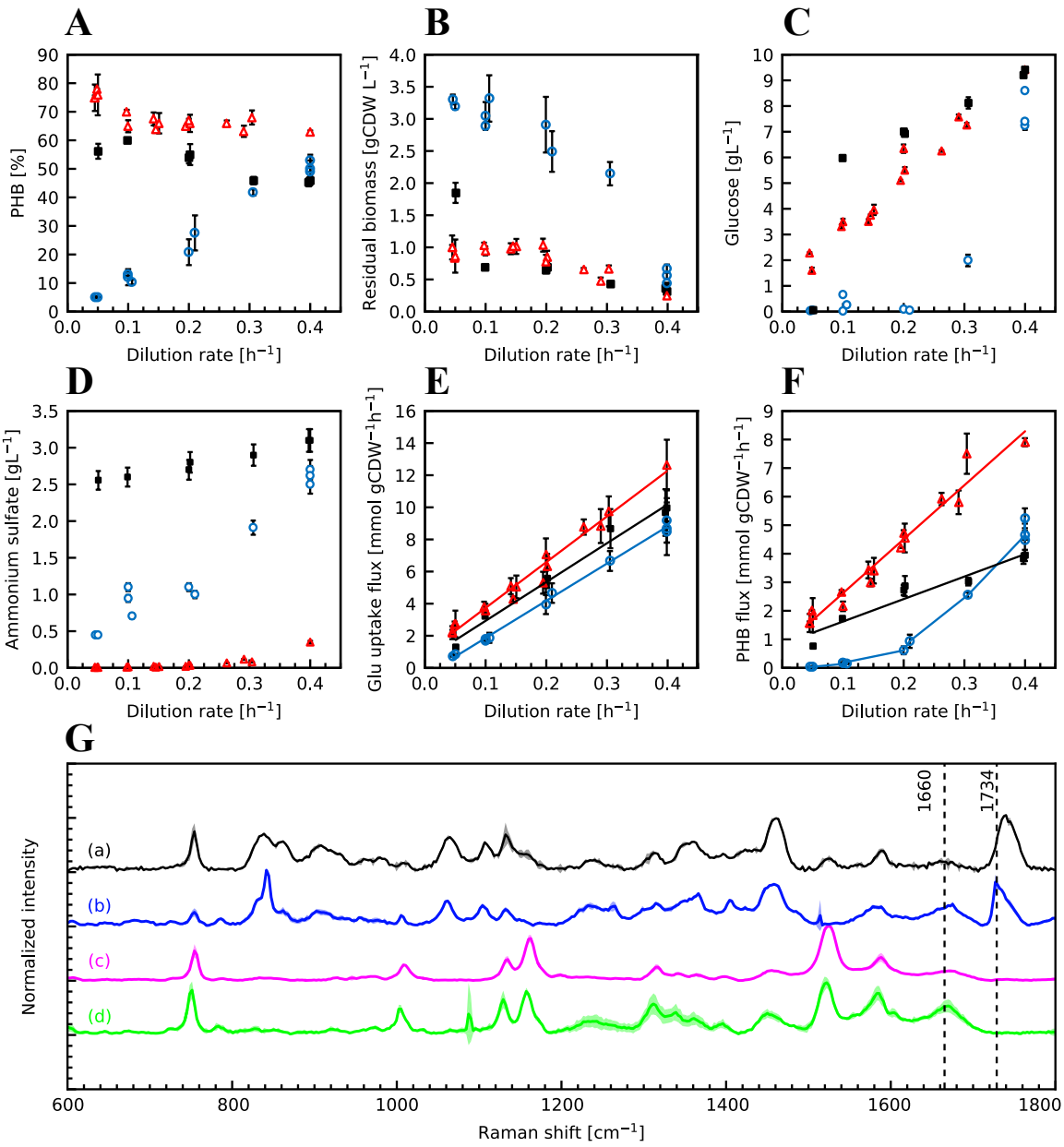

Figure 1. **Effects of the dilution rate and nutrient limitation in chemostat culture on PHB accumulation**. (A), residual (PHB free) biomass (B), glucose (C) and ammonium sulfate (D) concentration, specific glucose uptake rate per gram of residual biomass (E) and specific PHB accumulation rate per gram of residual biomass (F). Red triangles correspond to nitrogen-limited chemostats, black squares to oxygen-limited chemostats and blue circles to glucose-limited chemostats. Raman spectra of washed and dried biomass samples withdrawn from (G): (a) nitrogen-limited chemostat at D=0.05 h^{-1}, (b), (c) and (d) oxygen-limited chemostat at dilution rates of 0.3, 0.05 and 0.1 h^{-1}, respectively. The shaded area represents the standard deviation.

The maximum specific PHB accumulation rate (Figure 1, panel F) was found under nitrogen limitation at a D of 0.4 h^{-1} corresponding to 7.9 ± 0.14 mmol $gCDW^{-1}$ h^{-1} (equivalent to 0.69 gPHB $gCDW^{-1}$ h^{-1}). This value agrees with the instantaneous specific PHB synthesis rate reported by Wang and Lee (1997), with a maximum of 0.87 gPHB $gCDW^{-1}$ h^{-1} after the onset of nitrogen limitation in a batch culture of *A. lata* DSM1123 using sucrose as carbon and energy source. The difference can be explained by the increased specific sucrose uptake rate compared to the glucose uptake rate reported for this microorganism (Wang & Lee, 1997).

Comparatively, the PHB flux values found in this work are much higher, especially for the nitrogen-limited cultures, than for those found in nitrogen-limited chemostats with glucose as the carbon source for *C. necator* [0.15 gPHB $gCDW^{-1}$ h^{-1} (Atlić et al., 2011) or 0.23 gPHB $gCDW^{-1}$ h^{-1} (Henderson & Jones, 1997). A maximum of 10.6 mM of succinic acid was measured at a D=0.1 h^{-1} and 2 mM of malic acid at a D=0.2 h^{-1} (the complete set of organic acid measurements is presented in Table I-1, APPENDIX I).

4.1.2. Oxygen limited-chemostat cultures

PHB accumulation in chemostats under oxygen limitation showed a decrease of the PHB fraction at low dilution rates compared with the results obtained under ammonia-limited conditions (Figure 1, panel A).

Glucose and ammonium sulfate titers are consistent with an oxygen limited chemostat. PHB yield on glucose was 0.27 ± 0.03 g PHB g $glucose^{-1}$, irrespectively of the dilution rate. PHB content reached a maximum of 60% at a D=0.1 h^{-1} decreasing to 46% at a D=0.4 h^{-1}. Using a kinetic model for PHB production and cell growth in *A. lata* DSM 1123, Papapostolou et al. (2019) reported an intracellular PHB content of 43.3% at the end of a 43 hours fed-batch culture, where the dissolved oxygen concentration was maintained at 6% of its saturation value. A maximum of 7.9 mM succinic acid at a D=0.2 h^{-1} and 1.6 mM of malic acid at a D=0.1 h^{-1} were measured (see Table I-1, APPENDIX I).

4.1.3. Glucose-limited chemostat culture

The trends of PHB accumulation under oxygen and nitrogen are in agreement with the general behavior of PHB accumulation in other organisms: PHB accumulation triggers when a nutrient, different from the carbon source, is limiting (Steinbüchel & Hein, 2001). On the other hand, PHB accumulation in glucose limiting chemostats showed a completely different trend (Figure 1, panel A). At a D=0.05 h^{-1} the PHB percentage was as low as 4.85 ± 0.35 %, increasing linearly to 50.7 ± 2.1% at a D=0.4 h^{-1}. The PHB accumulation obtained at dilution rates of 0.3 and 0.4 h^{-1} were in good agreement with the PHB content of exponentially growing batch cultures (and of the exponential growth zone of fed-batch cultures) where the carbon source is the limiting nutrient, with reported values close to 50% PHB (Wang & Lee, 1997; Yamane et al., 1996) and 53% (Ramsay et al., 1990). This is the first report where a low PHB content is described in a culture of *A. lata* under glucose-limiting conditions. To confirm this result, samples of biomass were analyzed using Raman spectroscopy (Figure 1, panel G). The Raman spectrum revealed characteristic emission lines attributable to proteins (amide I at 1660-1662 cm^{-1}) and PHB (1734-1736 cm^{-1}) (Samek et al., 2016). A PHB standard (data no shown) shows several Raman peaks where the most intense peaks corresponded to 837 and 1734-1736 cm^{-1}. Samples from a nitrogen-limited chemostat at a D=0.05 h^{-1} (Figure 1, panel G, spectrum a) and glucose-limited chemostat at a D=0.3 h^{-1} showed clear PHB peak at 1734 cm^{-1}, with PHB to amide I peak heights ratios of 5.5 and 2.2, respectively. These results agree with the PHB content of the samples, 42% (D=0.3 h^{-1}, glucose-limited) and 75% (D=0.05 h^{-1}, nitrogen-limited) assuming that a positive linear correlation exists between the PHB/Amide I ratio and PHB content (Samek et al., 2016). The analysis of the glucose-limited chemostats at dilution rates of 0.05 and 0.1 h^{-1} (Figure 1, panel E, spectrums c and d) shows a nearly absent PHB peak at 1734 cm^{-1}, confirming the results of the GC analysis. The accumulation of PHA under unrestricted growth conditions at high dilution rates was also observed in cultures of *P. oleovorans*, although the maximum content was 10% (Durner et al., 2000).

Figure 1, panel E shows the calculated glucose uptake rates in mmol $gCDW^{-1}$ h^{-1}. Glucose uptake rates under oxygen and nitrogen limitation were found to be higher than those

obtained under glucose limiting conditions at every dilution rate. The specific glucose uptake rates in chemostats of *C. necator* operated at D= 0.1 h^{-1} were found to be similar and to decrease in the same order as the one found in our work: ammonia limited (4.2 mmol $gCDW^{-1}$ h^{-1}) followed by oxygen-limited (3.1 mmol $gCDW^{-1}$ h^{-1}) and glucose-limited (2.0 mmol $gCDW^{-1}$ h^{-1}) conditions (Henderson & Jones, 1997). The production of organic acids was negligible.

The PHB flux, (specific PHB productivity based on the residual biomass) is shown in Figure 1, panel F. A linear trend was found between PHB flux and the dilution rate for the ammonia limited and oxygen-limited chemostat. For the glucose-limited cultures, the relationship between PHB flux and dilution rate is best described considering two linear zones, with an almost negligible PHB accumulation rate at dilution rates below 0.1 h^{-1}. Interestingly, *Azohydromonas australica* DSM1124, a species closely related to *A. lata* DSM1123, showed no PHB accumulation during the growth phase in batch culture (before ammonium exhaustion) using glycerol as the sole carbon and energy source (Haage et al., 2001). The authors attributed this change in the behavior of a strain known for PHB accumulation during exponential growth to the use of a carbon source other than glucose (Haage et al., 2001). However, since the cells grew at a $\mu = 0.075$ h^{-1}, our results indicate that the reduced PHB accumulation it is not related to the nature of the substrate, but to the failure of glycerol to produce an uptake rate of carbon compatible with a μ sufficiently high to promote the accumulation of PHB.

4.1.4. Preliminary *in-vivo* depolymerization and viability assay in PHB accumulated cells of *A. lata* DSM 1123

By providing the environmental condition in which cells have high activity of intracellular PhaZ and low activity of Hbd, R3HBA could be produced with a yield of 96 % in only 30 min by *in-vivo* depolymerization of PHB in *A. lata* (Lee et al., 1999). In order to replicate the experiment of Lee et al. (1999), PHB accumulated cells of *A. lata* were incubated for 5 hours in phosphate buffer to assess PHB depolymerization at different pHs. At pH 4, the PHB conversion was 38.6 % higher than those obtained at pHs of 5 (29.4 %) and 7 (8.05 %) (Table

6). This pattern was consistent with the R3HBA titer and R3HBA yield of 2.42 g L^{-1} and 93.6 % at 4 pH and decreasing toward neutral pHs. The results are similar to the pioneering work of Lee et al. (1999) where the R3HBA yield reached up to 96 % in 30 min at pH 4, but not at higher pH values. The *in-vivo* depolymerization of *A. lata* is highly influenced by the effect of pH on PhaZ and Hbd activities. Lee et al. (1999) observed that the highest PhaZ activity is attained between pHs 3 and 4; whereas no activity was recorded at pH 4 for Hbd. Then R3HBA could not be converted to acetoacetate and was excreted to the extracellular medium.

Table 6. Summary of the PHB conversion, R3HBA excreted and cell viability at pH 4, 5 and 7 in *A. lata* cells

pH	**Initial biomass** [g L^{-1}]	**Initial PHB**	**Final PHB**	**R3HBA** [g L^{-1}]	**Yield R3HBA/PHB**	**Viable colonies**
4	3.50	63.9 %	25.3 %	2.42	93.6 %	2.72 %
5	3.14	59.4 %	30.0 %	0.196	9.32 %	10.8 %
7	3.60	66.0 %	58.0 %	0.019	1.76 %	32.2 %

After 5 hours of *in vivo* depolymerization, cells were plated on AL1 agar and the viability was quantified by colony counting. A viability of 50 % was considered positive. Table 6 indicated that the number of viable colonies increased with the pH toward neutral values, but no condition achieved 50 % of viability. A possible explanation is that *in-vivo* depolymerization and incubation with buffer phosphate can trigger cellular stress, thus causing death cell.

4.1.5. Sequential PHB depolymerization in a nitrogen-limited chemostat

A depolymerization bioreactor was coupled to the discharge of a nitrogen-limited chemostat operated at D=0.2 h^{-1} and was maintained at pH 4 with a 30 min of residence time. After ten residence times, a sample withdrawn from the depolymerization reactor showed a depolymerization yield of 92.3 ± 2.0% mol R3HBA per mol PHB calculated after measuring R3HBA using an enzymatic assay specific for R3HBA and PHB quantification by GC after

propanolysis. Considering the short residence time in the second bioreactor and the lack of metabolic activity of *A. lata* DSM1123 at pH 4, this result suggests that the PhaZ and Hbd are active under nitrogen-limited conditions. An HPLC measurement of the culture supernatant of the first reactor indicates the presence of R3HBA at a concentration of 18 mg L^{-1}. These results confirm the low activity of phaZ in neutral pHs as described by Lee et al.,(1999), where 40 mg L^{-1} of R3HBA titer was obtained at pH 7, the difference of amount obtained in this work with Lee and co-workers may be related by an active Hbd at this pH. Lee et al., (1999) showed Hbd activity of 15.12 U mg^{-1} protein at pH of 7 instead of 0 U mg^{-1} at 4 pH.

4.2. STUDY OF *in-vivo* PHB DEPOLYMERIZATION IN *M. parvus*

The results presented in this section, were published in the following paper "Production of (*R*)-3-hydroxybutyric acid from methane by in vivo depolymerization of polyhydroxybutyrate in *Methylocystis parvus* OBBP" with DOI: https://doi.org/10.1016/j.biortech.2022.127141

4.2.1. Influence of the presence of nitrate, O_2 and pH on PHB depolymerization

Figure 2 shows the CH_4 and O_2 consumption for the 48 hours depolymerization experiments performed with NMS (panels A and B) and NFMS (panels C and D) at pH 4, 7 and 11. Consumption of methane and oxygen was faster in the control experiment with NMS at pH 7 compared to that in NFMS medium, an expected result considering that NMS allows for balanced growth. In the absence of oxygen at pH 7, methane consumption was negligible in NFMS medium and close to 10% in the NMS cultures. In this regard, Bordel et al. (2019) showed that *M. parvus* can use stored PHB as an energy source under anoxic conditions only when nitrate is available in the cultivation broth. The annotated genome of *M. parvus* contains the genes involved in nitrate reduction and revealed that denitrification is the only mechanism supporting the use of methane or PHB as an energy source in the absence of oxygen (Bordel et al., 2019).

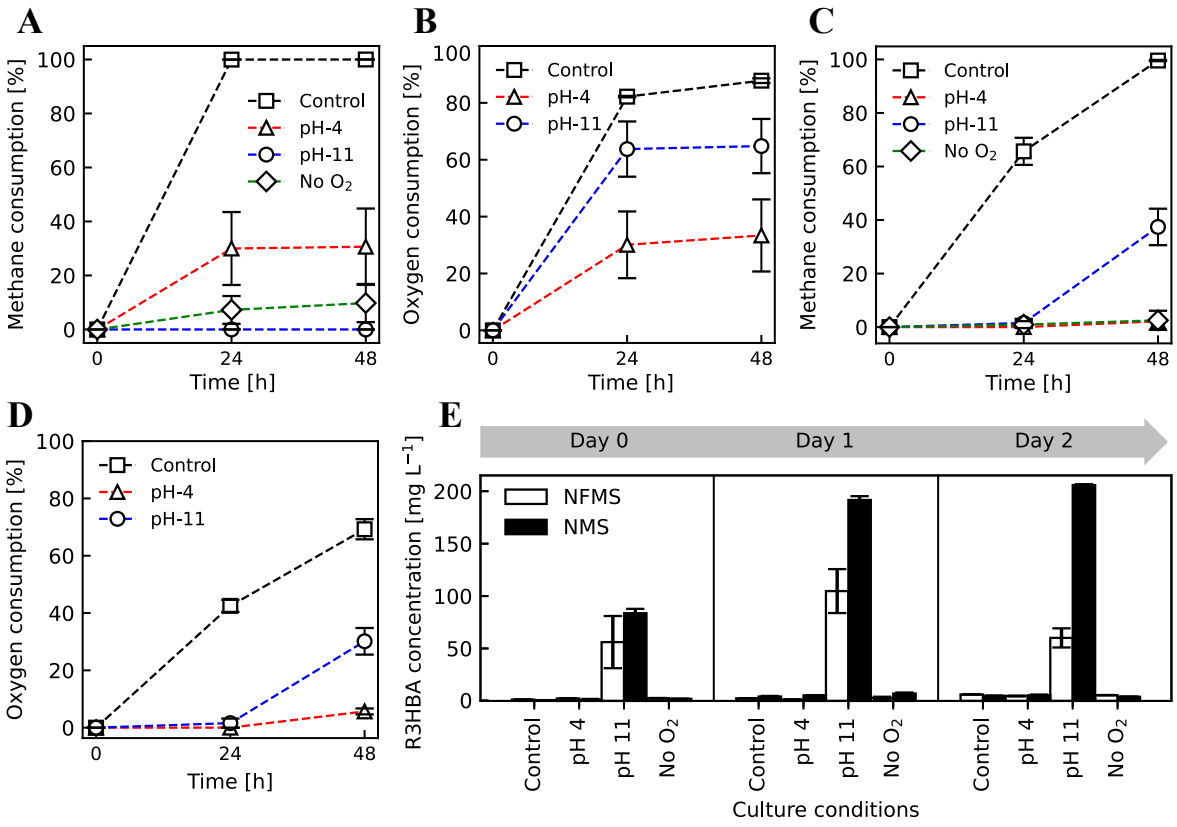

Figure 2. **CH_4 and O_2 consumption profile and R3HBA released at different depolymerization conditions in *M. parvus*.** CH_4 and O_2 consumption during PHB depolymerization in *M. parvus* cultivated in NMS (A, B) and NFMS (C, D) medium at pH 4 (triangles), pH 11 (circles), pH 7 (squares) and w/o oxygen at pH 7 (diamonds). (E) R3HBA released at pHs 4, 11, 7 (w/ and w/o oxygen) in NMS (black bars) and NFMS (white bars) medium.

On the other hand, neither methane nor oxygen consumption was recorded at pH 4 in NFMS medium. Similarly, at pH 11 the final consumption of CH_4 (37.41 ± 6.81 %) and the O_2 uptake (30.14 ± 4.65 %) were reduced compared to the control. In NMS, nitrate was consumed only in the control assays at pH 7 from the initial 130.1 mgN L^{-1} (measured as total nitrogen) to 47.8 ± 11.5 mgN L^{-1} at the end of the 48 hours incubation period. Nitrate consumption at pHs 4 and 11 was lower than 2.6 mgN L^{-1} during the same period and only 0.3 mgN L^{-1} was consumed in the assay at pH 7 in the absence of oxygen. Therefore, no significant cell growth occurred except in the control (neutral pH).

Interestingly, extracellular R3HBA was only detected at pH 11 in both NMS and NFMS medium (Figure 2, panel E). At pH 11 in NMS, 80.6 ± 0.8 % of PHB was depolymerized and R3HBA secretion reached 205.8 ± 1.2 mg L^{-1}, a higher concentration compared with the assay in NFMS, where 25.7 ± 7.9 % of PHB was depolymerized and a R3HBA titer of 60.1 ± 12.9 mg L^{-1} was measured after 48 h. The mechanisms by which nitrogen influences the depolymerization extent and rate seem to be related in other bacteria species to the alleviation of the stringent response. In the amino acid starved cells, the alarmone ppGpp accumulates and destabilizes the RNA polymerase σ70, resulting in an induction of genes under the control of alternative sigma σ factors, such as σ54 (Brigham et al., 2012). ppGpp has also been implicated in the inhibition of translation (Irving et al., 2021). In *C. necator* H16, PHB mobilization occurs in the absence of the alarmone ppGpp, which in turn requires the presence of a source of nitrogen (Juengert et al., 2017). As further evidence of this mechanism, the genome of *M. parvus* OBBP contains the necessary bifunctional (p)ppGpp synthetase/hydrolase (WP_016921527.1) required for the synthesis and degradation of ppGpp.

PHB depolymerization at pH 4 and pH 7 (with or without O_2) in NMS produced extracellular R3HBA titers of 5.42 ± 0.67 mg L^{-1}, 4.83 ± 0.37 mg L^{-1} and 4.01 ± 0.15 mg L^{-1}, respectively. Similarly, extracellular R3HBA concentrations of 4.68 ± 0.37 mg L^{-1}, 6.17 ± 0.22 mg L^{-1} and 5.50 ± 0.15 mg L^{-1} were measured after 48 hours in NFMS at pH 4 and pH 7 with or without oxygen, respectively. The final pH of the culture broth in the assays initially adjusted to pH 11 in NMS and NFMS media decreased to 8.28 and 6.23, respectively, confirming the secretion of the acidic R3HBA. No significant changes in pH were measured in the rest of the experiments, which agreed with the limited R3HBA release. The estimated Y_{R3HBA} are 31.5 ± 0.08 % and 28.9 ± 0.91 %, which equates to a PHB to R3HBA conversion of 25.4 ± 0.03 % and 7.4 ± 2.1 %, for the experiments at initial pH of 11 in NMS and NFMS respectively.

The *in-vivo* depolymerization of the intracellularly accumulated PHAs to hydroxy acids has been reported in several bacterial strains. For instance, the depolymerization process in *A. lata* was carried out in water without shaking to minimize oxygen transfer, at 37 °C and

pH 4 and achieved a depolymerization efficiency of 96% of the initial PHB to R3HBA in only 30 min (Lee et al., 1999). These authors also evaluated PHB depolymerization in *Pseudomonas aeruginosa* PAO1 (DSM 1707), *Pseudomonas oleovorans* (ATCC 29347) and *Cupriavidus necator* (NCIMB 11599) at pH values below 7 (Lee et al., 1999). The PHA to hydroxy acids conversion was 20 % for *C. necator* and less than 10 % for *Pseudomonas* species (Lee et al., 1999).

The conversion of PHA to hydroxy acids in *Pseudomonas putida* GPo1 was improved by changing the depolymerization conditions to an alkaline medium. This strain excreted R3HO and R3HHx at pH 11 in citrate buffer for 6 hours with a PHA degradation efficiency and monomer production yields above 90 % (w/w) (Ren et al., 2005). Ruth et al. (2007) engineered a depolymerization strategy at pH 10 in *P. putida* GPo1 under continuous mode with a production of R3HO, R3HHx, (*R*)-3-hydroxy-10-undecenoic acid, (*R*)-3-hydroxy-8-nonenoic acid, (*R*)-3-hydroxy-6-heptenoic acid, (*R*)-3-hydroxyundecanoic acid, (*R*)-3-hydroxynonanoic acid and (*R*)-3-hydroxyheptanoic acid. The study herein presented confirmed the key role of high pH on PHA depolymerization, which is a common feature in *Pseudomonas* species. Hence, *P. putida* GPo1 released 3-hydroxyoctanoic acid and 3-hydroxyhexanoic acid from intracellular PHA at pH 11 with conversions of 76 % (0.356 g L^{-1}) and 21% (0.015 g L^{-1}) in 6 hours, respectively (Ren et al., 2005). Similarly, *P. putida* Bet001 can depolymerize PHAs up to 98 % in 0.2 Tris-HCl buffer at pH 9.1 within 48 hours (Anis et al., 2018). In Type II methanotrophs, the production of hydroxy acids has only been described in a genetically engineered *Methylosinus trichosporum* OB3b strain able to synthesize (*R*)-4-hydroxybutyrate acid (R4HBA) from CH_4 via the tricarboxylic acid cycle (TCA cycle) and the overexpression phosphoenolpyruvate carboxylase (Ppc), isocitrate dehydrogenase (Icd) and 2-oxoglutarate dehydrogenase (SucAB). The highest 4-hydroxybutyrate titer obtained was 10.5 mg L^{-1} after 6 culture days (Nguyen et al., 2021).

PHB synthesis and degradation in methanotrophic bacteria seem to be similar to the metabolic processes carried out by most heterotrophic PHB producers (Vecherskaya et al., 2001). However, there is a limited understanding of the mechanisms that control the intracellular PHB depolymerization and the formation of its monomer acids such as R3HBA

and crotonic acid in Type II methanotrophs. Vecherskaya et al. (2001) demonstrated how products from the anaerobic fermentation of PHB in methanotrophs can be bioconverted in R3HBA, butyrate, acetate, succinate, and other reduced compounds. Figure 3 shows the pathways of PHB depolymerization and formation of different metabolites in *M. parvus* OBBP based on a genome-scale metabolic model (Bordel et al., 2019) that has been recently reported. This model shows the fluxes of the PHB degradation from crotonyl-CoA to methylmalyl-CoA, which is dissociated into glyoxylate and propionyl-CoA. The glyoxylate originated from methylmalyl-CoA is incorporated into the serine cycle and the propionyl-CoA is carboxylated into succinyl-CoA by the ethylmalonyl-CoA cycle (EMC) and then incorporated into the TCA cycle (Bordel et al., 2019). Another parallel pathway involves the enzymatic conversion of crotonyl-CoA to butyryl-CoA and finally to butyrate (Vecherskaya et al., 2001).

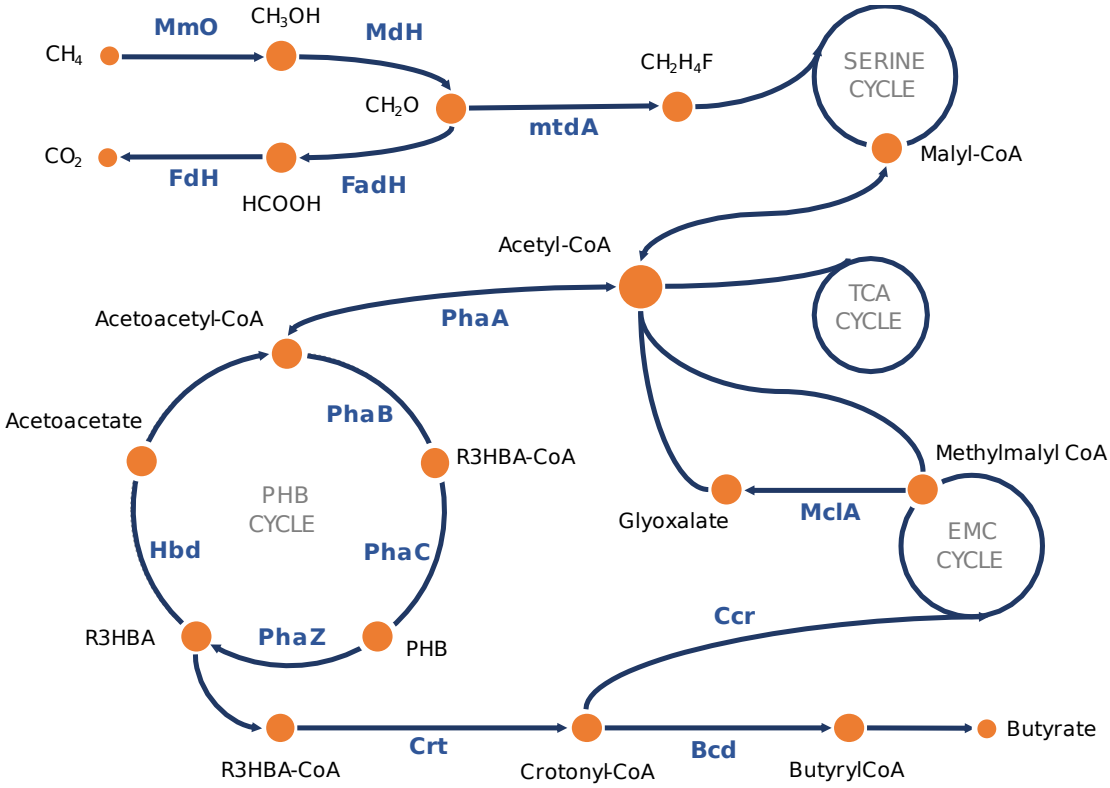

Figure 3. **Schematic metabolic pathways involved in the polymerization and depolymerization of PHB in *M. parvus*.** MmO, methane monooxygenase; MdH, methanol dehydrogenase; FadH, formaldehyde dehydrogenase; FdH, formate dehydrogenase; MtdA, methylene tetrahydromethanopterin dehydrogenase; PhaB, acetoacetyl-CoA reductase; Crt, 3-hydroxybutyryl-CoA dehydratase; Ccr, crotonyl-CoA carboxylase/reductase; MclA, malyl-CoA lyase; Bcd, butyryl-CoA dehydrogenase.

4.2.2. Optimization of pH during depolymerization

The results showed in Figure 4 indicate that PHB depolymerization at pH 11 in NMS was superior to the result obtained at low pHs in NFMS. However, these results do not clarify if pHs closer to 11 could result in higher R3HBA titers, if pH control could improve R3HBA yields or if methane plays a role in the depolymerization of PHB. In this context, *M. parvus* cells containing 18.1 % of PHB were resuspended in NMS medium at 1.32 ± 0.02 gTSS L^{-1} and depolymerization was assessed at pHs of 10, 11 and 12 as above described. Unlike previous experiments, the pH of the cultivation broth was periodically monitored and controlled with NaOH during the course of the depolymerization.

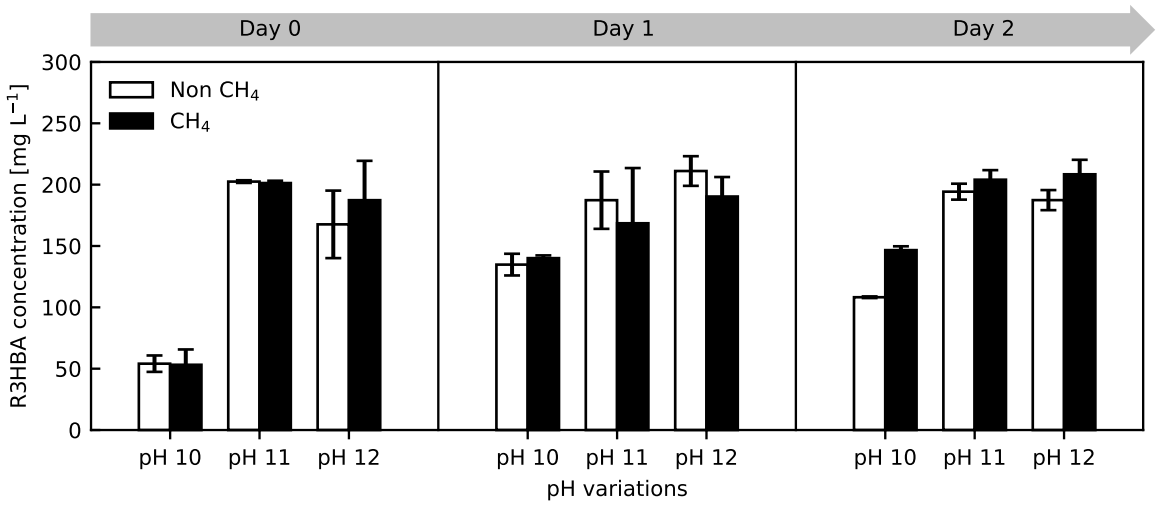

Figure 4. **R3HBA released at pH 10, 11 and 12 in presence or absence of CH_4 in *M. parvus***. PHB accumulated cells cultured in NMS medium with (black bars) or without (white bars) CH_4 for 48 h at 37°C.

M. parvus cells rapidly released R3HBA in the pH range of 10-12 following pH adjustment. Thus, the final extracellular monomer concentration reached 146.6 ± 3.11 mg L^{-1} and 108.2 ± 0.66 mg L^{-1} with or without methane at pH 10 (Figure 4). On the other hand, the influence of methane was negligible at pH 11 and pH 12, reaching a PHB depolymerization efficiency of 96.6 ± 2.22% and 92.9 ± 1.5%, respectively (corresponding to 204 ± 7.8 mg L^{-1} and 208.4 ± 11.8 mg L^{-1} of R3HBA) in the presence of CH_4. Similar PHB depolymerization

efficiencies of 98.2 ± 1.10% and 93.6 ± 1.33%, respectively (corresponding to 194.3 ± 6.5 mg L^{-1} and 187.4 ± 8.2 mg L^{-1} of R3HBA) were recorded in the absence of CH_4 at the end of the experiment at pH 11 and 12, respectively. These data suggested that methane did not play a significant role on PHB depolymerization and that pHs beyond 11 exerted little influence on R3HBA release. Based on these results, pH 11 in NMS and in the absence of CH_4 was selected for further experiments. Under this condition, a PHB to R3HBA conversion of 68.0 ± 3.2 % was estimated.

The fine-tuning of pH played a key role in R3HBA release and PHB depolymerization in other bacteria species. For instance, Ren et al. (2005) demonstrated that PHA depolymerization in *Pseudomonas* Gpo1 produced the highest titer of monomers (360 mg L^{-1} of (*R*)-3-hydroxyoctanoic acid at an initial pH of 11, while a significantly smaller concentration of monomers (50 mg L^{-1}) was measured at pH 12. Similarly, depolymerization and R3HBA release in *A. lata* peaked at a pH of 4 with a PHB to R3HBA conversion of 96 % in 30 min and decreased to 31 % at a pH 5 (Lee et al., 1999). The production of R3HBA *in-vivo* requires a concomitant high PHB depolymerization activity and a low enzymatic activity of Hbd (Jendrossek and Handrick, 2002). While intracellular depolymerases have an optimum pH range of 8-10 (Jendrossek; Handrick, 2002), Hbd activity is reported to be pH-dependent, with an activity range of 5-10 and an optimal pH range of 7.5-8.5, decreasing abruptly above pH 10 (Mountassif et al., 2010; Takanashi & Saito, 2006). In this context, this study suggests that the PhaZ enzyme, responsible of the depolymerization of PHB towards R3HBA, of *M. parvus* exhibits a high activity at pH 11.

4.2.3. Influence of temperature on the kinetic of PHB depolymerization

Since the optimal temperature for both growth and PHB accumulation in *M. parvus* is 30 °C and no growth occurs at temperatures greater than 40 °C (Soni et al., 1998), the kinetics of PHB depolymerization and R3HBA released were investigated at 25 and 35 °C, and pH 11 (manually adjusted to compensate for the R3HBA release). The R3HBA titers quantified at 25 and 35 °C were 240 ± 3.81 mg L^{-1} and 282 ± 20.04 mg L^{-1}, respectively, after 3 hours of depolymerization in a cell suspension with an initial PHB concentration of 1.86 ± 0.006 g L^{-1}.

The R3HBA production rates of initial PHB were 48.6 ± 6.0 mg R3HBA mg PHBi^{-1} h^{-1} at 25 °C and 52.7 ± 2.3 mg R3HBA mgPHBi^{-1} h^{-1} at 35 °C, while PHB depolymerization reached 16.5% (Y_{R3HBA}=64.5%) and 24.8% (Y_{R3HBA}=50.5%) at 25 and 35 °C, respectively. These results were similar to those obtained by Lee et al. (1999) during the depolymerization of PHB accumulated in *A. lata* at 30, 37 and 45 °C. A moderate increase in R3HBA production rate was found when the temperature increased from 30 to 37 °C, while PHB depolymerization suddenly stopped at 45 °C likely due to enzymatic denaturation. Since R3HBA production rate slightly increased with temperature, but R3HBA yields severely decreased, the following experiments were performed at 30 °C.

After 3 hours at 25 °C and pH 10.8, cells were harvested and cultured in NMS (to assess cell growth) and NFMS (to assess PHB accumulation) media in the presence of CH_4 to analyze the viability of the cells post-depolymerization.

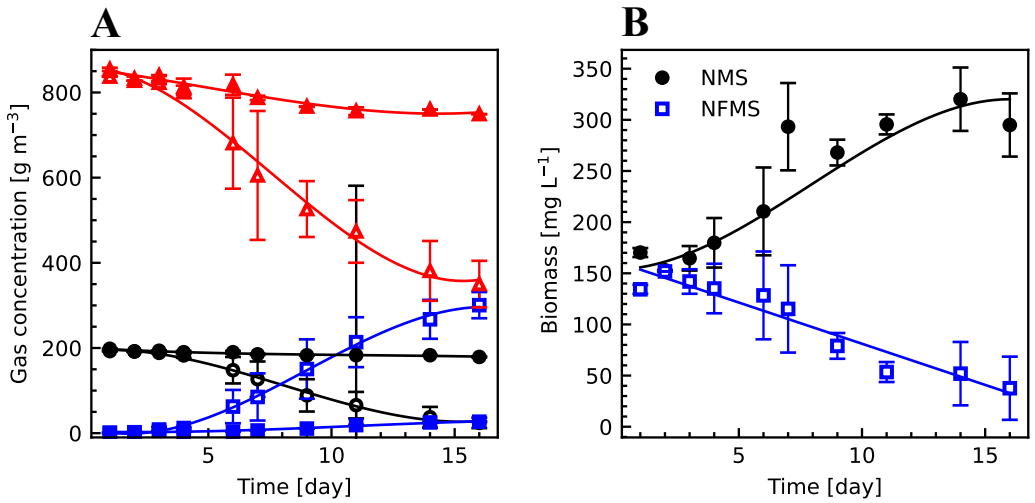

Figure 5. **Time course of biomass and CH_4, O_2 and CO_2 in viability assay of *M. parvus*.** Concentrations of biomass (A) and CH_4 (circles), O_2 (triangles) and CO_2 (square) (B) during the viability assays of *M. parvus* cells previously subjected to a 3 h depolymerization phase at pH 11. Filled and empty symbols correspond to the experiments carried out in NMS and NFMS media, respectively.

Cells incubated in NMS medium started to consume methane and oxygen by day 4, these gases fully being depleted after 16 days (Figure 5, panel A). Biomass concentration increased

from 170 mg L^{-1} to 295 mg L^{-1} (Figure 5, panel B). However, the μ of post-depolymerization cells was 0.058 h^{-1}, which has lower than the μ= 0.107 h^{-1} reported for fresh *M. parvus* cultures (Bordel et al., 2019). On the other hand, the culture incubated in NFMS medium experienced cell death during the cell viability experiment, presumably due to nitrogen limitation.

4.2.4. Influence of the aeration rate and R3HBA exogenous on PHB depolymerization

To assess the effect of oxygen availability on PHB depolymerization in *M. parvus*, three tests with different liquid to air surface ratios in E-flasks were carried out at a constant pH of 11. Figure 6 panel A, shows the kinetics of R3HBA release for the 72 hours experiment and the depolymerization, crotonic acid and R3HBA yields in Figure 6 panel B.

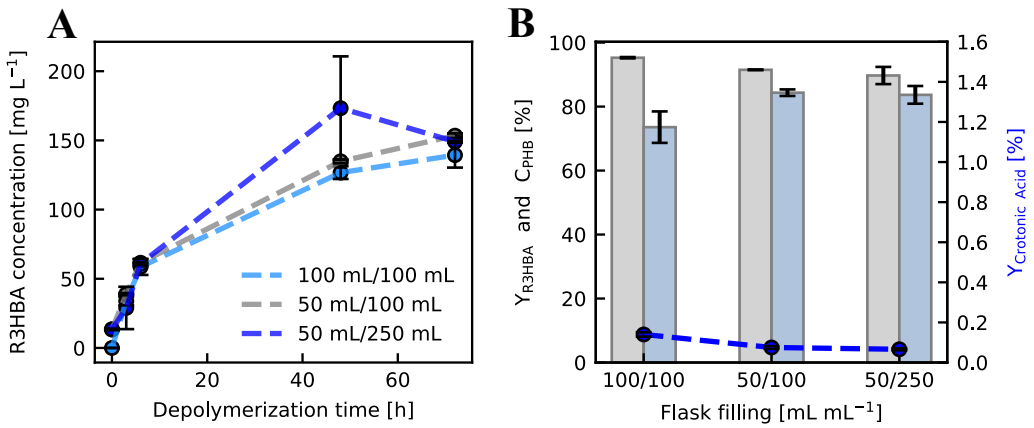

Figure 6. **Influence of the oxygen mass transfer rate on the kinetics of R3HBA release in *M. parvus*.** Timeline of the R3HBA release at different aeration conditions (A), depolymerization (grey bars) and R3HBA yields (blue bars) (B).

The final R3HBA concentration was similar regardless of the O_2 supply, while the largest differences were obtained for the R3HBA yield. Indeed, the lowest R3HBA yield (73.6 ± 4.9 %) occurred under the condition restricting O_2 mass transfer (100 mL of broth in a 100 mL E-flask) while under less restrictive O_2 supply rates, R3HBA yields reached 84.3 ± 1.0 % and 83.7 ± 2.8 % at 50 mL/100 mL and 50 mL/250 mL filling ratios, respectively. In terms of PHB to R3HBA conversion, these values correspond to 91.5 ± 0.1 %

and 89.7 ± 2.7 %, respectively. Literature suggests that the oxygen content during the depolymerization process could influence the fate of the monomers produced in rather unpredictable manners. In this regard, the PHB accumulated with glycerol as substrate can be depolymerized to R3HBA in *Halomonas* sp. KM-1 under microaerobic conditions (25 mL of broth in 200 mL E-flasks agitated at 50 rpm) in the presence of a nitrogen source. Indeed, 15.2 g L^{-1} of R3HBA were produced in 66 hours with a 76.6% PHB to R3HBA conversion under these conditions (Kawata et al., 2012). On the other hand, *Halomonas* sp. OITC1261 behaves differently despite its taxonomic closeness with *Halomonas* sp. KM-1, synthesizing R3HBA concomitantly with PHB under aerobic conditions without extra nitrogen supplementation (Yokaryo et al., 2017).

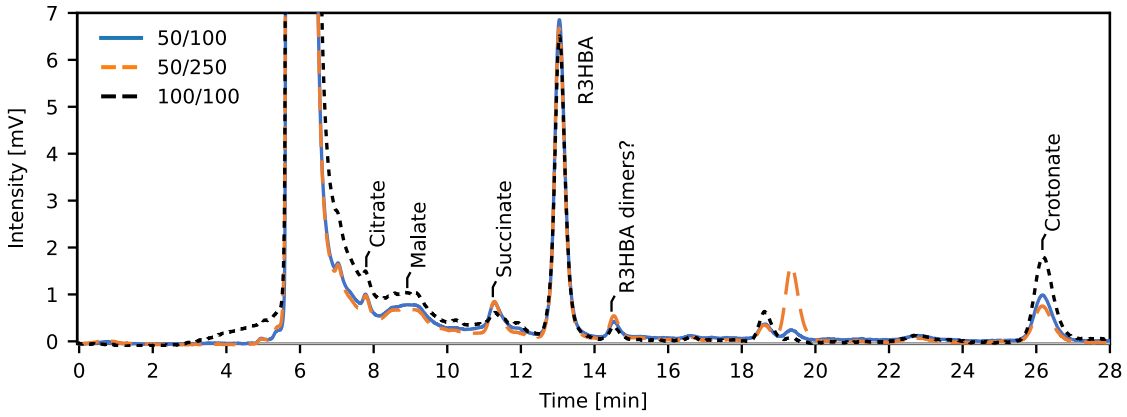

Figure 7. **HPLC chromatograms of depolymerization assays at different filling ratios in E-flasks**. Supernant of samples culture taken after 72 h of depolymerization at pH 11in NMS medium.

HPLC analysis (Figure 7) of the depolymerization broth at 72 hours showed that citric acid (ranging between 1 and 3 mg L^{-1} depending on the O_2 supply rate), malate (20-45 mg L^{-1}), succinate (5-20 mg L^{-1}) and crotonate (less than 0.2 mg L^{-1}) were present along with R3HBA and two unidentified compounds at 18.5 and 19.5 min in the incubation broth drawn after 72 hours of depolymerization assay. In addition, a peak at 14.6 min was resolved, presumably corresponding to R3HBA dimers based on previous reports (Lu et al., 2014).

The oxygen consumption during the PHB depolymerization process at pH 11 (Figure 2, panel B) and the fact that the yield of R3HBA decreased as the supply of oxygen decreased

below a certain threshold, suggests that part of the electrons released from the conversion of the depolymerized PHB towards acetyl-CoA are aerobically oxidized for the provision of maintenance energy. This follows from the subsequent findings: (i) the production of acetoacetate from R3HBA produces a molecule of NADH that could be used for ATP production if O_2 is available, (ii) a negligible nitrate consumption was measured at pH 11 during the depolymerization experiment, thus growth can be disregarded, (iii) a limited supply of O_2, achieved by carrying out the depolymerization process in an almost filled E-flask, decreased the R3HBA yield, suggesting that R3HBA was routed towards other metabolites to provide energy for maintenance. The latter finding can be considered as a less extreme version of the experiments by Vecherskaya et al. (2001) under anaerobic conditions, where products characteristics of a fermentative metabolism for energy production were obtained.

On the other hand, R3HBA might act as an inhibitor of the enzymatic depolymerization activity. To test this hypothesis in *M. parvus*, depolymerization assays were carried out adding exogenous R3HBA before the onset of the depolymerization at concentrations ranging from 0 to 650 mg L^{-1}. The higher limit was higher than the R3HBA titers achieved in previous experiments, where values slightly above 200 mg L^{-1} were found after 48 hours of depolymerization at pH 11 with or without methane.

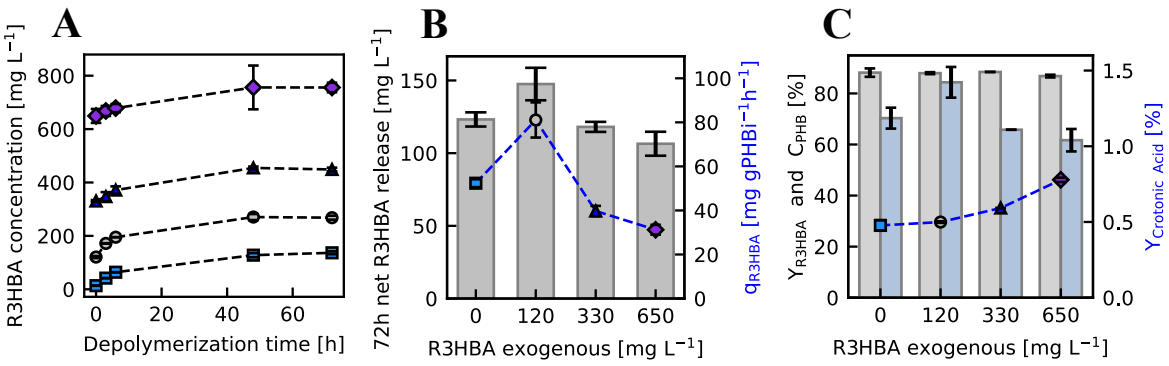

Figure 8. **Influence of R3HBA exogenous in the R3HBA excretion in *M. parvus*.** Time course of R3HBA concentration at 0 (square), 120 (circle), 330 (triangle) and 650 (diamond) mg L^{-1} of initial R3HBA (A), net release (bars) and initial production rate of R3HBA (scatter plot) (B) and R3HBA yield (blue bars), depolymerization yield (gray bars) and crotonic acid yields (scatter plot) (C) at pH 11 and NMS medium in *M. parvus* after 72 h.

Figure 8 panel A shows the total R3HBA concentration during the 72 hours depolymerization experiment, while the net R3HBA released at the end of the experiment (72 h) is shown in Figure 8 panel B. No significant differences were found between R3HBA concentration released after 72 hours with no added R3HBA and any of the experiments with addition of exogenous R3HBA. Figure 8 panel B, also shows the specific initial rate of R3HBA release calculated during the first 6 hours. This parameter increased from 52.4 ± 1.8 mg of R3HBA per gram of initial PHB (PHBi) per hour in the absence of exogenous R3HBA to 81.1 ± 8.0 mg g PHBi^{-1}h^{-1} in the presence of 120 mg R3HBA L^{-1}. This increase could be related to impurities in the *in-house* produced R3HBA, although this was not further investigated. Additional increases in the initial R3HBA concentration led to a decrease in the specific initial rate of R3HBA release. Finally, Figure 8 panel C shows no differences on the depolymerization yield regardless of the initial R3HBA concentration. Interestingly, the Y_{R3HBA} was reduced at 330 and 650 mg L^{-1} (65.8 ± 0 and 61.7 ± 4.40 %) compared to non R3HBA addition or to 120 mg R3HBA L^{-1} added, while an increment of the crotonic acid yield to 0.78 ± 0.014 % was evidenced at the highest initial R3HBA concentration.

Surprisingly, literature is scarce regarding the effect of R3HBA on the depolymerization kinetics, although R3HBA is the main reaction product. Scherer et al, (1999) found that an extracellular PHB depolymerase from *Aspergillus fumigatus* was reversibly inhibited by trimers of R3HBA, but no data was presented concerning inhibition by R3HBA.

4.3. PLASMID CONSTRUCTION FOR *tesB* EXPRESSION IN *C. necator* H16 AND *M. parvus*

The implementation of the TSS system in *M. parvus* was explored by the construction of an expression vector containing *tesB*. A synthetic operon including promoter. *tesB* and terminator cassette was amplified from a pUC57 plasmid and assembled in the pAWP89 backbone resulting in pLY01 plasmid. Figure 9C1-C3 showed the bands of approximately 1300 bp corresponding to the promoter, *tesB* and terminator cassette assembled in pLY01 plasmid. Then, this was sequenced in order to confirm the correct construction of the plasmid. Figure 10 indicates the comparison between the main features in the designed pAWP89-*tesB*

(Figure 10A) and the constructed and sequenced plasmid pLY01 (Figure 10B). Although *tesB* is present, the construction of the plasmid yield and unexpected result. The features displayed in pLY01 such as *Amp*^{R} and *lac* promoter did not correspond to the features of the backbone pAWP89 plasmid, suggesting that incorrect fragments of the pUC57 plasmid were assembled in pLY01 instead of the corresponding *tesB* cassette. The reasons of the inconsistent construction are unknown, consequently the application of TSS system in *M. parvus* was not possible.

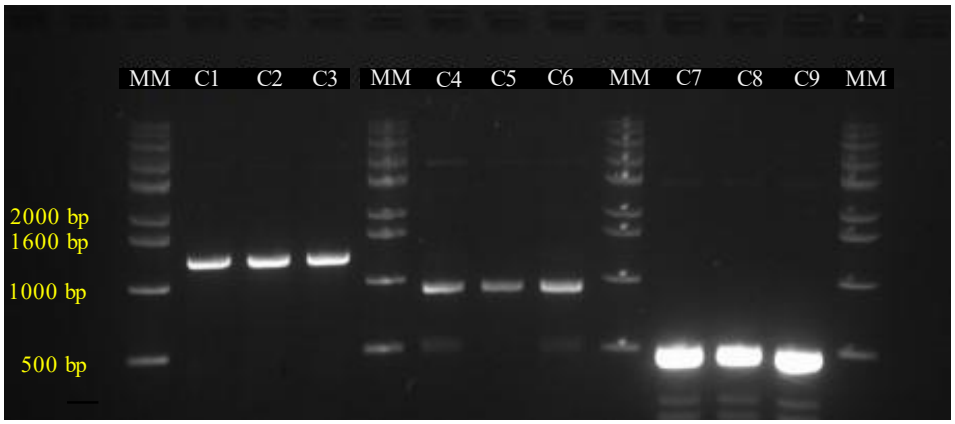

Figure 9. **PCR product amplification of plasmids constructed for the expression of *tesB* in *M. parvus* and *C. necator* H16**. Samples from constructed plasmids in *E. coli* DH5α for visualization through agarose gel by electrophoresis at 90 V for 45 min and using a molecular size marker (MM) of 1 kb DNA AccuLadder from Bionner. The bands, C1-C3 are the cassette containing promoter, *tesB* and terminator gene amplified from pLY01 plasmid; the following lanes correspond to amplified products from pLY02 plasmid, C4-C6: *tesB* gene, C7-C9: terminator fragment.

For the construction of vector carrying *tesB* gene for its expression in *C. necator* H16, the fragments *tesB* and terminator were amplified from pUC57 and pBAD24-sfGFPx2 plasmid and assembled through Gibson using the backbone plasmid pBBR1MCS2 (details in methods section), resulting in pLY02 plasmid. Then, the assembled plasmid was transferred to the chemocompetent *E. coli* DH5α and the confirmation of the insertion of *tesB* and terminators fragment is presented in Figure 9C4-C9.

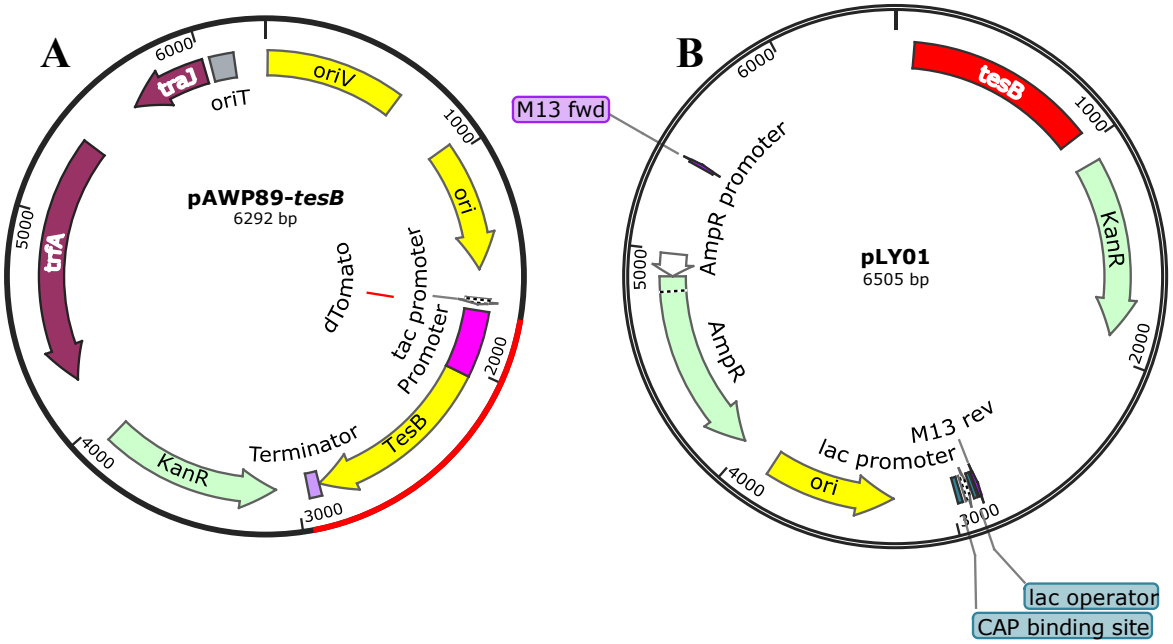

Figure 10. **Maps of the plasmid designed for *tesB* expression in *M. parvus***. Main features contained in the plasmids (A) pAWP89-*tesB* (6292 bp) and (B) pLY01 plasmid from Gibson assembly (6505 bp). Created by SnapGene® 6.1.1.

According to Figure 9, the lanes C4-C9 shows the amplified bands corresponding to *tesb* (Figure 9 C4-C6) and terminator (Figure 9 C7-C9) fragments with 900 bp and 450 bp, respectively. Thus, plasmid was sequenced in order to confirm the correct insertion of the fragments. Figure 11 revealed the main features obtained in the sequenced pLY02 plasmid (Figure 11B) in comparison to the designed pBBR1MCS2-*tesB* (Figure 11A). pLY02 had a total length of 6522 bp and contains the *tesB* and Amp^R gene, the last one not corresponding with the antibiotic resistance gene of pBBR1MCS2-*tesB*. The Amp^R gene is contained in pBAD24-sfGFPx2 and pUC57 plasmids, suggesting that the terminator fragment wasn't assembled in the Gibson cocktail and remnants of pBAD24-sfGFPx2 or pUC57 plasmids were linked to the product plasmid, pLY02. Moreover, the origin replication site and protein replication fragment from pBBR1MCS-2-*tesB* backbone plasmid does not appear pLY01_tesb. Due these negative results, the application of TSS system in *C. necator* was not possible.

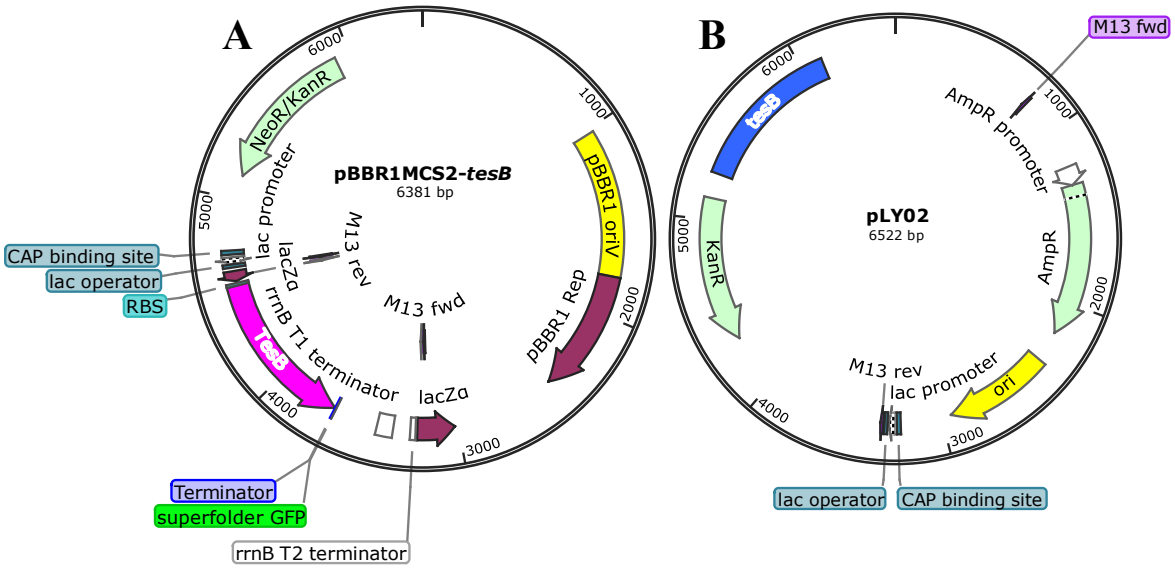

Figure 11. **Maps of the plasmid designed for *tesB* expression in *C. necator* H16**. Main features contained in the plasmids (A) pBBR1MCS2-*tesB* (6381 bp) and (B) pLY02 from Gibson assembly (6522 bp). Created by SnapGene® 6.1.1.

4.4. GENERATION OF MUTANT STRAINS OF *C. necator* VIA SUICIDE VECTOR pT18mobsacB

Another way of studying the production of R3HBA can be through redirecting fluxes in the PHB metabolic pathway that allows the release of R3HBA without being converted into acetoacetate. Two mutant strains were constructed via suicide vector pT18mobsacB. The first strain was *C. necator* Δ*phaC* which is a mutant strain with a *phaC* knock out, the gene encoding for the only active PHA synthase in *C. necator*. This strain is unable to polymerize PHB. The second strain is *C. necator* Δ*phaC* Δ*hbd*, which is the same *C. necator* Δ*phaC* with the deletion of *hbd* gene encoding for the hydroxybutyrate dehydrogenase, unable to polymerize PHB and to transform R3HBA into acetoacetate.

The Figure 12 shows the amplification of *phaC* and *hbd* genes in the *C. necator* strains studied. The total length of *phaC* in *C. necator* H16 corresponds to 1770 pb (Figure 12A *phaC* lane 1), which have the same length with *C. necator* 541 because is a chemically induced mutant with G320A point mutation in *phaC* gene that cause a stop codon producing a truncated and non-functional PHA synthase (Raberg et al., 2014). Lanes 3 and 4 (Figure

12A *phaC*) correspond to *C. necator* Δ*phaC* and *C. necator* Δ*phaC* Δ*hbd* which showed a length of 1000 bp with a *phaC* null fragment (Figure 12B). This confirms the deletion of the *phaC* gene in these mutant strains.

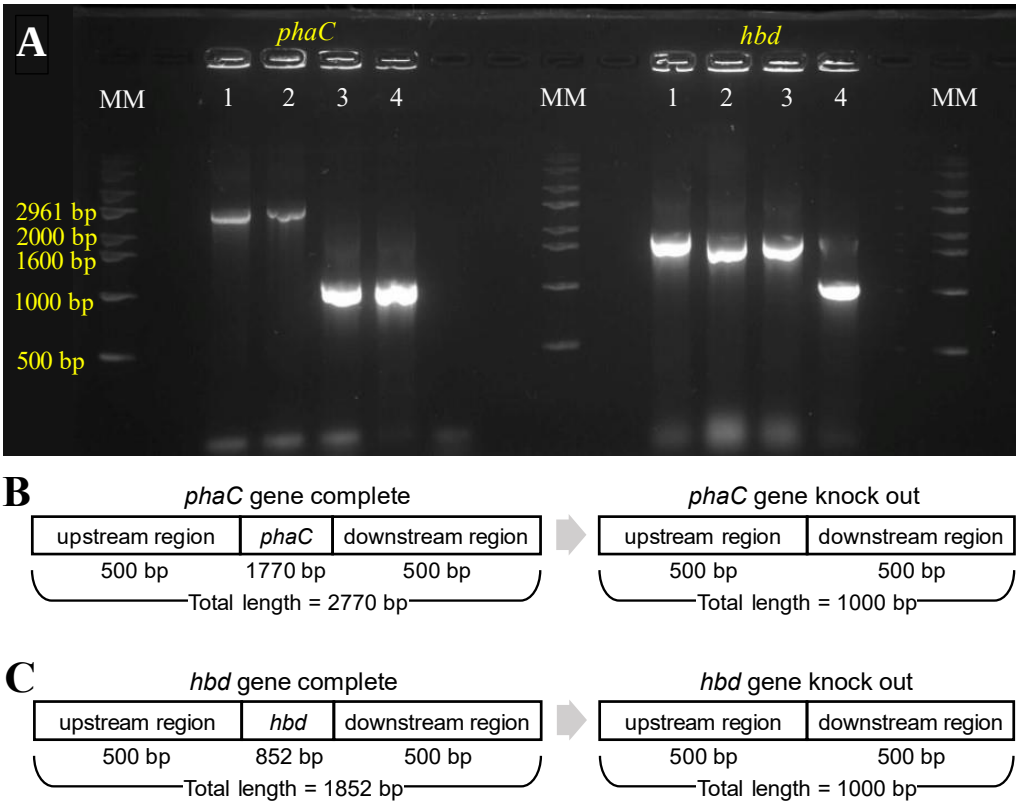

Figure 12. **PCR colony amplification of *phaC* and *hbd* genes in wild type and mutant *C. necator* strains**. The lanes positions (1) *C. necator* H16; (2) *C. necator* 541; (3) *C. necator* Δ*phaC* and (4) *C. necator* Δ*phaC* Δ*hbd*. The molecular size marker (MM) used is 1 kb DNA AccuLadder from Bionner. The left and right positions indicated the *phaC* or *hbd* gene amplified with the primers listed in materials section. Samples were analyzed by electrophoresis through a 1 % agarose gel and visualized by GelRed staining. (A). Schematic representation of the lengths of *phaC* (B) and *hbd* (C) fragments.

A null *hbd* mutant was successfully obtained. Figure 12 shows a band length of 1000 bp confirming the successful deletion of *hbd* in *C. necator* Δ*phaC* Δ*hbd* (Figure 12 *hbd* lane 4) in comparison with the band obtained for the wild type strain with 1852 pb (Figure 12 *hbd* lane 1). *C. necator* 541 and *C. necator* Δ*phaC* had a total band length of 1852 bp, which confirmed the conservation of the expression of *hbd* gene.

4.4.1. Biomass, PHB and R3HBA production in *C. necator* and knockout mutant strains

In order to elucidate the growth, fructose consumption and R3HBA production patterns, all strains were cultured at 30 °C for 48 hours in RE1 mineral medium with approximately 20 g L^{-1} fructose and 1.0 g L^{-1} of ammonium sulphate. During the first 10 h, *C. necator* H16 reached a total biomass concentration of 0.237 ± 0.024 g L^{-1} and μ=0.21 h^{-1} (Figure 13). The mutant, *C. necator* 541 grew faster than the wild type with a μ=0.25 h^{-1}, and reached lower cell concentration of 0.49 ± 0.014 g L^{-1} (Figure 14, panel A). Similarly, the mutant strains *C. necator* Δ*phaC* and *C. necator* Δ*phaC* Δ*hbd* attained biomass concentration at 10 hours of culture equal to 0.252 ± 0.019 g L^{-1} and 0.213 ± 0.003 g L^{-1} with a specific growth rate of 0.21 h^{-1} and 0.20 h^{-1}, respectively (Figures 15-16, panel A). These results show that the maximum specific growth rate was not affected by the deletion of *phaC* and *hbd*. After 48 hours of growth and PHB accumulation, important differences were found between the wild type and mutant strains PHB accumulation in cells occurred only *C. necator* H16 (80 %), whereas in the mutant PHB was null, confirming the successful gene knock out of *phaC* in these strains.

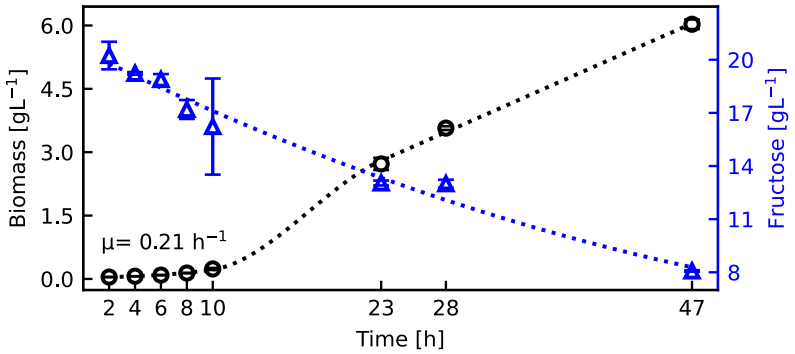

Figure 13. **Cell growth and fructose consumption in *C. necator* H16**. The cultures were carried out in RE1 medium with 20 g L^{-1} of fructose and 1.0 g L^{-1} of ammonium sulphate at pH 7 and incubated at 30 °C for 48 h.

Figures 13-16 panel A, describes the continuous consumption of fructose. The highest final fructose consumption occurred for *C. necator* H16 (12.4 ± 0.040 g L^{-1}) followed by *C. necator* Δ*phaC* (9.00 ± 0.25 g L^{-1}), *C. necator* 541 (7.16 ± 0.39 g L^{-1}) and

C. necator Δ*phaC* Δ*hbd* (6.32 ± 0.19 g L^{-1}). These results suggest that fructose was not the limiting nutrient and that the nitrogen source was totally consumed. The maximum biomass concentration free of PHB attained for all cultures in *C. necator* H16 (1.21 ± 0.02 g L^{-1}) is consistent with a complete consumption of the nitrogen source.

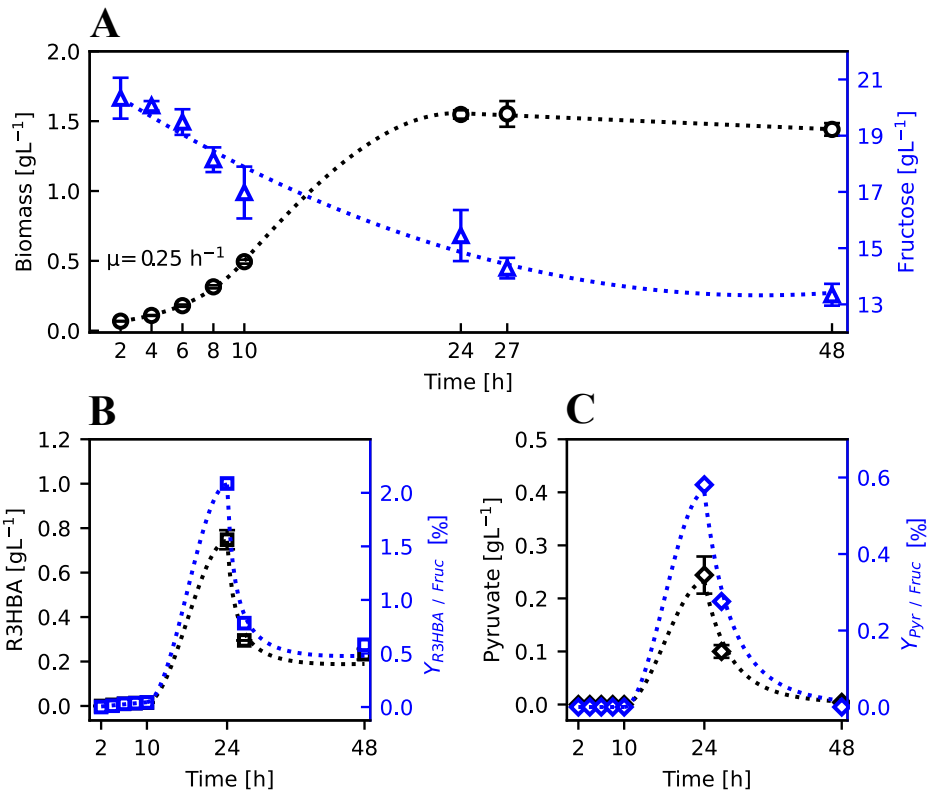

Figure 14. **Cell growth, fructose consumption, R3HBA and pyruvate production and yield in *C. necator* 541**. The cultures were carried out in RE1 medium with 20 g L^{-1} of fructose and 1.0 g L^{-1} of ammonium sulphate at pH 7 and incubated at 30 °C for 48 h.

All mutant strains presented the first R3HBA peak production at 23 hours with 0.748 ± 0.043 g L^{-1}, 0.492 ± 0.027 g L^{-1}, 0.115 ± 0.025 g L^{-1} for *C. necator* 541, *C. necator* Δ*phaC* Δ*hbd* and *C. necator* Δ*phaC*, respectively (Figures 14-16, panel B). Interestingly, at the end of the culture, the R3HBA production of *C. necator* Δ*phaC* Δ*hbd* increased to 0.677 ± 0.050 g L^{-1} with a carbon mole of R3HBA per carbon mole o fructose yield of $Y_{R3HBA/Fruc}$=12.5 %, whereas in *C. necator* 541 decreased to 0.233 ± 0.024 g L^{-1} ($Y_{R3HBA/Fruc}$=0.58 %) and in *C. necator* Δ*phaC* of 0.068 ± 0.013 g L^{-1}

($Y_{R3HBA/Fruc}$=1.13 %). No significant peaks were obtained for *C. necator* H16. The second confirmation of the successful *hbd* gene knock out for *C. necator* Δ*phaC* Δ*hbd* was evidenced by the reduced mobilization of R3HBA.

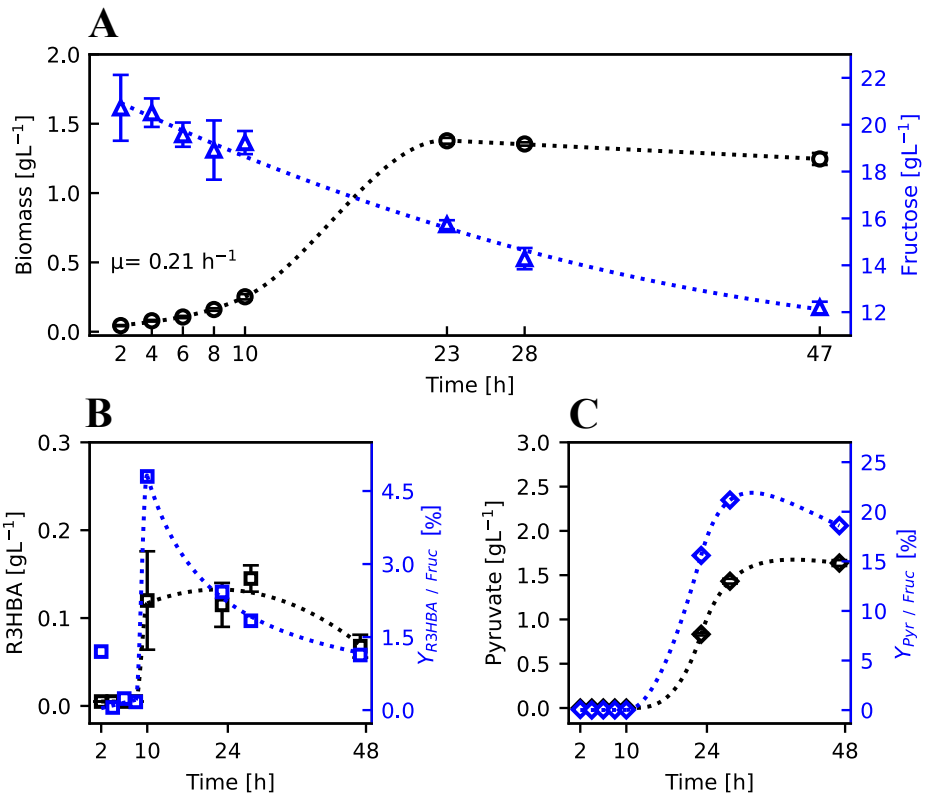

Figure 15. **Cell growth, fructose consumption, R3HBA and pyruvate production and yield in *C. necator* Δ*phaC***. The cultures were carried out in RE1 medium with 20 g L^{-1} of fructose and 1.0 g L^{-1} of ammonium sulphate at pH 7 and incubated at 30 °C for 48 h.

Shiraki et al. (2006) constructed a *C. necator* strain (H16_*bhd1*) capable of accumulating PHB but without Hbd activity by the deletion of *hbd* gene using suicide vector. After 60 hours of culture, both the wild type *C. necator* and the Δ*hbd* accumulated nearly 50% PHB from 2 % w/v of fructose. In this point, the culture was spiked with ammonium sulphate to yield 5 g L^{-1}. Under aerobic conditions, a spike of R3HBA was produced with a maximum of 10 mM (1 g L^{-1}) after 24 hours of depolymerization. The released R3HBA rapidly decreased by an unidentified mechanism. On the other hand, under anaerobic conditions in presence of ammonium sulphate, the R3HBA released by H16_*bhd1* increased to 3.1 g L^{-1}., higher than

the titer achieved using the wild-type strain, which released 0.520 g L^{-1}. Unfortunately, these titers required a depolymerization time of 100 hours under anaerobic conditions.

The strategy presented by Shiraki et al., (2006) relied on the depolymerization of the accumulated PHB. On the other hand, the *C. necator* Δ*phaC* and *C. necator* Δ*phaC* Δ*hbd* strains are unable to accumulate PHB but still release R3HBA, suggesting the presence of a native thioesterase enzyme that removes the CoA of R3HBA. A search in MetaCyc of thioesterase enzymes of *C. necator* resulted in 24 enzymes that were compared by protein BLAST analysis with *E. coli*'s Ycia enzyme sequence. The analysis showed that one enzyme in *C. necator*, WP_037025319.1 shows a percent identity of 44 % with Ycia. Probably this homologous thioesterase is related to the R3HBA release by removing a CoA when the PhaC are absent, but its mechanism and activation conditions are currently unknown.

The extracellular concentration of pyruvate was measured during the cultivation. After 23 hours of cultivation and when nitrogen was the limiting nutrient, pyruvate excretion of *C. necator* Δ*phaC* strain was 0.833 ± 0.014 g L^{-1} (Figure 15, panel C) and 24 hours after this concentration increased by 2-fold up to 1.64 ± 0.033 g L^{-1} ($Y_{Pyr/Fruc}$=18.6 %). It was hypothesized that pyruvate during unbalanced conditions started to accumulate inside the cell by the blockage of PHB synthesis and then was excreted into extracellular medium. The effect of a truncated PHB pathway produce an accumulation of acetyl-CoA, acetoacetyl-CoA and R3HBA-CoA, where the release of pyruvate is a response of the inhibitory effect of acetyl-CoA on the activity of pyruvate dehydrogenase (Jung & Lee, 1997). This behavior is a general characteristic of PHB-negative mutant strains and it has been previously described that the pyruvate excretion pattern of the PHB-negative mutant strains is according to the PHB accumulation pattern in the wild type strain (Jung & Lee, 1997). However, when a nitrogen source is added, pyruvate is consumed (Cook & Schlegel, 1978). The maximum value at 23 h time for *C. necator* 541 and *C. necator* Δ*phaC* Δ*hbd* of 0.244 ± 0.035 g L^{-1} (Figure 14, panel C), 0.576 ± 0.009 g L^{-1} (Figure 16, panel C) and then decreased almost to zero both according to the yield pattern of the pyruvate. Probably, the pyruvate consumed directs to synthesis of several amino acids (Raberg et al., 2014).

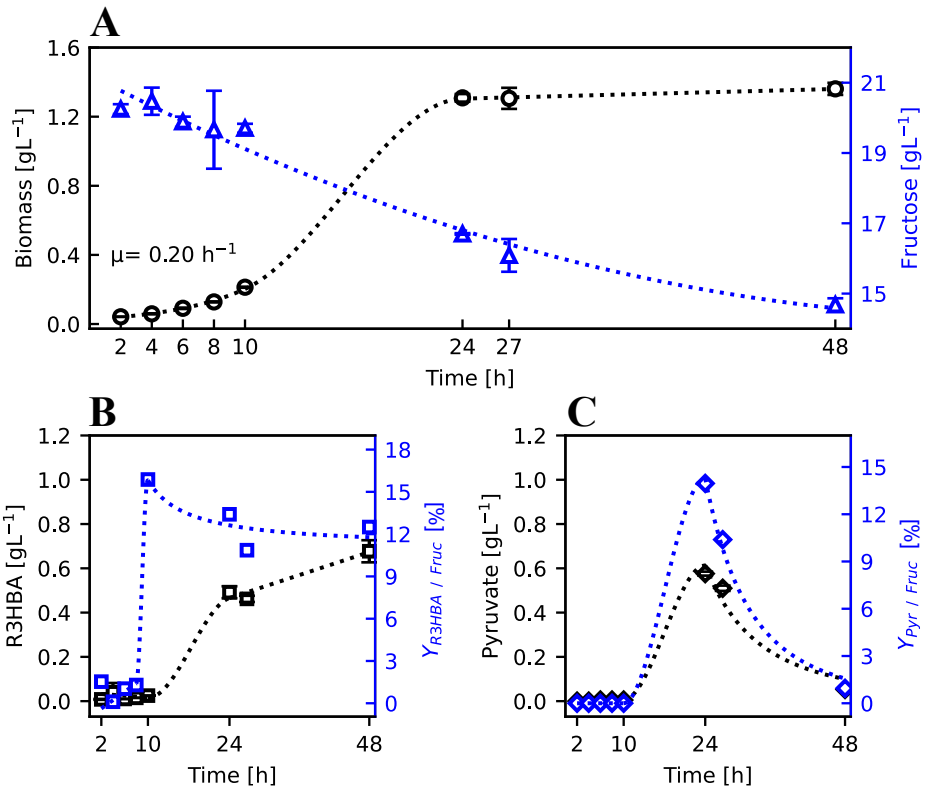

Figure 16. **Cell growth, fructose consumption, R3HBA and pyruvate production and yield in *C. necator* Δ*phaC* Δ*hbd***. The cultures were carried out in RE1 medium with 20 g L^{-1} of fructose and 1.0 g L^{-1} of ammonium sulfate at pH 7 and incubated at 30 °C for 48 h.

Finally, an experiment for confirming the influence of nitrogen and different pHs on the PHB depolymerization and R3HBA release in *C. necator* H16 was assayed. Figure 17 shows an assay for the R3HBA production in presence of a nitrogen source. *C. necator* H16 cells containing 80 % (8.92 ± 0.19 g L^{-1}) of PHB were washed and cultured in RE1 medium without fructose at 30 °C and, 250 rpm for 24 hours and subjected to pHs of 4, 7 and 10. The PHB concentration decreased under all pHs conditions. While at pH 4 and 7, similar PHB titer was found (4.69 ± 0.40 g L^{-1}, 3.99 ± 0.39 g L^{-1}), at pH 10 the PHB titer was reduced to 2.64 ± 0.44 g L^{-1} with a R3HBA concentration of title of 10 mg L^{-1} and a final pH of 8. At the initial pHs of 4 and 7, no R3HBA could be detected, suggesting that PHB was mobilized and used for growth and maintenance due to the presence of a nitrogen source and the constant aeration by the agitation. (Handrick et al, 2000).

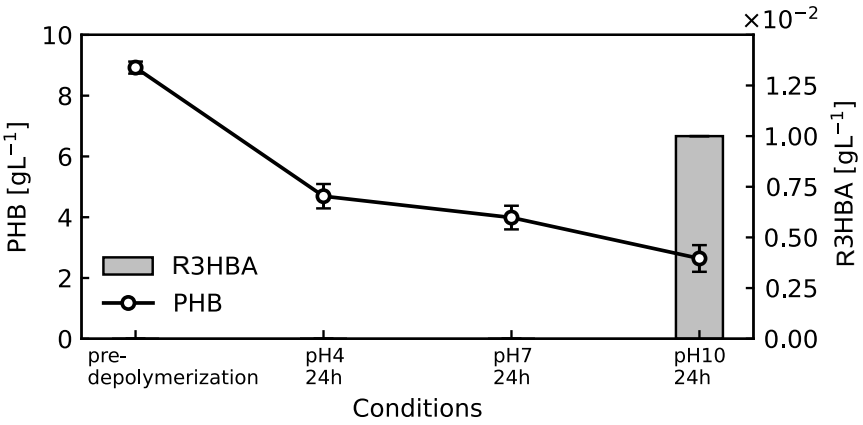

Figure 17. **Influence of pHs conditions in PHB depolymerization and R3HBA release in *C. necator* H16**. PHB accumulated cells of *C. necator* H16 were resuspended in RE1 medium w/o fructose at 4, 7, 10 pHs and incubated at 30 °C, 250 rpm for 24 h.

5. CONCLUSIONS

The results obtained in this work demonstrated the feasibility of R3HBA production by reducing or eliminating the fluxes of the reactions consuming R3HBA via operational manipulation as described in *M. parvus* and *A. lata* or via gene knock outs in *C. necator*.

A. lata DSM 1123 is a gram-negative facultative autotroph, with a growth associated PHB production. A complete characterization of this strain under chemostat cultures was undertaking in this thesis. Results showed that a significant PHB accumulation occurred under nitrogen, oxygen and especially in glucose-limited conditions. Dilution rates higher than 0.2 h^{-1} under glucose-limited chemostat resulted in an overflow of PHB. This suggests a counterintuitive PHB accumulation under glucose-limited conditions when only biomass production should be affected as seen in other bacteria (Ackermann & Babel, 1997; Page & Knosp, 1989). On other hand, *in vivo* PHB depolymerization was possible with a R3HBA yield of 93.4% at pH 4, but cell recycling was not feasible after incubation at acidic pH. The successful depolymerization in a two stage chemostat (a polymerization reactor followed by depolymerization tank) suggests that the genes PhaZ and Hbd are active under nitrogen-limited conditions.

R3HBA can be obtained in the supernatant from PHB accumulated cells of *M. parvus* using CH_4 as the sole carbon and energy source. The process, which involves the *in-vivo* depolymerization of PHB (PDS system) mediated by intracellular enzymes of *M. parvus*, attained a PHB to R3HBA conversion of 77.2 ± 0.9% after 72 hours of depolymerization at pH 11 in a mineral medium containing nitrate under aerobic conditions. The reduction of O_2 supply affected negatively the R3HBA yield, reducing it to 73% under microaerobic conditions. Similarly, increasing concentrations of exogenous R3HBA added to the broth at the beginning of the depolymerization process hindered the initial R3HBA release rate and the R3HBA yield, but not the PHB depolymerization yield. Finally, cells exposed to a reduced depolymerization time of 3 hours at pH 11 were able to grow in the presence of nitrogen and CH_4. However, the long times required at pH 11 for full PHB depolymerization (up to 72 h) limit the applicability of cell recycling.

The implementation of PDS system in *C. necator* was studied through the construction of two mutants: *C. necator* Δ*phaC* and *C. necator* Δ*phaC* Δ*hbd*. No accumulation of PHB was recorded. A maximum R3HBA titer of 0.145 ± 0.015 g L^{-1} was reached out in *C. necator* Δ*phaC* at 28 hours whereas for *C. necator* Δ*phaC* Δ*hbd* a R3HBA titer of 0.677 ± 0.05 g L^{-1} at 48 hours was observed, as expected by the *hbd* deletion. Interestingly, the truncated pathway of PHB synthesis provided an insight into the cell's metabolic situation: cells released R3HBA, exposed to a significant titer of pyruvate (as high as 1.63 ± 0.03 g L^{-1} in the strain *C. necator* Δ*phaC*), which was likely caused by the inhibitory effect of acetyl-CoA on the activity of pyruvate dehydrogenase (Jung & Lee, 1997).

C. necator Δ*phaC, C. necator* Δ*phaC* Δ*hbd* and *C. necator* 541 attained a peak R3HBA titer at 24 hours of culture, which was then completely consumed except in *C. necator* Δ*phaC* Δ*hbd* that R3HBA was not converted into acetoacetate. These results suggest that a native thioesterase of *C. necator* may play a role in the release of R3HBA by removing CoA from R3HBA-CoA. A protein homology on the genome of *C. necator* showed an enzyme encoded as WP_037025319.1 with a percent identity of 44 % in comparison with Ycia that may trigger R3HBA release.

The implementation of TSS system through of *tesB* via expression vector was not possible by inconsistencies in the assembly of the fragments in the constructed plasmids pLY01 and pLY02. These plasmids contained the *tesB* gene but showed other features as antibiotic resistance, an incomplete promoter fragment, and the origin replication site that were not suitable for the transformation in *C. necator* and *M. parvus*.

5.1. Future directions

A. lata showed an overflown metabolism that led to PHB accumulation under glucose conditions but it is necessary to identify the possible internal bottlenecks in fluxes of the central metabolism.

To further understand the effects of high R3HBA concentrations on the depolymerization kinetics in *M. parvus*, future work will include depolymerization experiments carried out at high initial PHB concentrations. Indeed, PHB concentrations between 1-100 g L^{-1} could be attained through biomass concentration using centrifugation to test the possibility of achieving high R3HBA titers without sacrificing yield or increasing the depolymerization time.

A first approach for the implementation of TSS in *M. parvus* will consider the elimination of fluxes involved in the reactions that consume R3HBA using genetic strategies via gene knock outs and could be complemented by the expression of *tesB* and *ycia* genes.

This work showed the R3HBA release in *C. necator* mutants with truncated PHB pathway synthesis, which suggests the existence of a native thioesterase that may act by removing the CoA of R3HBA-CoA. A natural next step should be addressing the knockout and the overexpression of this enzyme in *C. necator* Δ*phaC* and *C. necator* Δ*phaC* Δ*hbd* to investigate its physiological role and its biotechnological potential.

REFERENCES

Ackermann, J. U & Babel, W. (1997). Growth-associated synthesis of poly(hydroxybutyric acid) in *Methylobacterium rhodesianum* as an expression of an internal bottleneck. *Applied Microbiology and Biotechnology*, *47*(2), 144–149. https://doi.org/10.1007/s002530050903

Adkins, J., Pugh, S., McKenna, R., & Nielsen, D. R. (2012). Engineering microbial chemical factories to produce renewable "biomonomers." *Frontiers in Microbiology*, *3*(Aug), 1–12. https://doi.org/10.3389/fmicb.2012.00313

Agarwal, A. S., Zhai, Y., Hill, D., & Sridhar, N. (2011). The electrochemical reduction of carbon dioxide to formate/formic acid: Engineering and economic feasibility. *ChemSusChem*, *4*(9), 1301–1310. https://doi.org/10.1002/cssc.201100220

Amulya, K., Jukuri, S., & Venkata Mohan, S. (2015). Sustainable multistage process for enhanced productivity of bioplastics from waste remediation through aerobic dynamic feeding strategy: Process integration for up-scaling. *Bioresource Technology*, *188*, 231–239. https://doi.org/10.1016/j.biortech.2015.01.070

Anis, S. N. S., Annuar, M. S. M., & Simarani, K. (2018). Microbial biosynthesis and *in vivo* depolymerization of intracellular medium-chain-length poly-3-hydroxyalkanoates as potential route to platform chemicals. *Biotechnology and Applied Biochemistry*, *65*(6), 784–796. https://doi.org/10.1002/bab.1666

Asenjo, J. A., & Suk, J. S. (1986). Microbial Conversion of Methane into poly-β-hydroxybutyrate (PHB): Growth and intracellular product accumulation in a type II methanotroph. *Journal of Fermentation Technology*, *64*(4), 271–278. https://doi.org/10.1016/0385-6380(86)90118-4

Atlić, A., Koller, M., Scherzer, D., Kutschera, C., Grillo-Fernandes, E., Horvat, P., Chiellini, E., & Braunegg, G. (2011). Continuous production of poly([R]-3-hydroxybutyrate) by *Cupriavidus necator* in a multistage bioreactor cascade. *Applied Microbiology and Biotechnology*, *91*(2), 295–304. https://doi.org/10.1007/s00253-011-3260-0

Beaumont, L. J., Pitman, A., Perkins, S., Zimmermann, N. E., Yoccoz, N. G., & Thuiller, W. (2011). Impacts of climate change on the world's most exceptional ecoregions. *Proceedings of the National Academy of Sciences of the United States of America*, *108*(6), 2306–2311. https://doi.org/10.1073/pnas.1007217108

Bera, A., Dubey, S., Bhayani, K., Mondal, D., Mishra, S., & Ghosh, P. K. (2015). Microbial synthesis of polyhydroxyalkanoate using seaweed-derived crude levulinic acid as co-nutrient. *International Journal of Biological Macromolecules*, *72*, 487–494. https://doi.org/10.1016/j.ijbiomac.2014.08.037

Bertani, G. (1951). Studies on lysogenesis. I. The mode of phage liberation by lysogenic Escherichia coli. *Journal of Bacteriology*, *62*(3), 293–300.

Bhati, R., & Mallick, N. (2016). Carbon dioxide and poultry waste utilization for production of polyhydroxyalkanoate biopolymers by *Nostoc muscorum* Agardh: a sustainable approach. *Journal of Applied Phycology*, *28*(1), 161–168. https://doi.org/10.1007/s10811-015-0573-x

Bordel, S., Rojas, A., & Muñoz, R. (2019). Reconstruction of a Genome Scale Metabolic Model of the polyhydroxybutyrate producing methanotroph *Methylocystis parvus* OBBP. *Microbial Cell Factories*, *18*(1), 1–11. https://doi.org/10.1186/s12934-019-1154-5

Borrero-de Acuña, J. M., Aravena-Carrasco, C., Gutierrez-Urrutia, I., Duchens, D., & Poblete-Castro, I. (2019). Enhanced synthesis of medium-chain-length poly(3-hydroxyalkanoates) by inactivating the tricarboxylate transport system of *Pseudomonas putida* KT2440 and process development using waste vegetable oil. *Process Biochemistry*, *77*, 23–30. https://doi.org/10.1016/j.procbio.2018.10.012

Braunegg, G., Bona, R; Koller, M. (2004). Sustainable polymer production. *Polymer-Plastics Technology and Engineering*, *43*, 1779–1793. https://doi.org/doi: 10.1081/PPT-200040130

Bresan, S., Sznajder, A., Hauf, W., Forchhammer, K., Pfeiffer, D., & Jendrossek, D. (2016). Polyhydroxyalkanoate (PHA) granules have no phospholipids. *Scientific Reports*, *6*(March), 1–13. https://doi.org/10.1038/srep26612

Brigham, C. (2019). Perspectives for the biotechnological production of biofuels from CO_2 and H_2 using *Ralstonia eutropha* and other 'Knallgas' bacteria. *Applied Microbiology and Biotechnology*, *103*(5), 2113–2120. https://doi.org/10.1007/s00253-019-09636-y

Brigham, C. J., Speth, D. R., Rha, C. K., & Sinskey, A. J. (2012). Whole-genome microarray and gene deletion studies reveal regulation of the polyhydroxyalkanoate production cycle by the stringent response in *Ralstonia eutropha* H16. *Applied and Environmental Microbiology*, *78*(22), 8033–8044. https://doi.org/10.1128/AEM.01693-12

Bugnicourt, E., Cinelli, P., Lazzeri, A., & Alvarez, V. (2014). Polyhydroxyalkanoate (PHA): Review of synthesis, characteristics, processing and potential applications in packaging. *Express Polymer Letters*, *8*(11), 791–808. https://doi.org/10.3144/expresspolymlett.2014.82

Cao, Q., Zhang, J., Liu, H., Wu, Q., Chen, J., & Chen, G. Q. (2014). The mechanism of anti-osteoporosis effects of 3-hydroxybutyrate and derivatives under simulated microgravity. *Biomaterials*, *35*(28), 8273–8283. https://doi.org/10.1016/j.biomaterials.2014.06.020

Carmichael, J. T., & Brulle, R. J. (2017). Elite cues, media coverage, and public concern: an integrated path analysis of public opinion on climate change, 2001–2013. *Environmental Politics*, *26*(2), 232–252. https://doi.org/10.1080/09644016.2016.1263433

Chen, G. Q. (2009). A microbial polyhydroxyalkanoates (PHA) based bio- and materials industry. *Chemical Society Reviews*, *38*(8), 2434–2446. https://doi.org/10.1039/b812677c

Chen, G. Q., König, K. H., & Lafferty, R. M. (1991). Production of poly-D(-)-3-hydroxybutyrate and poly-D(-)-3-hydroxyvalerate by strains of *Alcaligenes latus*. *Antonie van Leeuwenhoek*, *60*(1), 61–66. https://doi.org/10.1007/BF00580443

Chen, G. Q., & Wu, Q. (2005). Microbial production and applications of chiral hydroxyalkanoates. *Applied Microbiology and Biotechnology*, *67*(5), 592–599. https://doi.org/10.1007/s00253-005-1917-2

Chen, X., Zhou, L., Tian, K., Kumar, A., Singh, S., Prior, B. A., & Wang, Z. (2013). Metabolic engineering of *Escherichia coli*: A sustainable industrial platform for bio-based chemical production. *Biotechnology Advances*, *31*(8), 1200–1223. https://doi.org/10.1016/j.biotechadv.2013.02.009

Chiba, T., & Nakai, T. (1985). a Synthetic Approach To (+)-Thienamycin From Methyl (R)-3-Hydroxybutanoate. a New Entry To (3 R , 4 R)-3-[(R)-1-Hydroxyethyl]-4-Acetoxy-2-Azetidinone. *Chemistry Letters*, *14*(5), 651–654. https://doi.org/10.1246/cl.1985.651

Choi, M. H., Yoon, S. C., & Lenz, R. W. (1999). Production of poly(3-hydroxybutyric acid-Co-4-hydroxybutyric acid) and poly(4-hydroxybutyric acid) without subsequent degradation by *Hydrogenophaga pseudoflava*. *Applied and Environmental Microbiology*, *65*(4), 1570–1577. https://doi.org/10.1128/aem.65.4.1570-1577.1999

Cook, A. M., & Schlegel, H. G. (1978). Metabolite concentrations in *Alcaligenes eutrophus* H 16 and a mutant defective in poly-β-hydroxybutyrate synthesis. *Archives of Microbiology*, *119*(3), 231–235. https://doi.org/10.1007/BF00405400

Crépin, L., Lombard, E., & Guillouet, S. E. (2016). Metabolic engineering of *Cupriavidus necator* for heterotrophic and autotrophic alka(e)ne production. *Metabolic Engineering*, *37*, 92–101. https://doi.org/10.1016/j.ymben.2016.05.002

Cruz, M. V., Freitas, F., Paiva, A., Mano, F., Dionísio, M., Ramos, A. M., & Reis, M. A. M. (2016). Valorization of fatty acids-containing wastes and byproducts into short- and medium-chain length polyhydroxyalkanoates. *New Biotechnology*, *33*(1), 206–215. https://doi.org/10.1016/j.nbt.2015.05.005

Cruz, M. V., Paiva, A., Lisboa, P., Freitas, F., Alves, V. D., Simões, P., Barreiros, S., & Reis, M. A. M. (2014). Production of polyhydroxyalkanoates from spent coffee grounds oil obtained by supercritical fluid extraction technology. *Bioresource Technology*, *157*, 360–363. https://doi.org/10.1016/j.biortech.2014.02.013

de Paula, F. C., Kakazu, S., de Paula, C. B. C., Gomez, J. G. C., & Contiero, J. (2017). Polyhydroxyalkanoate production from crude glycerol by newly isolated *Pandoraea* sp. Polyhydroxyalkanoate production from crude glycerol. *Journal of King Saud University - Science*, *29*(2), 166–173. https://doi.org/10.1016/j.jksus.2016.07.002

de Roo, G., Kellerhals, M. B., Ren, Q., Witholt, B., & Kessler, B. (2002). Production of Chiral R -3-Hydroxyalkanoic Acids and R -3-Hydroxyalkanoic Acid Methylesters via Hydrolytic Degradation of Polyhydroxyalkanoate Synthesized by *Pseudomonas* sp. 3–8. https://doi.org/10.1002/bit.10134

del Cerro, C., García, J. M., Rojas, A., Tortajada, M., Ramón, D., Galán, B., Prieto, M. A., & García, J. L. (2012). Genome sequence of the methanotrophic poly-β-hydroxybutyrate producer *Methylocystis parvus* OBBP. *Journal of Bacteriology*, *194*(20), 5709–5710. https://doi.org/10.1128/JB.01346-12

Dietrich, K., Dumont, M. J., Del Rio, L. F., & Orsat, V. (2017). Producing PHAs in the bioeconomy—Towards a sustainable bioplastic. *Sustainable Production and Consumption*, *9*, 58–70. https://doi.org/10.1016/j.spc.2016.09.001

Dlugokencky, E. (2020). *Trends in Atmospheric Methane*. https://gml.noaa.gov/ccgg/trends_ch4/

Dmitrieva-Posocco, O., Wong, A. C., Lundgren, P., Golos, A. M., Descamps, H. C., Dohnalová, L., Cramer, Z., Tian, Y., Yueh, B., Eskiocak, O., Egervari, G., Lan, Y., Liu, J., Fan, J., Kim, J., Madhu, B., Schneider, K. M., Khoziainova, S., Andreeva, N., et al. (2022). β-Hydroxybutyrate suppresses colorectal cancer. *Nature*, *605*(7908), 160–165. https://doi.org/10.1038/s41586-022-04649-6

Doi, Y., Segawa, A., Kawaguchi, Y., & Kunioka, M. (1990). Cyclic nature of poly(3-hydroxyalkanoate) metabolism in *Alcaligenes eutrophus*. *FEMS Microbiology Letters*, *67*(1–2), 165–169. https://doi.org/10.1111/j.1574-6968.1990.tb13856.x

Durner, R., Witholt, B., & Egli, T. (2000). Accumulation of poly[(R)-3-hydroxyalkanoates] in *Pseudomonas oleovorans* during growth with octanoate in continuous culture at different dilution rates. *Applied and Environmental Microbiology*, *66*(8), 3408–3414. https://doi.org/10.1128/AEM.66.8.3408-3414.2000

Edenhofer, O. (2014). IPCC 2014 Mitigation of Climate Change. Contribution of Working Group III to the Fifth Assessment Report of the Intergovernmental Panel on Climate Change. In *Cambridge: Cambridge University Press*.

Estrada, J. M., Lebrero, R., Quijano, G., Pérez, R., Figueroa-González, I., García-Encina, P. A., & Muñoz, R. (2014). Methane abatement in a gas-recycling biotrickling filter: Evaluating innovative operational strategies to overcome mass transfer limitations. *Chemical Engineering Journal*, *253*, 385–393. https://doi.org/10.1016/j.cej.2014.05.053

Etminan, M., Myhre, G., Highwood, E. J., & Shine, K. P. (2016). Radiative forcing of carbon dioxide, methane, and nitrous oxide: A significant revision of the methane radiative forcing. *Geophysical Research Letters*, *43*(24),614-623. https://doi.org/10.1002/2016GL071930

Fei, T., Cazeneuve, S., Wen, Z., Wu, L., & Wang, T. (2016). Effective Recovery of Poly-β-Hydroxybutyrate (PHB) Biopolymer from *Cupriavidus necator* Using a Novel and Environmentally Friendly Solvent System. *Biotechnology progress*. 32(3), 678–685 https://doi.org/10.1002/btpr.2247

Follonier, S., Riesen, R., & Zinn, M. (2015). Pilot-scale production of functionalized mcl-PHA from grape pomace supplemented with fatty acids. *Chemical and Biochemical Engineering Quarterly*, *29*(2), 113–121. https://doi.org/10.15255/CABEQ.2014.2251

Fuhrmann, E., & Talbiersky, J. (2005). Synthesis of alkyl aryl ethers by catalytic Williamson ether synthesis with weak alkylation agents. *Organic Process Research and Development*, *9*(2), 206–211. https://doi.org/10.1021/op050001h

Gao, X., Chen, J. C., Wu, Q., & Chen, G. Q. (2011). Polyhydroxyalkanoates as a source of chemicals, polymers, and biofuels. *Current Opinion in Biotechnology*, *22*(6), 768–774. https://doi.org/10.1016/j.copbio.2011.06.005

Gebauer, B., & Jendrossek, D. (2006). Assay of poly(3-hydroxybutyrate) depolymerase activity and product determination. *Applied and Environmental Microbiology*, *72*(9), 6094–6100. https://doi.org/10.1128/AEM.01184-06

Geyer, R., Jambeck, J. R., & Law, K. L. (2017). Production, use, and fate of all plastics ever made. *Science Advances*, *3*(7), 3–8. https://doi.org/10.1126/sciadv.1700782

Ghasemi Ghodrat, A., Tabatabaei, M., Aghbashlo, M., & Mussatto, S. I. (2018). Waste Management Strategies; the State of the Art. In M. Tabatabaei & H. Ghanavati (Eds.), *Biogas: Fundamentals, Process, and Operation* (pp. 1–33). Springer International Publishing. https://doi.org/10.1007/978-3-319-77335-3_1

Gibson, D. G., Young, L., Chuang, R. Y., Venter, J. C., Hutchison, C. A., & Smith, H. O. (2009). Enzymatic assembly of DNA molecules up to several hundred kilobases. *Nature Methods*, *6*(5), 343–345. https://doi.org/10.1038/nmeth.1318

Gómez Cardozo, J. R., Mora Martínez, A. L., Yepes Pérez, M., & Correa Londoño, G. A. (2016). Production and Characterization of Polyhydroxyalkanoates and Native Microorganisms Synthesized from Fatty Waste. *International Journal of Polymer Science*, *2016*, 6541718. https://doi.org/10.1155/2016/6541718

Gorenflo, V., Schmack, G., Vogel, R., & Steinbu, A. (2001). Development of a Process for the Biotechnological Large-Scale Production of 4-Hydroxyvalerate-Containing Polyesters and Characterization of Their Physical and Mechanical Properties. 45–57. *Biomacromolecules*. 20012 (1),45-57. doi: 10.1021/bm0000992

Grousseau, E., Blanchet, E., Déléris, S., Albuquerque, M. G. E., Paul, E., & Uribelarrea, J. L. (2013). Impact of sustaining a controlled residual growth on polyhydroxybutyrate yield and production kinetics in *Cupriavidus necator*. *Bioresource Technology*, 148, 30–38. https://doi.org/10.1016/j.biortech.2013.08.120

Guevara-Martínez, M., Perez-Zabaleta, M., Gustavsson, M., Quillaguamán, J., Larsson, G., & van Maris, A. J. A. (2019). The role of the acyl-CoA thioesterase "YciA" in the production of (R)-3-hydroxybutyrate by recombinant *Escherichia coli*. *Applied Microbiology and Biotechnology*, *103*(9), 3693–3704. https://doi.org/10.1007/s00253-019-09707-0

Haage, G., Wallner, E., Bona, R., Schellauf, F., & Braunegg, G. (2001). Production of Poly-3-hydroxybutyrate-co-3-hydroxy-valerate with *Alcaligenes latus* DSM 1124 on Various Carbon Sources. *Biorelated Polymers*, 147–155. https://doi.org/10.1007/978-1-4757-3374-7_13

Haas, C., Steinwandter, V., De Apodaca, E. D., Madurga, B. M., Smerilli, M., Dietrich, T., & Neureiter, M. (2015). Production of PHB from chicory roots-Comparison of three *Cupriavidus necator* strains. *Chemical and Biochemical Engineering Quarterly*, *29*(2), 99–112. https://doi.org/10.15255/CABEQ.2014.2250

Hahn, S. K., Chang, Y. K., Kim, B. S., & Chang, H. N. (1994). Optimization of microbial poly(3-hydroxybutyrate) recover using dispersions of sodium hypochlorite solution and chloroform. *Biotechnology and Bioengineering*, 44(2), 256–261. https://doi.org/10.1002/bit.260440215

Hamilton, Li. A., Feit, S., Muffet, C., Kelso, M., Rubright, S., & Bernhardt, Co. (2019). *Executive Summary. Plastic Proliferation Threatens the Climate on a Global Scale*. https://www.ciel.org/wp-content/uploads/2019/05/Plastic-and-Climate-FINAL-2019.pdf

Hanahan, D. (1983). Studies on transformation of *Escherichia coli* with plasmids. *Journal of Molecular Biology*, *166*(4), 557–580. https://doi.org/10.1016/S0022-2836(83)80284-8

Handrick, R., Reinhardt, S., Focarete, M. L., Scandola, M., Adamus, G., Kowalczuk, M., & Jendrossek, D. (2001). A New Type of Thermoalkalophilic Hydrolase of *Paucimonas lemoignei* with High Specificity for Amorphous Polyesters of Short Chain-length Hydroxyalkanoic Acids. *Journal of Biological Chemistry*, 276(39), 36215–36224. https://doi.org/10.1074/jbc.M101106200

Handrick, R., Reinhardt, S., & Jendrossek, D. (2000). Mobilization of poly(3-hydroxybutyrate) in *Ralstonia eutropha*. *Journal of Bacteriology*, 182(20), 5916–5918. https://doi.org/10.1128/JB.182.20.5916-5918.2000

Hänggi, U. J. (1990). Pilot scale production of PHB with *Alcaligenes latus*. *Novel Biodegradable Microbial Polymers*, 65–70. https://doi.org/10.1007/978-94-009-2129-0_6

Hanson, R. S., & Hanson, T. E. (1996). Methanotrophic bacteria. *Microbiological Reviews*, *60*(2), 439–471. https://doi.org/10.1128/mr.60.2.439-471.1996

Hazer, D. B., Kiliçay, E., & Hazer, B. (2012). Poly(3-hydroxyalkanoate)s: Diversification and biomedical applications: A state of the art review. *Materials Science and Engineering C*, *32*(4), 637–647. https://doi.org/10.1016/j.msec.2012.01.021

Henderson, R. A., & Jones, C. W. (1997). Physiology of poly-3-hydroxybutyrate (PHB) production by *Alcaligenes eutrophus* growing in continuous culture. *Microbiology*, *143*(7), 2361–2371. https://doi.org/10.1099/00221287-143-7-2361

Hiroe, A., Chek, M. F., Hakoshima, T., Sudesh, K., & Taguchi, S. (2019). Synthesis of Polyesters III: Acyltransferase as Catalyst. In: Enzymatic Polymerization towards Green Polymer Chemistry. Green Chemistry and Sustainable Technology. *Springer* https://doi.org/10.1007/978-981-13-3813-7_7

Holmes, P. A. (1985). Applications of PHB - A microbially produced biodegradable thermoplastic. *Physics in Technology*, *16*(1), 32–36. https://doi.org/10.1088/0305-4624/16/1/305

Howe, P. D., Mildenberger, M., Marlon, J. R., & Leiserowitz, A. (2015). Geographic variation in opinions on climate change at state and local scales in the USA. *Nature Climate Change*, *5*(6), 596–603. https://doi.org/10.1038/nclimate2583

IEA. (2020). *Methane Tracker 2020*. https://www.iea.org/reports/methane-tracker-2020

Irving, S. E., Choudhury, N. R., & Corrigan, R. M. (2021). The stringent response and physiological roles of (pp)pGpp in bacteria. *Nature Reviews Microbiology*, *19*(4), 256–271. https://doi.org/10.1038/s41579-020-00470-y

J. A. Ramsay, E. Berger, R. Voyer, C. Chavarie, B. A. R. (1994). Extraction of poly-3-hydroxybutyrate using chlorinated solvents. *8*(8), 589–594.

James, B. W., Mauchline, W. S., Dennis, P. J., Keevil, C. W., & Wait, R. (1999). Poly-3-hydroxybutyrate in *Legionella pneumophila*, an energy source for survival in low-nutrient environments. *Applied and Environmental Microbiology*, *65*(2), 822–827. https://doi.org/10.1128/aem.65.2.822-827.1999

Jawaharraj, K., Shrestha, N., Chilkoor, G., Dhiman, S. S., Islam, J., & Gadhamshetty, V. (2020). Valorization of methane from environmental engineering applications: A critical review. *Water Research*, *187*, 116400. https://doi.org/10.1016/j.watres.2020.116400

Jendrossek, D; Handrick, R. (2002). Microbial degradation of polyhydroxyalkanoates. *Annual Review of Microbiology*, *56*(1), 403–432. https://doi.org/10.1146/annurev.micro.56.012302.160838

Jers, C., Kalantari, A., Garg, A., & Mijakovic, I. (2019). Production of 3-Hydroxypropanoic Acid From Glycerol by Metabolically Engineered Bacteria. *Frontiers in Bioengineering and Biotechnology*, *7*(May), 1–15. https://doi.org/10.3389/fbioe.2019.00124

Jossek, R., Reichelt, R., & Steinbüchel, A. (1998). *In vitro* biosynthesis of poly(3-hydroxybutyric acid) by using purified poly(hydroxyalkanoic acid) synthase of *Chromatium vinosum*. *Applied Microbiology and Biotechnology*, *49*(3), 258–266. https://doi.org/10.1007/s002530051166

Juengert, J. R., Borisova, M., Mayer, C., Wolz, C., Brigham, C. J., & Sinskey, A. J. (2017). Absence of ppGpp Leads to Increased Mobilization of Intermediately Accumulated Poly(3-Hydroxybutyrate) in *Ralstonia eutropha* H16. *Applied and Environmental Microbiology*, *83*(13), 1–16. https://doi.org/https://doi.org/10.1128/AEM.00755-17

Juengert, J. R., Cameron, P., Dieter, J., & Maia, K. (2018). Poly(3-Hydroxybutyrate) (PHB) Polymerase PhaC1 and PHB Depolymerase PhaZa1 of *Ralstonia eutropha* Are Phosphorylated *In Vivo*. *Applied and Environmental Microbiology*, *84*(13), e00604-18. https://doi.org/10.1128/AEM.00604-18

Jung, Young-Mi; Lee, Y.-H. (1997). Investigation of Regulatory Mechanism of Flux of Acetyl-CoA in *Alcaligenes eutrophus* Using PHB-negative Mutant and Transformants Harboring Cloned *phbCAB* Genes. *Journal of Microbiology and Biotechnology*, *7*(4), 215–222.

Kashiwaya, Y., Takeshima, T., Mori, N., Nakashima, K., Clarke, K., & Veech, R. L. (2000). D-β-hydroxybutyrate protects neurons in models of Alzheimer's and Parkinson's disease. *Proceedings of the National Academy of Sciences of the United States of America*, *97*(10), 5440–5444. https://doi.org/10.1073/pnas.97.10.5440

Katayama, M., Hiraide, A., Sugimoto, H., Yoshioka, T., & Sugimoto, T. (1994). Effect of Ketone Bodies on Hyperglycemia and Lactic Acidemia in Hemorrhagic Stress. *Journal of Parenteral and Enteral Nutrition*, *18*(5), 442–446. https://doi.org/10.1177/0148607194018005442

Kawata, Y., Ando, H., Matsushita, I., & Tsubota, J. (2014). Efficient secretion of (R)-3-hydroxybutyric acid from *Halomonas* sp. KM-1 by nitrate fed-batch cultivation with glucose under microaerobic conditions. *Bioresource Technology*, *156*, 400–403. https://doi.org/10.1016/j.biortech.2014.01.073

Kawata, Y., Kawasaki, K., & Shigeri, Y. (2012). Efficient secreted production of (R)-3-hydroxybutyric acid from living *Halomonas* sp. KM-1 under successive aerobic and microaerobic conditions. *Applied Microbiology and Biotechnology*, *96*(4), 913–920. https://doi.org/10.1007/s00253-012-4218-6

Kawata, Y., Nojiri, M., Matsushita, I., & Tsubota, J. (2015). Improvement of (R)-3-hydroxybutyric acid secretion during *Halomonas* sp. KM-1 cultivation with saccharified Japanese cedar by the addition of urea. *Letters in Applied Microbiology*, *61*(4), 397–402. https://doi.org/10.1111/lam.12473

Khosravi-Darani, K., & Bucci, D. Z. (2015). Application of poly(hydroxyalkanoate) in food packaging: Improvements by nanotechnology. In *Chemical and Biochemical Engineering Quarterly* (Vol. 29, Issue 2, pp. 275–285). https://doi.org/10.15255/CABEQ.2014.2260

Khosravi-Darani, K., Mokhtari, Z. B., Amai, T., & Tanaka, K. (2013). Microbial production of poly(hydroxybutyrate) from C1 carbon sources. *Applied Microbiology and Biotechnology*, *97*(4), 1407–1424. https://doi.org/10.1007/s00253-012-4649-0

Kim, B. S., Lee, S. C., Lee, S. Y., Chang, H. N., Chang, Y. K., & Woo, S. I. (1994). Production of poly(3-hydroxybutyric acid) by fed-batch culture of *Alcaligenes eutrophus* with glucose concentration control. *Biotechnology and Bioengineering*, *43*, 892–898. doi: 10.1002/bit.260430908

Kim, M., Cho, K., Ryu, H. W., Lee, E. G., & Chang, Y. K. (2003). Recovery of poly (3-hydroxybutyrate) from high cell density culture of *Ralstonia eutropha* by direct addition of sodium dodecyl sulfate. *Biotechnology Letters*, 25(1), 55–59. doi: 10.1023/a:1021734216612

Kim, T.W., Park, J.S., & Lee, Y.H. (1996). Enzymatic Characteristics of Biosynthesis and Degradation of Poly-β-hydroxybutyrate of *Alcaligenes latus*. Journal of Microbiology and Biotechnology, 6, 425-431.

Knoll, M., Hamm, T. M., Wagner, F., Martinez, V., & Pleiss, J. (2009). The PHA Depolymerase Engineering Database : A systematic analysis tool for the diverse family of polyhydroxyalkanoate (PHA) depolymerases. *BMC Bioinformatics*, 10, 1–8. https://doi.org/10.1186/1471-2105-10-89

Koller, M. (2014). Poly(hydroxyalkanoates) for Food Packaging: Application and Attempts towards Implementation. *Applied Food Biotechnology*, *1*, 3–15. https://doi.org/doi.org/10.22037/afb.v1i1.7127

Kosseva, M. R., & Rusbandi, E. (2018). International Journal of Biological Macromolecules Trends in the biomanufacture of polyhydroxyalkanoates with focus on downstream processing. *International Journal of Biological Macromolecules*, *107*, 762–778. https://doi.org/10.1016/j.ijbiomac.2017.09.054

Kumar, P., Ray, S., & Kalia, V. C. (2016). Production of co-polymers of polyhydroxyalkanoates by regulating the hydrolysis of biowastes. *Bioresource Technology*, *200*, 413–419. https://doi.org/10.1016/j.biortech.2015.10.045

Kunasundari, B., & Sudesh, K. (2011). Isolation and recovery of microbial polyhydroxyalkanoates. *Polymer letters*, *5*(7), 620–634. https://doi.org/10.3144/expresspolymlett.2011.60

Lafferty, R. M., & Heinzle, E. (1977). Cyclic carbonic acid esters as solvents for poly-(β)-hydroxybutyric acid. In *U.S. Patent*. https://patents.google.com/patent/US4101533

Latimer, A. A., Kakekhani, A., Kulkarni, A. R., & Nørskov, J. K. (2018). Direct Methane to Methanol: The Selectivity-Conversion Limit and Design Strategies. *ACS Catalysis*, *8*(8), 6894–6907. https://doi.org/10.1021/acscatal.8b00220

Lawrence, A. G., Schoenheit, J., He, A., Tian, J., Liu, P., Stubbe, J., & Sinskey, A. J. (2005). Transcriptional analysis of *Ralstonia eutropha* genes related to poly-(R)-3-hydroxybutyrate homeostasis during batch fermentation. *Applied Microbiology and Biotechnology*, *68*(5), 663–672. https://doi.org/10.1007/s00253-005-1969-3

Lee, I. Y., Kim, M. K., Chang, H. N., & Park, Y. H. (1995). Regulation of poly-β-hydroxybutyrate biosynthesis by nicotinamide nucleotide in *Alcaligenes eutrophus*. In *FEMS Microbiology Letters*, 131(1), 35–39. https://doi.org/10.1016/0378-1097(95)00231-S

Lee, S. Y., & Lee, Y. (2003). Metabolic Engineering of *Escherichia coli* for Production of Enantiomerically Pure (R)-(-)-Hydroxycarboxylic Acids. *Applied and Environmental Microbiology*, *69*(6), 3421–3426. https://doi.org/10.1128/AEM.69.6.3421-3426.2003

Lee, S. Y., Lee, Y., & Wang, F. (1999). Chiral compounds from bacterial polyesters: Sugars to plastics to fine chemicals. *Biotechnology and Bioengineering*, *65*(3), 363–368. https://doi.org/10.1002/(SICI)1097-0290(19991105)65:3<363::AID-BIT15>3.0.CO;2-1

Lee, Y., Hyun, S., Taek, I., Han, K., & Yup, S. (2000). Preparation of alkyl (R)-(–)-3-hydroxybutyrate by acidic alcoholysis of poly-(R)-(–)-3-hydroxybutyrate. *Enzyme and Microbial Technology*, *27*, 33–36. https://doi.org/10.1016/s0141-0229(00)00146-0

Levett, I., Birkett, G., Davies, N., Bell, A., Langford, A., Laycock, B., Lant, P., & Pratt, S. (2016). Techno-economic assessment of poly-3-hydroxybutyrate (PHB) production from methane - The case for thermophilic bioprocessing. *Journal of Environmental Chemical Engineering*, *4*(4), 3724–3733. https://doi.org/10.1016/j.jece.2016.07.033

Li, F., Zhang, C., Liu, Y., Liu, D., Xia, H., & Chen, S. (2016). Efficient production of (R)-3-hydroxybutyric acid by *Pseudomonas* sp. DS1001a and its extracellular poly(3-hydroxybutyrate) depolymerase. *Process Biochemistry*, *51*(3), 369–373. https://doi.org/10.1016/j.procbio.2015.12.016

Liddell, J. M. (1999). Process for the recovery of Polyhydroxyalkanoic acid. In *U.S. Patent*.

Listewnik, H. F., Wendlandt, K. D., Jechorek, M., & Mirschel, G. (2007). Process design for the microbial synthesis of Poly-β-hydroxybutyrate (PHB) from natural gas. *Engineering in Life Sciences*, *7*(3), 278–282. https://doi.org/10.1002/elsc.200620193

Liu, Q., Ouyang, S. P., Chung, A., Wu, Q., & Chen, G. Q. (2007). Microbial production of R-3-hydroxybutyric acid by recombinant *E. coli* harboring genes of *phbA*, *phbB*, and *tesB*. *Applied Microbiology and Biotechnology*, *76*(4), 811–818. https://doi.org/10.1007/s00253-007-1063-0

Loo, C. Y., Lee, W. H., Tsuge, T., Doi, Y., & Sudesh, K. (2005). Biosynthesis and characterization of poly(3-hydroxybutyrate-co-3- hydroxyhexanoate) from palm oil products in a *Wautersia eutropha* mutant. *Biotechnology Letters*, *27*(18), 1405–1410. https://doi.org/10.1007/s10529-005-0690-8

Loow, Y. L., Wu, T. Y., Jahim, J. M., Mohammad, A. W., & Teoh, W. H. (2016). Typical conversion of lignocellulosic biomass into reducing sugars using dilute acid hydrolysis and alkaline pretreatment. *Cellulose*, *23*(3), 1491–1520. https://doi.org/10.1007/s10570-016-0936-8

Lu, J., Brigham, C. J., Gai, C. S., & Sinskey, A. J. (2012). Studies on the production of branched-chain alcohols in engineered *Ralstonia eutropha*. *Applied Microbiology and Biotechnology*, *96*(1), 283–297. https://doi.org/10.1007/s00253-012-4320-9

Lu, J., Brigham, C. J., Li, S., & Sinskey, A. J. (2016). *Ralstonia eutropha* H16 as a Platform for the Production of Biofuels, Biodegradable Plastics, and Fine Chemicals from Diverse Carbon Resources. In *Biotechnology for Biofuel Production and Optimization*. Elsevier B.V. https://doi.org/10.1016/B978-0-444-63475-7.00012-1

Lu, J., Takahashi, A., & Ueda, S. (2014). 3-Hydroxybutyrate oligomer hydrolase and 3-hydroxybutyrate dehydrogenase participate in intracellular polyhydroxybutyrate and polyhydroxyvalerate degradation in *Paracoccus denitrificans*. *Applied and Environmental Microbiology*, *80*(3), 986–993. https://doi.org/10.1128/AEM.03396-13

Lu, J., Tappel, R. C., & Nomura, C. T. (2009). Mini-review: Biosynthesis of poly(hydroxyalkanoates). *Polymer Reviews*, *49*(3), 226–248. https://doi.org/10.1080/15583720903048243

Martin, Robert; Thomas, Jhon; Soni, M. (2021). Evaluation of the generally recognized as safe *(GRAS)* status of D-6-hydroxybutyrate (D-BHB) as a food ingredient. https://www.fda.gov/media/157969/download

Massieu, L., Haces, M. L., Montiel, T., & Hernández-Fonseca, K. (2003). Acetoacetate protects hippocampal neurons against glutamate-mediated neuronal damage during glycolysis inhibition. *Neuroscience*, *120*(2), 365–378. https://doi.org/10.1016/S0306-4522(03)00266-5

Matsuyama, A., Yamamoto, H., Kawada, N., & Kobayashi, Y. (2001). Industrial production of (R)-1,3-butanediol by new biocatalysts. *Journal of Molecular Catalysis B: Enzymatic*, *11*(4–6), 513–521. https://doi.org/10.1016/S1381-1177(00)00032-1

Mikkili, I., Karlapudi, A.P., JohnBabu, D., Nath, S., & Kodali, V.P. (2014). Isolation, Screening and Extraction of Polyhydroxybutyrate (PHB) producing bacteria from Sewage sample. *International Journal of PharmTech Research*, 6(2), 850-857

Misra, S. K., Valappil, S. P., Roy, I., & Boccaccini, A. R. (2006). Polyhydroxyalkanoate (PHA)/inorganic phase composites for tissue engineering applications. *Biomacromolecules*, *7*(8), 2249–2258. https://doi.org/10.1021/bm060317c

Mohamad Noh, N. (2017). Catalytic Route for the Synthesis of Cyclic Organic Carbonates from Renewable Polyols [Doctoral disertation]. https://livrepository.liverpool.ac.uk/id/eprint/3012167

Mothes, G., Schnorpfeil, C., & Ackermann, J. U. (2007). Production of PHB from crude glycerol. *Engineering in Life Sciences*, *7*(5), 475–479. https://doi.org/10.1002/elsc.200620210

Mountassif, D., Andreoletti, P., Cherkaoui-Malki, M., Latruffe, N., & Kebbaj, M. S. El. (2010). Structural and catalytic properties of the D-3-hydroxybutyrate dehydrogenase from *Pseudomonas aeruginosa*. *Current Microbiology*, *61*(1), 7–12. https://doi.org/10.1007/s00284-009-9568-7

Mozejko-Ciesielska, J., Dabrowska, D., Szalewska-Palasz, A., & Ciesielski, S. (2017). Medium-chain-length polyhydroxyalkanoates synthesis by *Pseudomonas putida* KT2440 relA/spoT mutant: bioprocess characterization and transcriptome analysis. *AMB Express*, *7*(1). https://doi.org/10.1186/s13568-017-0396-z

Możejko-Ciesielska, J., & Kiewisz, R. (2016). Bacterial polyhydroxyalkanoates: Still fabulous? *Microbiological Research*, *192*(2016), 271–282. https://doi.org/10.1016/j.micres.2016.07.010

Naggert, J., Narasimhan, M. L., DeVeaux, L., Cho, H., Randhawa, Z. I., Cronan, J. E., Green, B. N., & Smith, S. (1991). Cloning, sequencing, and characterization of *Escherichia coli* thioesterase II. *Journal of Biological Chemistry*, *266*(17), 11044–11050. https://doi.org/10.1016/s0021-9258(18)99125-8

Naranjo, J. M., Posada, J. A., Higuita, J. C., & Cardona, C. A. (2013). Valorization of glycerol through the production of biopolymers: The PHB case using *Bacillus megaterium*. *Bioresource Technology*, *133*, 38–44. https://doi.org/10.1016/j.biortech.2013.01.129

Nguyen, D. T. N., Lee, O. K., Nguyen, T. T., & Lee, E. Y. (2021). Type II methanotrophs: A promising microbial cell-factory platform for bioconversion of methane to chemicals. *Biotechnology Advances*, *47*(January), 107700. https://doi.org/10.1016/j.biotechadv.2021.107700

Obruca, S., Sedlacek, P., Mravec, F., Samek, O., & Marova, I. (2016). Evaluation of 3-hydroxybutyrate as an enzyme-protective agent against heating and oxidative damage and its potential role in stress response of poly(3-hydroxybutyrate) accumulating cells. *Applied Microbiology and Biotechnology*, *100*(3), 1365–1376. https://doi.org/10.1007/s00253-015-7162-4

Oh, Y. H., Lee, S. H., Jang, Y. A., Choi, J. W., Hong, K. S., Yu, J. H., Shin, J., Song, B. K., Mastan, S. G., David, Y., Baylon, M. G., Lee, S. Y., & Park, S. J. (2015). Development of rice bran treatment process and its use for the synthesis of polyhydroxyalkanoates from rice bran hydrolysate solution. *Bioresource Technology*, *181*, 283–290. https://doi.org/10.1016/j.biortech.2015.01.075

Page, W. J., & Knosp, O. (1989). Hyperproduction of poly-β-hydroxybutyrate during exponential growth of *Azotobacter vinelandii* UWD. *Applied and Environmental Microbiology*, *55*(6), 1334–1339. https://doi.org/10.1128/aem.55.6.1334-1339.1989

Papapostolou, A., Karasavvas, E., & Chatzidoukas, C. (2019). Oxygen mass transfer limitations set the performance boundaries of microbial PHA production processes – A model-based problem investigation supporting scale-up studies. *Biochemical Engineering Journal*, *148*(March), 224–238. https://doi.org/10.1016/j.bej.2019.04.024

Pérez-Fortes, M., Schöneberger, J. C., Boulamanti, A., & Tzimas, E. (2016). Methanol synthesis using captured CO_2 as raw material: Techno-economic and environmental assessment. *Applied Energy*, *161*, 718–732. https://doi.org/10.1016/j.apenergy.2015.07.067

Peypoux, F., Bonmatin, J. M., & Wallach, J. (1999). Recent trends in the biochemistry of surfactin. *Applied Microbiology and Biotechnology*, *51*(5), 553–563. https://doi.org/10.1007/s002530051432

Pieja, A. J., Sundstrom, E. R., & Criddle, C. S. (2011). Poly-3-hydroxybutyrate metabolism in the type II Methanotroph *Methylocystis parvus* OBBP. *Applied and Environmental Microbiology*, *77*(17), 6012–6019. https://doi.org/10.1128/AEM.00509-11

Poblete-Castro, I., Binger, D., Oehlert, R., & Rohde, M. (2014). Comparison of mcl-poly(3-hydroxyalkanoates) synthesis by different *Pseudomonas putida* strains from crude glycerol: Citrate accumulates at high titer under PHA-producing conditions. *BMC Biotechnology*, *14*(1), 1–11. https://doi.org/10.1186/s12896-014-0110-z

Poirier, Y., Nawrath, C., & Somerville, C. (1995). Production of Polyhydroxyalkanoates, a Family of Biodegradable Plastics and Elastomers, in Bacteria and Plants. *Bio/Technology*, *13*(2), 142–150. https://doi.org/10.1038/nbt0295-142

Polyák, P., Dohovits, E., Nagy, G. N., Vértessy, B. G., Vörös, G., & Pukánszky, B. (2018). Enzymatic degradation of poly-[(R)-3-hydroxybutyrate]: Mechanism, kinetics, consequences. *International Journal of Biological Macromolecules*, *112*, 156–162. https://doi.org/10.1016/j.ijbiomac.2018.01.104

Posada, J. A., Naranjo, J. M., López, J. A., Higuita, J. C., & Cardona, C. A. (2011). Design and analysis of poly-3-hydroxybutyrate production processes from crude glycerol. *Process Biochemistry*, *46*(1), 310–317. https://doi.org/10.1016/j.procbio.2010.09.003

Raberg, M., Voigt, B., Hecker, M., & Steinbüchel, A. (2014). A closer look on the polyhydroxybutyrate- (PHB-) negative phenotype of *Ralstonia eutropha* PHB^{-}4. *PLOS ONE*, *9*(5), 1–11. https://doi.org/10.1371/journal.pone.0095907

Ramsay, B. A., Lomaliza, K., Chavarie, C., Dube, B., Bataille, P., & Ramsay, J. A. (1990). Production of poly-(beta-hydroxybutyric-co-beta-hydroxyvaleric) acids. *Applied and Environmental Microbiology*, *56*(7), 2093–2098. https://doi.org/https://doi.org/10.1128/aem.56.7.2093-2098.1990

Ramsay, J. A., Berger, E., Ramsay, B. A., & Chavarie, C. (1990). Recovery of Poly-3-hydroxyalkanoic acid granules by a surfactant-hypochlorite treatment. *Biotechnology Techniques*, *4*(4), 221–226.

Rathbone, S., Furrer, P., Lübben, J., Zinn, M., & Cartmell, S. (2010). Biocompatibility of polyhydroxyalkanoate as a potential material for ligament and tendon scaffold material. *Journal of Biomedical Materials Research - Part A*, *93*(4), 1391–1403. https://doi.org/10.1002/jbm.a.32641

Rehm, B. H. A., Krüger, N., & Steinbüchel, A. (1998). A new metabolic link between fatty acid de *novo* synthesis and polyhydroxyalkanoic acid synthesis. The *phaG* gene from *Pseudomonas putida* KT2440 encodes a 3-hydroxyacyl-acyl carrier protein-coenzyme a transferase. *Journal of Biological Chemistry*, *273*(37), 24044–24051. https://doi.org/10.1074/jbc.273.37.24044

Reinecke, F., & Steinbüchel, A. (2009). *Ralstonia eutropha* Strain H16 as Model Organism for PHA Metabolism and for Biotechnological Production of Technically Interesting Biopolymers. *Microbial Physiology*, *16*(1–2), 91–108. https://doi.org/10.1159/000142897

Ren, Q., Grubelnik, A., Hoerler, M., Ruth, K., Hartmann, R., Felber, H., & Zinn, M. (2005). Bacterial poly(hydroxyalkanoates) as a source of chiral hydroxyalkanoic acids. *Biomacromolecules*, *6*(4), 2290–2298. https://doi.org/10.1021/bm050187s

Ren, Q., Ruth, K., Thöny-Meyer, L., & Zinn, M. (2007). Process engineering for production of chiral hydroxycarboxylic acids from bacterial polyhydroxyalkanoates. *Macromolecular Rapid Communications*, *28*(22), 2131–2136. https://doi.org/10.1002/marc.200700389

Riahi, K; R. Schaeffer, J; Arango, K. et al. (2022). *IPCC, 2022: Climate Change 2022: Mitigation of Climate Change. Chapter 3: Mitigation pathways compatible with long-term goals.*

Rodríguez, Y., Firmino, P. I. M., Arnáiz, E., Lebrero, R., & Muñoz, R. (2020). Elucidating the influence of environmental factors on biogas-based polyhydroxybutyrate production by *Methylocystis hirsuta* CSC1. *Science of the Total Environment*, *706*. https://doi.org/10.1016/j.scitotenv.2019.135136

Rodríguez, Y., García, S., Pérez, R., Lebrero, R., & Muñoz, R. (2022). Optimization of nitrogen feeding strategies for improving polyhydroxybutyrate production from biogas by *Methylocystis parvus* str. OBBP in a stirred tank reactor. *Chemosphere*, *299*. https://doi.org/10.1016/j.chemosphere.2022.134443

Roohi, Zaheer, M. R., & Kuddus, M. (2018). PHB (poly-β-hydroxybutyrate) and its enzymatic degradation. In *Polymers for Advanced Technologies*, 29(1), 30–40. https://doi.org/10.1002/pat.4126

Rostkowski, K. H., Pfluger, A. R., & Criddle, C. S. (2013). Stoichiometry and kinetics of the PHB-producing Type II methanotrophs *Methylosinus trichosporium* OB3b and *Methylocystis parvus* OBBP. *Bioresource Technology*, *132*, 71–77. https://doi.org/10.1016/j.biortech.2012.12.129

Ruth, K., Grubelnik, A., Hartmann, R., Egli, T., Zinn, M., & Ren, Q. (2007). Efficient production of (R)-3-hydroxycarboxylic acids by biotechnological conversion of polyhydroxyalkonoates and their purification. *Biomacromolecules*, *8*(1), 279–286. https://doi.org/10.1021/bm060585a

Samek O, Obruča S, Šiler M, Sedláček P, Benešová P, Kučera D, Márova I, Ježek J, Bernatová S, Zemánek P. (2016). Quantitative Raman Spectroscopy Analysis of Polyhydroxyalkanoates Produced by *Cupriavidus necator* H16. *Sensors*, 16(11), 1808. https://doi.org/10.3390/s16111808

Scherer, T. M., Fuller, R. C., Lenz, R. W., & Goodwin, S. (1999). Production, purification and activity of an extracellular depolymerase from *Aspergillus fumigatus*. *Journal of Environmental Polymer Degradation*, *7*(3), 117–125. https://doi.org/10.1023/A:1022881204565

Schweitzer, D., Mullen, C. A., Boateng, A., & Snell, K. D. (2015). Biobased n-Butanol Prepared from Poly-3-hydroxybutyrate: Optimization of the Reduction of n-Butyl Crotonate to n-Butanol. *Organic Process Research and Development*, *19*(7), 710–714. https://doi.org/10.1021/op500156b

Scott, F., Yañez, L., Conejeros, R., Araya, B., & Vergara-Fernández, A. (2021). Two internal bottlenecks cause the overflow metabolism leading to poly(3-hydroxybutyrate) production in *Azohydromonas lata* DSM1123. *Journal of Environmental Chemical Engineering*, *9*(4). https://doi.org/10.1016/j.jece.2021.105665

Seebach, D., Albert, M., Arvidsson, P. I., Rueping, M., & Schreiber, J. V. (2001). From the Biopolymer PHB to Biological Investigations of Unnatural β- and γ-Peptides. *CHIMIA*, 55(4), 345. https://doi.org/10.2533/chimia.2001.345

Seebach, D., Beck, A. K., Breitschuh, R., & Job, K. (2003). Direct Degradation of the Biopolymer Poly[(R)-3-Hydroxybutyric Acid] to (R)-3-Hydroxybutanoic Acid and its Methyl Ester. In *Organic Syntheses*, *71*, 39. https://doi.org/https://doi.org/10.1002/0471264180.os071.05

Seebach, D., Chow, H. -F, Jackson, R. F. W., Sutter, M. A., Thaisrivongs, S., & Zimmermann, J. (1986). (+)-11,11′-Di-O-methylelaiophylidene – preparation from elaiophylin and total synthesis from (R)-3-hydroxybutyrate and (S)-malate. *Liebigs Annalen Der Chemie*, *1986*(7), 1281–1308. https://doi.org/10.1002/jlac.198619860714

Shah, M., Naseer, M. I., Choi, M. H., Kim, M. O., & Yoon, S. C. (2010). Amphiphilic PHA-mPEG copolymeric nanocontainers for drug delivery: Preparation, characterization and in vitro evaluation. *International Journal of Pharmaceutics*, *400*(1–2), 165–175. https://doi.org/10.1016/j.ijpharm.2010.08.008

Shiraki, M., Endo, T., & Saito, T. (2006). Fermentative production of (R)-(-)-3-hydroxybutyrate using 3-hydroxybutyrate dehydrogenase null mutant of *Ralstonia eutropha* and recombinant *Escherichia coli*. *Journal of Bioscience and Bioengineering*, *102*(6), 529–534. https://doi.org/10.1263/jbb.102.529

Soni, B. K., Conrad, J., Kelley, R. L., & Srivastava, V. J. (1998). Effect of temperature and pressure on growth and methane utilization by several methanotrophic cultures. *Applied Biochemistry and Biotechnology*, *70–72*, 729–738. https://doi.org/10.1007/BF02920184

Srivatsan, A., & Wang, J. D. (2008). Control of bacterial transcription, translation and replication by (p)ppGpp. *Current Opinion in Microbiology*, *11*(2), 100–105. https://doi.org/10.1016/j.mib.2008.02.001

Steinbüchel, A., & Hein, S. (2001). Biochemical and molecular basis of microbial synthesis of polyhydroxyalkanoates in microorganisms. *Advances in Biochemical Engineering/Biotechnology*, *71*, 81–123. https://doi.org/10.1007/3-540-40021-4_3

Steinbüchel, A., & Valentin, H. E. (1995). Diversity of bacterial polyhydroxyalkanoic acids. *FEMS Microbiology Letters*, *128*(3), 219–228. https://doi.org/10.1016/0378-1097(95)00125-O

Strong, P. J., Xie, S., & Clarke, W. P. (2015). Methane as a resource: Can the methanotrophs add value? *Environmental Science and Technology*, *49*(7), 4001–4018. https://doi.org/10.1021/es504242n

Strong, P., Laycock, B., Mahamud, S., Jensen, P., Lant, P., Tyson, G., & Pratt, S. (2016). The Opportunity for High-Performance Biomaterials from Methane. *Microorganisms*, *4*(1), 11. https://doi.org/10.3390/microorganisms4010011

Suriyamongkol, P., Weselake, R., Narine, S., Moloney, M., & Shah, S. (2007). Biotechnological approaches for the production of polyhydroxyalkanoates in microorganisms and plants - A review. *Biotechnology Advances*, *25*(2), 148–175. https://doi.org/10.1016/j.biotechadv.2006.11.007

Sznajder, A., Pfeiffer, D., & Jendrossek, D. (2015). Comparative proteome analysis reveals four novel polyhydroxybutyrate (PHB) granule-associated proteins in *Ralstonia eutropha* H16. *Applied and Environmental Microbiology*, *81*(5), 1847–1858. https://doi.org/10.1128/AEM.03791-14

Taidi, B., Mansfield, D. A., & Anderson, A. J. (1995). Turnover of poly(3-hydroxybutyrate) (PHB) and its influence on the molecular mass of the polymer accumulated by *Alcaligenes eutrophus* during batch culture. *FEMS Microbiology Letters*, *129*(2–3), 201–205. https://doi.org/10.1016/0378-1097(95)00158-2

Tajima, K., Han, X., Hashimoto, Y., Satoh, Y., Satoh, T., & Taguchi, S. (2016). *In vitro* synthesis of polyhydroxyalkanoates using thermostable acetyl-CoA synthetase, CoA transferase, and PHA synthase from thermotorelant bacteria. *Journal of Bioscience and Bioengineering*, *122*(6), 660–665. https://doi.org/10.1016/j.jbiosc.2016.06.001

Tajima, K., Han, X., Satoh, Y., Ishii, A., Araki, Y., Munekata, M., & Taguchi, S. (2012). *In vitro* synthesis of polyhydroxyalkanoate (PHA) incorporating lactate (LA) with a block sequence by using a newly engineered thermostable PHA synthase from *Pseudomonas* sp. SG4502 with acquired LA-polymerizing activity. *Applied Microbiology and Biotechnology*, *94*(2), 365–376. https://doi.org/10.1007/s00253-011-3840-z

Takanashi, M., & Saito, T. (2006). Characterization of two 3-hydroxybutyrate dehydrogenases in poly(3-hydroxybutyrate)-degradable bacterium, *Ralstonia pickettii* T1. *Journal of Bioscience and Bioengineering*, *101*(6), 501–507. https://doi.org/10.1263/jbb.101.501

Tamer, I. M., Moo-young, M., & Chisti, Y. (1998). Disruption of *Alcaligenes latus* for Recovery of Poly (β-hydroxybutyric acid): Comparison of High-Pressure Homogenization , Bead Milling , and Chemically Induced Lysis. *Industrial and Engineering Chemistry Research*, *5885*(97), 1807–1814.

Tanaka, K., Ishizaki, A., Kanamaru, T., & Kawano, T. (1995). Production of poly (D-3-hydroxybutyrate) from CO_2, H_2, and O_2 by high cell density autotrophic cultivation of *Alcaligenes eutrophus*. *Biotechnology and Bioengineering*, *45*(3), 268–275. http://onlinelibrary.wiley.com/doi/10.1002/bit.260450312/abstract

Tanaka, K., Miyawaki, K., Yamaguchi, A., Khosravi-Darani, K., & Matsusaki, H. (2011). Cell growth and P(3HB) accumulation from CO_2 of a carbon monoxide-tolerant hydrogen-oxidizing bacterium, *Ideonella* sp. O-1. *Applied Microbiology and Biotechnology*, *92*(6), 1161–1169. https://doi.org/10.1007/s00253-011-3420-2

Tieu, K., Perier, C., Caspersen, C., Teismann, P., Wu, D. C., Yan, S. Du, Naini, A., Vila, M., Jackson-Lewis, V., Ramasamy, R., & Przedborski, S. (2003). D-β-Hydroxybutyrate rescues mitochondrial respiration and mitigates features of Parkinson disease. *Journal of Clinical Investigation*, *112*(6), 892–901. https://doi.org/10.1172/JCI200318797

Tokiwa, Y., & Ugwu, C. U. (2007). Biotechnological production of (R)-3-hydroxybutyric acid monomer. *Journal of Biotechnology*, *132*(3), 264–272. https://doi.org/10.1016/j.jbiotec.2007.03.015

Uchino, K., Saito, T., Gebauer, B., & Jendrossek, D. (2007). Isolated poly(3-hydroxybutyrate) (PHB) granules are complex bacterial organelles catalyzing formation of PHB from acetyl coenzyme A (CoA) and degradation of PHB to acetyl-CoA. *Journal of Bacteriology*, *189*(22), 8250–8256. https://doi.org/10.1128/JB.00752-07

Ueda, H., & Tabata, Y. (2003). Polyhydroxyalkanonate derivatives in current clinical applications and trials. *Advanced Drug Delivery Reviews*, *55*(4), 501–518. https://doi.org/10.1016/S0169-409X(03)00037-1

Ugwu, C. U., Tokiwa, Y., Aoyagi, H., Uchiyama, H., & Tanaka, H. (2008). UV mutagenesis of *Cupriavidus necator* for extracellular production of (R)-3-hydroxybutyric acid. *Journal of Applied Microbiology*, *105*(1), 236–242. https://doi.org/10.1111/j.1365-2672.2008.03774.x

Ugwu, C. U., Tokiwa, Y., & Ichiba, T. (2011). Production of (R)-3-hydroxybutyric acid by fermentation and bioconversion processes with *Azohydromonas lata*. *Bioresource Technology*, *102*(12), 6766–6768. https://doi.org/10.1016/j.biortech.2011.03.073

van der Linden, S., Leiserowitz, A., Rosenthal, S., Maibach, E., Howe, P. D., Mildenberger, M., Marlon, J. R., & Leiserowitz, A. (2017). Inoculating the Public against Misinformation about Climate Change. *Global Challenges*, *1*(2), 596–603. https://doi.org/10.1002/gch2.201600008

Vecherskaya, M., Dijkema, C., Saad, H. R., & Stams, A. J. M. (2009). Microaerobic and anaerobic metabolism of a *Methylocystis parvus* strain isolated from a denitrifying bioreactor. *Environmental Microbiology Reports*, *1*(5), 442–449. https://doi.org/10.1111/j.1758-2229.2009.00069.x

Vecherskaya, M., Dijkema, C., & Stams, A. J. M. (2001). Intracellular PHB conversion in a Type II methanotroph studied by 13C NMR. *Journal of Industrial Microbiology and Biotechnology*, *26*(1–2), 15–21. https://doi.org/10.1038/sj.jim.7000086

Vergé, X. P. C., De Kimpe, C., & Desjardins, R. L. (2007). Agricultural production, greenhouse gas emissions and mitigation potential. *Agricultural and Forest Meteorology*, *142*(2–4), 255–269. https://doi.org/10.1016/j.agrformet.2006.06.011

Volova, T; Shishatskaya, E; Sevastianov, V; Efremov, S; andMogilnaya, O. (2003). Results of biomedical investigations of PHB and PHB/PHV fibers. *Biochemical Engineering Journal*, *16*, 125–133.

Wang, B., Xiong, W., Yu, J., Maness, P. C., & Meldrum, D. R. (2018). Unlocking the photobiological conversion of CO_2 to (R)-3-hydroxybutyrate in cyanobacteria. *Green Chemistry*, *20*(16), 3772–3782. https://doi.org/10.1039/c8gc01208c

Wang, F., & Lee, S. Y. (1997). Poly(3-hydroxybutyrate) production with high productivity and high polymer content by a fed-batch culture of *Alcaligenes latus* under nitrogen limitation. *Applied and Environmental Microbiology*, *63*(9), 3703–3706. https://doi.org/10.1128/aem.63.9.3703-3706.1997

Wang, L., Armbruster, W., & Jendrossek, D. (2007). *Production of medium-chain-length hydroxyalkanoic acids from Pseudomonas putida* in pH stat. *Applied Microbiology and Biotechnology*, *75*(5), 1047–1053. https://doi.org/10.1007/s00253-007-0920-1

Wang, S. Y., Wang, Z., Liu, M. M., Xu, Y., Zhang, X. J., & Chen, G. Q. (2010). Properties of a new gasoline oxygenate blend component: 3-Hydroxybutyrate methyl ester produced from bacterial poly-3-hydroxybutyrate. *Biomass and Bioenergy*, *34*(8), 1216–1222. https://doi.org/10.1016/j.biombioe.2010.03.020

Wang, Y. W., Wu, Q., Chen, J., & Chen, G. Q. (2005). Evaluation of three-dimensional scaffolds made of blends of hydroxyapatite and poly(3-hydroxybutyrate-co-3-hydroxyhexanoate) for bone reconstruction. *Biomaterials*, 26(8), 899–904. https://doi.org/10.1016/j.biomaterials.2004.03.035

Wendlandt, K. D., Jechorek, M., Helm, J., & Stottmeister, U. (2001). Producing poly-3-hydroxybutyrate with a high molecular mass from methane. *Journal of Biotechnology*, *86*(2), 127–133. https://doi.org/10.1016/S0168-1656(00)00408-9

Windhorst, C., & Gescher, J. (2019). Efficient biochemical production of acetoin from carbon dioxide using *Cupriavidus necator* H16. *Biotechnology for Biofuels*, *12*(1), 1–11. https://doi.org/10.1186/s13068-019-1512-x

Witholt, B., & Kessler, B. (1999). Perspectives of medium chain length poly(hydroxyalkanoates), a versatile set of bacterial bioplastics. *Current Opinion in Biotechnology*, *10*(3), 279–285. https://doi.org/10.1016/S0958-1669(99)80049-4

Yamanashi, T., Iwata, M., Kamiya, N., Tsunetomi, K., Kajitani, N., Wada, N., Iitsuka, T., Yamauchi, T., Miura, A., Pu, S., Shirayama, Y., Watanabe, K., Duman, R. S., & Kaneko, K. (2017). Beta-hydroxybutyrate, an endogenic NLRP3 inflammasome inhibitor, attenuates stress-induced behavioral and inflammatory responses. *Scientific Reports*, *7*(1), 7677. https://doi.org/10.1038/s41598-017-08055-1

Yamane, T., Fukunaga, M., & Lee, Y. W. (1996). Increased PHB productivity by high-cell-density fed-batch culture of *Alcaligenes latus*, a growth-associated PHB producer. *Biotechnology and Bioengineering*, *50*(2), 197–202. https://doi.org/10.1002/(sici)1097-0290(19960420)50:2<197::aid-bit8>3.3.co;2-6

Yishai, O., Lindner, S. N., Gonzalez de la Cruz, J., Tenenboim, H., & Bar-Even, A. (2016). The formate bio-economy. *Current Opinion in Chemical Biology*, *35*, 1–9. https://doi.org/10.1016/j.cbpa.2016.07.005

Yokaryo, Hiroto; Teruya, Morimi ; Hanashiro, Ryuji ; Goda, Masahiro; Tokiwa, Y. (2017). Direct Production of (R)-3-Hydroxybutyric Acid of High Optical Purity by *Halomonas* sp. OITC1261 Under Aerobic conditions. *Biotechnology Journal*, *13*(2), 1–23. https://doi.org/10.1002/biot.201700343

Yun, E. J., Kwak, S., Kim, S. R., Park, Y. C., Jin, Y. S., & Kim, K. H. (2015). Production of (S)-3-hydroxybutyrate by metabolically engineered *Saccharomyces cerevisiae*. *Journal of Biotechnology*, *209*, 23–30. https://doi.org/10.1016/j.jbiotec.2015.05.017

Zhang, X., Luo, R., Wang, Z., Deng, Y., and Chen, G.-Q. (2009). Application of (R)-3-Hydroxyalkanoate Methyl Esters Derived from Microbial Polyhydroxyalkanoates as Novel Biofuels. *Biomacromolecules*, *10*, 707–711. https://doi.org/https://doi.org/10.1021/bm801424e

Zhang, J., Cao, Q., Li, S., Lu, X., Zhao, Y., Guan, J. S., Chen, J. C., Wu, Q., & Chen, G. Q. (2013). 3-Hydroxybutyrate methyl ester as a potential drug against Alzheimer's disease via mitochondria protection mechanism. *Biomaterials*, *34*(30), 7552–7562. https://doi.org/10.1016/j.biomaterials.2013.06.043

Zheng, Zhong; Gong, Qiang; Chen, G. (2004). A Novel Method for Production of 3-Hydroxydecanoic Acid by Recombinant *Escherichia coli* and *Pseudomonas putida*. *Chinese Journal of Chemical Engineering*, *12*(4), 550–555.

APPENDICES

APPENDIX I. RAW DATA AND CALIBRATION CURVES

Table I-1. Acids concentration in nutrient limitation chemostats in *A. lata* by HPLC

Nutrient limited	**D** [h^{-1}]	**Citric** [mM in broth]	**Malic** [mM in broth]	**Succinic** [mM in broth]	**Pyruvic** [mM in broth]	**R3HBA** [mM in broth]
O_2	0.05	0.18	0.32	0.57	0.01	0.01
	0.05	0.15	0.28	1.83	0.02	0.88
	0.10	0.38	1.61	4.75	0.01	0.01
	0.20	0.73	0.98	7.86	0.01	0.01
Gluc	0.05	0.08	0.58	1.24	0.00	0.33
	0.05	0.03	0.25	0.60	0.03	0.00
	0.10	0.03	0.24	0.53	0.01	0.01
	0.20	0.00	0.00	0.00	0.01	0.00
	0.40	0.00	0.00	0.00	0.22	0.01
N	0.05	0.10	0.00	0.17	0.00	0.22
	0.10	0.34	1.56	10.65	0.01	0.01
	0.20	0.51	2.02	3.43	0.00	0.01
	0.20	0.00	1.14	5.26	0.01	0.22

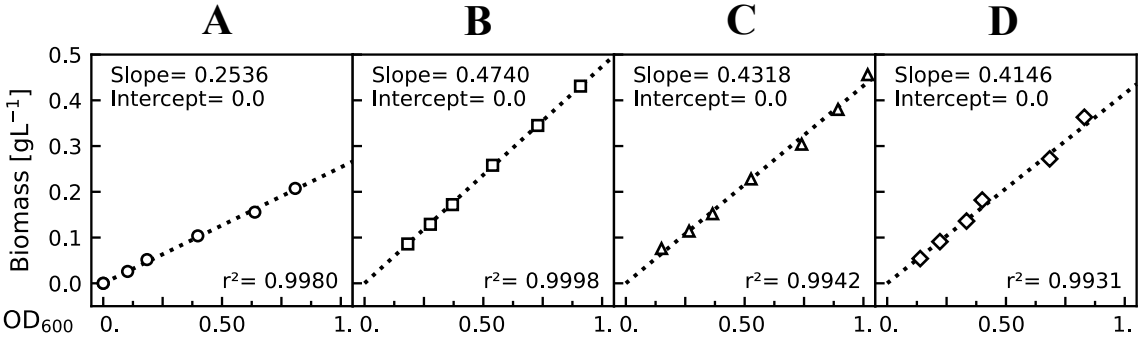

Figure I-1. **Calibration curves of absorbance and *C. necator* derived mutants concentration**. Correlation of the specific absorbance (600 nm) and cell concentration in RE1 medium at different dilution factors. (A) *C. necator* H16; (B) *C. necator* 541; (C) *C. necator* Δ*phaC* and (D) *C. necator* Δ*phaC* Δ*hbd*.

APPENDIX II. PRIMERS AND GENES FOR THE CONSTRUCTION OF *tesB* EXPRESSION VECTOR

Table II-1. Primers used for the expression of *tesB* in *M. parvus* and *C. necator* H16

Primers	**Sequence 5'- 3'**	**Plasmid**
tesb_parvus_F	GAAACAGCTataaacgacgattggcgtatttttgatg	pAWP89_tesb
tesb_parvus_F	CCCGACAACTAttatcttgtgcaatgccatggtttattg	pAWP89_tesb
vector_p89_F	cacaagataaTAGTTGTCGGGAAGATGCGTGATCTGA	pAWP89_tesb
vector_p89_R	cgtcgtttatAGCTGTTTCCTGTGTGAATACCTCC	pAWP89_tesb
tesb_pbbr1_FOR	ACAAAAGCTGATGAGTCAGAAAGGAGGACAACCATGAGTCAGGCGCTAAAAAATTTACTGAC	pBBR1MCS2_tesb
tesb_pbbr1_REV	TCTAGACCTTCCTTCCTTAATTGTGATTACGCATCACC	pBBR1MCS2_tesb
T1T2_FOR	ATTAAGGAAGGAAGGTCTAGAGTCGACCTGCAG	pBBR1MCS2_tesb
T1T2_REV	GCGAATTGCGCAAAAAAAAAAGGCCATCCGTCAGGATGG	pBBR1MCS2_tesb
vector.for	CTGACTCATCAGCTTTTGTTCCCTTTAGTGAGGG	pBBR1MCS2_tesb
vector.rev	TTTTTGCGCAATTCGCCCTATAGTGAGTCGTAT	pBBR1MCS2_tesb

II-1. Sequences synthetized ordered for the expression of *tesB* in *M. parvus* or *C. necator* H16

tesB gene from *E. coli* K12 (without codon optimization)

5'−ATGAGTCAGGCGCTAAAAAATTTACTGACATTGTTAAATCTGGAAAAAATT
GAGGAAGGACTCTTTCGCGGCCAGAGTGAAGATTTAGGTTTACGCCAGGTGTT
TGGCGGCCAGGTCGTGGGTCAGGCCTTGTATGCTGCAAAAGAGACCGTCCCTG
AAGAGCGGCTGGTACATTCGTTTCACAGCTACTTTCTTCGCCCTGGCGATAGTA
AGAAGCCGATTATTTATGATGTCGAAACGCTGCGTGACGGTAACAGCTTCAGC
GCCCGCCGGGTTGCTGCTATTCAAAACGGCAAACCGATTTTTTATATGACTGCC

TCTTTCCAGGCACCAGAAGCGGGTTTCGAACATCAAAAAACAATGCCGTCCGC
GCCAGCGCCTGATGGCCTCCCTTCGGAAACGCAAATCGCCCAATCGCTGGCGC
ACCTGCTGCCGCCAGTGCTGAAAGATAAATTCATCTGCGATCGTCCGCTGGAA
GTCCGTCCGGTGGAGTTTCATAACCCACTGAAAGGTCACGTCGCAGAACCACA
TCGTCAGGTGTGGATCCGCGCAAATGGTAGCGTGCCGGATGACCTGCGCGTTC
ATCAGTATCTGCTCGGTTACGCTTCTGATCTTAACTTCCTGCCGGTAGCTCTACA
GCCGCACGGCATCGGTTTTCTCGAACCGGGGATTCAGATTGCCACCATTGACCA
TTCCATGTGGTTCCATCGCCCGTTTAATTTGAATGAATGGCTGCTGTATAGCGT
GGAGAGCACCTCGGCGTCCAGCGCACGTGGCTTTGTGCGCGGTGAGTTTTATAC
CCAAGACGGCGTACTGGTTGCCTCGACCGTTCAGGAAGGGGTGATGCGTAATC
ACAATTAA−3’

Promoter gene extracted from GenBank accession number AJTV00000000

5’−ATAAACGACGATTGGCGTATTTTTTGATGGTTGTCGGTTTCTTCTCGGTCGCC
ATACGCCTGACAGTGCTCCCCTCGCCGCTCGGGCAGCCTAAAAAAAGGTCAAG
CCCAGCCGATTGACGATAGACGCATTTTGGCGCCTGCGGCAATATTTTCCTTGG
CGAAGCCTTTCGCTCCCCCCCCAATTCCGTGCAAAACGGGCCGCGGCTTGACGA
ACGCAAGCGCGAAATGCTCAACCACATCCGCCCCGGCCGGGCGCTGAGGGCCT
CGAGAGCTCGACCATCTTTAAAAGGGAGACAGAT−3’

Terminator gene extracted from GenBank accession number AJTV00000000

5’−GGAAGGCGCGGGCATCGCTTTTTCTATAAATCATCCGGCCATTTTTGAGCAA
TAAA−3’

APPENDIX III. PUBLICATIONS

Bioresource Technology 353 (2022) 127141

Contents lists available at ScienceDirect

Bioresource Technology

journal homepage: www.elsevier.com/locate/biortech

Production of (*R*)-3-hydroxybutyric acid from methane by *in vivo* depolymerization of polyhydroxybutyrate in *Methylocystis parvus* OBBP

Luz Yáñez [a,b], Yadira Rodríguez [a], Felipe Scott [b], Alberto Vergara-Fernández [b], Raúl Muñoz [a,*]

[a] Institute of Sustainable Processes, Universidad de Valladolid, Doctor Mergelina s/n, 47011, Spain
[b] Green Technology Research Group, Facultad de Ingeniería y Ciencias Aplicadas, Universidad de Los Andes, 7550000, Chile

HIGHLIGHTS

- PHB accumulated in *M. parvus* was depolymerized under alkaline conditions.
- The depolymerization produced (R)-3-hydroxybutyrate with a 77% conversion.
- The presence of a nitrogen source promoted depolymerization and monomer release.
- Low O_2 supply rates and high monomers concentration reduced PHB depolymerization.

GRAPHICAL ABSTRACT

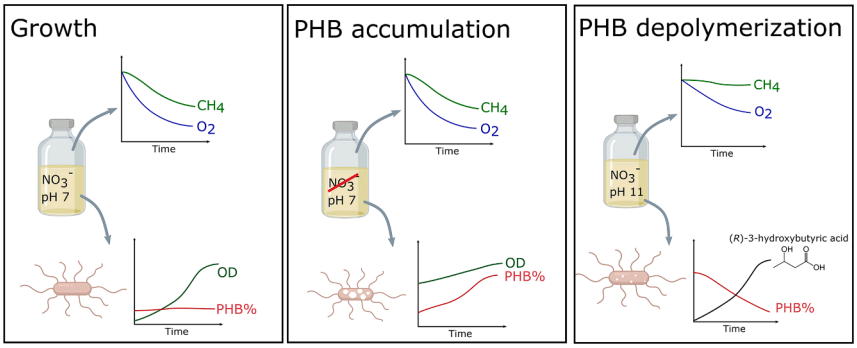

ARTICLE INFO

Keywords:
(*R*)-3-hydroxybutyrate
Chiral compounds
Greenhouse gas valorization
Methanotrophic bacteria
Polyhydroxybutyrate

ABSTRACT

Methylocystis parvus OBBP accumulates polyhydroxybutyrate (PHB) using methane as the sole carbon and energy source. In this work, the feasibility of producing (*R*)-3-hydroxybutyric acid (R3HBA) via intracellularly accumulated PHB through depolymerization (*in-vivo)* was investigated. Results showed that a PHB to R3HBA conversion of 77.2 ± 0.9% (R3HBA titer of 0.153 ± 0.002 g L^{-1}) can be attained in a mineral medium containing 1 g L^{-1} KNO_3 at 30 °C with shaking at 200 rpm and a constant pH of 11 for 72 h. Nitrogen deprivation and neutral or acidic pHs strongly reduced the excreted R3HBA concentration. Reduced oxygen availability negatively affected the R3HBA yield, which decreased to 73.6 ± 4.9% (titer of 0.139 ± 0.01 g L^{-1}) under microaerobic conditions. Likewise, the presence of increasing concentrations of R3HBA in the medium before the onset of PHB depolymerization reduced the initial R3HBA release rate and R3HBA yield.

1. Introduction

Methane (CH_4) is an inexpensive, colorless, odorless, and abundant gas that represents a widely available carbon and energy source. In 2019, CH_4 accounted for nearly 10 % of all U.S. anthropogenic greenhouse gas emissions (Jackson et al., 2020). The largest CH_4 sources included anthropogenic emissions from agriculture, waste and the extraction and use of fossil fuels (Kirschke et al., 2013; Saunois et al.,

* Corresponding author.
E-mail addresses: lfyanez@miuandes.cl (L. Yáñez), yadira.rodriguez@uva.es (Y. Rodríguez), fscott@miuandes.cl (F. Scott), aovergara@miuandes.cl (A. Vergara-Fernández), mutora@iq.uva.es (R. Muñoz).

https://doi.org/10.1016/j.biortech.2022.127141
Received 9 March 2022; Received in revised form 6 April 2022; Accepted 7 April 2022
Available online 9 April 2022

2016). The Global Methane Assessment report shows that decreasing methane emission by 45% during this decade would avoid 0.3 °C of global warning by 2045. Moreover, nearly a quarter-million premature deaths and 25 million tons of crop losses could be prevented annually (Ravishankara et al., 2021). CH_4 emissions contribute to almost one-quarter of the cumulative radiative forcing of carbon dioxide (CO_2), CH_4 and nitrous oxide (N_2O) combined since 1750 (Etminan et al., 2016). Although the lifetime of CH_4 in the atmosphere is much shorter than that of CO_2, it absorbs thermal infrared radiation much more efficiently. Indeed, CH_4 exhibits a global warming potential 86 times stronger per unit of mass than CO_2 on a 20-year timescale and approximately 28 times more powerful on a 100-year time scale (Edenhofer, 2014). Today, CH_4 can be captured from landfills (38 Mt/year), wastewater treatment (21 Mt/year), agriculture (11–30 Mt/year), biomass (10 Mt/year), and natural gas production (92 Mt/year) (Strong et al., 2015). This methane can be valorized as an energy vector or as a feedstock for the biological production of products such as ectoine, biopolymers, and single cell proteins, among others (Jawaharraj et al., 2020) or for the catalytic production of methanol (Latimer et al., 2018). In this context, CH_4 represents a carbon and energy source for a group of gram-negative bacteria known as methanotrophs. These bacteria are classified according to the pathways used for the assimilation of the formaldehyde directly derived from CH_4 into type I and type II methanotrophs. Type I using the ribulose monophosphate pathway for formaldehyde assimilation, and type II methanotrophs using the serine pathway (Nguyen et al., 2021). *Methylocystis parvus* is a type II methanotroph that shows a higher specific growth rate compared to other species of the *Methylocystis* genera (Bordel et al., 2019) and the ability to synthesize the biopolymer polyhydroxybutyrate (PHB) under nitrogen-limited conditions (Rostkowski et al., 2013). *M. parvus* has been reported to accumulate more than 50% (Pieja et al., 2011; Wendlandt et al., 2001) of its dry weight as PHB, which renders it a suitable industrial biopolymer producer.

In *M. parvus,* PHB synthesis starts with the condensation of two acetyl-CoA molecules, see Fig. 2A (Bordel et al., 2019). This pathway is conserved in many bacteria such as *Ralstonia eutropha*, *Azohydromonas* spp., *Azotobacter* spp., among others (McAdam et al., 2020), where acetyl-CoA molecules can be supplied from a wide range of carbon sources. These include simple sugars and organic acids (Sirohi et al., 2020), food residues, and industrial by-products (Liu et al., 2021). Bacteria rely on PHB depolymerases (PhaZ), located intracellularly, to catabolize this stored reserve of carbon and energy (Müller-Santos et al., 2021), yielding the monomer (*R*)-3-hydroxybutyric acid (R3HBA) and dimers (Jendrossek and Handrick, 2002). If conditions are permissive for growth, the released R3HBA will act as a source of carbon and energy (Donoso et al., 2011), starting with the conversion of R3HBA to acetoacetate by the NADH-dependent enzyme (*R*)-3-hydroxybutyrate dehydrogenase (Bdh) (Tokiwa and Ugwu, 2007). If environmental conditions do not support growth, or part of the R3HBA consumption pathway is blocked, the monomer is excreted to the media (Lee et al., 1999). This strategy has been implemented in non-methanotrophic PHB producers to obtain R3HBA in the cultivation broth during PHB depolymerization. While for *Azohydromonas lata* a pH of 4.0 produced the highest titer and yield of R3HBA, a pH of 9.2 was required for the liberation of hydroxyalkanoic acids from polyhydroxyalkanoates in *Pseudomonas putida* (Ruth et al., 2007).

R3HBA is a chiral molecule that can be applied as a building block in the synthesis of fine chemicals and pharmaceutical products such as biopolymers, antibiotics (Ren et al., 2005), insecticides and fragrances (Matsuyama et al., 2001; Yañez et al., 2020). R3HBA and its derivatives have been also used as potential drugs. For example, the infusion of 3RHBA improved ATP production in mitochondria and confers partial protection against neurodegenerative disease in a Parkinson mice model (Tieu et al., 2003). Outcomes of depression (Yamanashi et al., 2017), osteoporosis (Cao et al., 2014), Alzheimer (Zhang et al., 2013), and cardiovascular diseases (Nielsen et al., 2019) have been shown to improve using a 3HBA infusion. As a dietary supplement, the price of 3HBA is within 130–160 USD/kg (Fruggo," 2021). However, the conventional synthesis, extraction and purification of R3HBA from PHB produced from sugar-based bacterial processes is nowadays expensive (Pérez-Rivero et al., 2019), which requires alternative PHB production pathways with streamlined downstream processes in order to enhance process economics.

This work aims at determining the environmental conditions (presence or absence of carbon and nitrogen sources, pH, temperature) that lead to the production of R3HBA in the culture supernatant using the native PHB depolymerization pathway in *M. parvus*. The underlying hypothesis is that a combination of these variables would result in an active PHB depolymerase and an inactive or inhibited (*R*)-3-hydroxybutyrate dehydrogenase, as previously shown for other gram negative bacteria (Lee et al., 1999; Ren et al., 2005, 2007; Ruth et al., 2007).

2. Materials and methods

2.1. Mineral salt medium

Nitrate mineral salt (NMS) medium (pH 6.8) was composed of (g L^{-1}): 1.0 KNO_3, 1.1 $MgSO_4{\cdot}7H_2O$, 0.8 $Na_2HPO_4{\cdot}12H_2O$, 0.26 KH_2PO_4 and 0.2 $CaCl_2{\cdot}2H_2O$; and 1 mL of trace element solution (g L^{-1}): 0.3 $Na_2MoO_4{\cdot}2H_2O$, 0.3 $Na_2EDTA{\cdot}2H_2O$, 1 $CuSO_4{\cdot}5H_2O$, 0.5 $FeSO_4{\cdot}7H_2O$, 0.4 $ZnSO_4{\cdot}7H_2O$, 0.03 $CoCl_2$, 0.02 $MnCl_2{\cdot}4H_2O$, 0.015 H_3BO_3, 0.01 $NiCl_2{\cdot}6H_2O$ and 0.38 Fe-EDTA. Nitrate-free mineral salt (NFMS) medium was identical to NMS medium except that potassium nitrate was omitted. The reagents were acquired from PanReac AppliChem (Spain), except KNO_3, which was purchased from COFARCAS (Spain).

2.2. Inocula preparation

The methanotrophic strain *Methylocystis parvus* OBBP, kindly provided by Biopolis S.L. (Valencia, Spain), was inoculated (10% v/v) under sterile conditions in 125-mL crimp-sealed serum bottles containing 50 mL of (NMS) medium. The headspace (75 mL) of the bottles was flushed under sterile conditions for 5 min with filtered oxygen (0.22 μm, Millex GP, Merck). Then, 25 mL of the oxygen headspace atmosphere was replaced with sterile methane, resulting in an O_2:CH_4 concentration ratio of 66.7:33.3% (v/v). The cultures were incubated at 30 °C and 230 rpm in an orbital shaker (MaxQ 4000; Thermo Scientific, USA) for 5 days, unless otherwise stated. The headspace atmosphere of the bottles was replaced 6 times upon CH_4 depletion.

Then, biomass was collected and transferred into 2.2 L serum bottles containing 0.4 L of NMS, crimp sealed under a O_2:CH_4 atmosphere of 66.7%:33.3% until complete methane depletion (~10 days). The headspace atmosphere was obtained by flushing for 3 min a gas mixture as described above from a 100 L-Tedlar gas sampling bag (Sigma-Aldrich, USA). The cultures were grown at 25 °C (thermostated room) with an initial pH of 6.9 and magnetically stirred at 300 rpm (Poly 15 Variomag, Thermo Fisher Scientific).

When methane was depleted, the biomass was collected by centrifugation at 10000 rpm for 8 min (Sorvall Legend RT+; Thermo Scientific, USA) and re-suspended into 0.4 L of NFMS medium to promote PHB accumulation for ~ 10 days under similar incubation conditions.

2.3. Optimization of PHB depolymerization in M. Parvus

Unless otherwise indicated, the experiments were performed batch wise using PHB containing biomass in 125 mL serum bottles (working volume of 45 mL) crimp sealed (three biological replicates). The bottles were incubated at 30 °C (except Test 3) and 230 rpm in an orbital shaker.

2.3.1. Test 1. Influence of the presence of nitrate and O_2, and pH on PHB depolymerization

The assays were performed with NMS and NFMS media at both pH 4 and pH 11 in triplicate for 48 h. All cultures were inoculated with 10 mL of concentrated *M. parvus* culture previously grown in NFMS for 10 days (1.3 gTSS L^{-1} with 51,4% of PHB) and were incubated for two days under an O_2:CH_4 headspace (66.7%:33.3%) and a He:CH_4 atmosphere (66.7%:33.3%). A control test at pH 7 under a O_2:CH_4 headspace (66.7%:33.3%) and NMS media was also carried out. Culture samples were collected periodically for the quantification of the R3HBA concentration. Total suspended solids (TSS), total nitrogen, PHAs, and pH were determined at the beginning and end of the experiment.

2.3.2. Test 2. Optimization of pH during PHB depolymerization

PHB depolymerization under an O_2:CH_4 atmosphere (66.7%:33.3%) was assessed in triplicate at pH 10, pH 11 and pH 12 with NMS medium as above described for 48 h. The pH of the cultures was monitored three times per day and manually adjusted using 5 M NaOH, while the concentration of extracellular R3HBA was quantified once per day. The biomass concentration (estimated as TSS) and PHB cells content were determined at the beginning and the end of the experiment.

2.3.3. Test 3. Influence of temperature on the kinetic of PHB depolymerization

PHB depolymerization at pH 11 on NMS medium was assessed in triplicate at 25 and 35 °C for 3 h using fresh *M. parvus* with a concentration and PHB cell content of 4.17 gTSS L^{-1} and 44.7%. The determination of extracellular R3HBA concentration was conducted at 15, 30, 60, 120 and 180 min. At the end of the experiment, cell viability was evaluated using the pellets obtained after centrifugation of the biomass from depolymerized cells. Cell viability tests were performed at 25 °C in 2.2 L serum bottles with a working volume of 0.4 L of both NMS and NFMS medium. The bottles were capped with aluminum caps and chlorobutyl rubber stoppers under and O_2:CH_4 atmosphere (66.7:33.3%) and incubated as above described (section 2.2) until complete CH_4 depletion. TSS, CH_4, O_2 and CO_2 concentrations were periodically measured.

2.3.4. Test 4. Influence of the initial R3HBA concentration and aeration rate on PHB depolymerization

The influence of the oxygen mass transfer rate on PHB depolymerization and R3HBA yield was investigated in Erlenmeyer flasks (E-flasks) incubated at 200 rpm and 30 °C in an orbital shaker for 72 h. The lowest oxygen mass transfer rate was achieved in 100 mL E-flasks containing 100 mL of medium, while the highest oxygen transfer rate was reached in 250 mL E-flasks containing 50 mL of cultivation broth. An intermediate condition was tested in 100 mL E-flasks containing 50 mL of cultivation broth. The initial biomass concentration and PHB content of the cell suspension was 0.51 ± 0.005 gTSS L^{-1} and 31.9 ± 1.88% PHB, respectively. The experiments were conducted in duplicate.

The potential inhibitory effect of extracellular R3HBA over PHB depolymerization was investigated using R3HBA produced *in-house* following the procedure described by Lee et al. (1999). Briefly, *Azohydromonas lata* (DSM 1123, Leibniz Institute, Germany) was cultivated from a frozen stock culture in a nutrient agar plate. A single colony was picked and used to inoculate a 500 mL E-flask with 100 mL of AL1 medium (Wang and Lee, 1997). This culture served as the inoculum for a batch bioreactor cultivation of this bacterium in a Labfors 5 bioreactor (Infors HT, Switzerland). The bioreactor was operated with 1 L of AL2 medium containing an initial glucose concentration of 30 g L^{-1} and an initial ammonium sulfate concentration of 2 g L^{-1}. Dissolved oxygen was maintained above 40% saturation by varying the stirring speed up to 700 rpm at 1 vvm air. When necessary, pure oxygen was automatically mixed with the inlet air flow under a cascade control. After 24 h of cultivation, approximately 12.0 g L^{-1} of biomass were retrieved containing a PHB cell content of 75%. Cells were collected by centrifugation, washed twice with distilled water, and resuspended in water at a concentration of approximately 120 gTSS L^{-1}. PHB depolymerization was started by adjusting the pH to 4.0 with HCl and lasted for 1 h. The pH was controlled at 4.0 using 2 M NaOH. Following the purification procedure outlined in Lee et al. (1999), a solution containing 34.2 g L^{-1} of sodium (*R*)-3-hydroxybutyrate was obtained. HPLC analysis indicated that the solution contained trace levels of other unidentified compounds and crotonic acid. Finally, *M. parvus* cells containing PHB were washed and resuspended in NMS medium at pH 11 supplemented with R3HBA at concentrations of 0, 120, 330 and 650 mg L^{-1}. Cell incubation was performed in 100 mL E-flasks containing 50 mL of cell suspension with the corresponding R3HBA concentration at 30 °C and 200 rpm in an orbital shaker.

Culture samples were collected at 0, 3, 6, 48 and 72 h for R3HBA and crotonic acid quantification. The biomass and PHB cell content were monitored at the beginning and the end of experiments.

2.4. PHB depolymerization and R3HBA yields calculation

The PHB depolymerization percentage conversion (%) was calculated according to Eq. (1):

$$C_{PHB} = 100 \times \frac{X^i_{PHB} - X^f_{PHB}}{X^i_{PHB}} \quad (1)$$

The R3HBA molar yield was calculated as the ratio of the moles of R3HBA excreted and the moles of PHB consumed, considering that PHB hydrolysis consumes one mol of water per mol of R3HBA produced (Eq. (2)):

$$Y_{R3HBA} = 100\left(\frac{104.10 - 18.01}{104.10}\right)\frac{X^f_{R3HBA} - X^i_{R3HBA}}{X^i_{PHB} - X^f_{PHB}} \quad (2)$$

where X^i_{PHB} and X^f_{PHB} correspond to the initial and final PHB concentrations (g L^{-1}), and X^i_{3HBA} and X^f_{3HBA} represent the initial and final concentrations of R3HBA (g L^{-1}). A similar calculation was used for the crotonic acid yield (Y_{crot}). The conversion of PHB to R3HBA can be calculated as the product $0.01 \cdot Y_{R3HBA} \cdot C_{PHB}$.

Finally, the specific R3HBA release rate per gram of initial intracellular PHB (q_{R3HBA}) was calculated as follows.

$$q_{R3HBA} = \frac{m}{X^i_{PHB}} \quad (3)$$

Where *m* is the slope of the line whose independent and dependent variables are the depolymerization time and R3HBA concentration (in mg L^{-1}), respectively.

2.5. Analytical procedures

CH_4, CO_2 and O_2 gas concentrations were measured in gas a chromatograph coupled with a thermal conductivity detector (Bruker 430 GC-TCD, Bruker Corporation, USA) following the method described by Estrada et al. (2014). The optical density of the cultures samples was measured by spectrophotometry at 600 nm (UV-2550, Shimadzu, Japan). TSS and pH were analyzed according to Rodríguez et al. (2020). PHB was quantified via gas chromatography-mass spectrometry (GC–MS) (Rodríguez et al., 2020) or GC-FID (Scott et al., 2021). The concentration of R3HBA was determined using a commercial (*R*)-3-Hydroxybutyric Acid Assay Kit (Megazyme, Ireland) according to manufacturer's protocol or using HPLC with a UV–Vis detector at 210 nm and a refractive index detector (Prominence, Shimadzu) according to Scott et al. (2021). Citrate, succinate, malate and crotonic acids (Sigma-Aldrich catalog number, 113018) were quantified using the HPLC-UV-IR method described by Scott et al. (2021). The organic acids standard was purchased from Biorad (catalog number, 125–0586).

3. Results and discussion

3.1. Influence of the presence of nitrate and O_2, and pH on PHB depolymerization

Fig. 1 shows the methane and oxygen consumption for the 48 h depolymerization experiments performed with NMS (Fig. 1A and B) and NFMS (Fig. 1C and D) at pH 4, 7 and 11. Consumption of methane and oxygen was faster in the control experiment with NMS at pH 7 compared to that in NFMS medium, an expected result considering that NMS allows for balanced growth. In the absence of oxygen at pH 7, methane consumption was negligible in NFMS medium and close to 10% in the NMS cultures. In this regard, Bordel et al., (2019) showed that *M. parvus* can use stored PHB as an energy source under anoxic conditions only when nitrate is available in the cultivation broth. The annotated genome of *M. parvus* contains the genes involved in nitrate reduction and revealed that denitrification is the only mechanism supporting the use of methane or PHB as an energy source in the absence of oxygen (Bordel et al., 2019).

Both pHs of 11 and 4 induced an important reduction in the consumption of methane and oxygen compared to the control tests. Thus, methane consumption was negligible at pH 11 in NMS medium, while the final consumption of oxygen accounted for 64.8 ± 9.54% of the initial O_2 present in the headspace (compared to 87.8 ± 0.82% of the control), suggesting the occurrence of a respiratory metabolism fueled by a substrate different than methane. pH 4 supported an oxygen and methane final consumption of 33.4 ± 12.67 and 30.6 ± 14.14%, respectively. On the other hand, neither methane nor oxygen consumption was recorded at pH 4 in NFMS medium. Similarly, at pH 11 the final consumption of CH_4 (37.41 ± 6.81%) and the O_2 uptake (30.14 ± 4.65) were reduced compared to the control.

In NMS, nitrate was consumed only in the control assays at pH 7 from the initial 130.1 mgN L^{-1} (measured as total nitrogen) to 47.8 ± 11.5 mgN L^{-1} at the end of the 48 h incubation period. Nitrate consumption at pHs 4.0 and 11.0 was lower than 2.6 mgN L^{-1} during the same period, and only 0.3 mgN L^{-1} was consumed in the assay at pH 7 in the absence of oxygen. Therefore, no significant cell growth occurred except in the control assay at neutral pH.

Interestingly, extracellular R3HBA was only detected at pH 11 in both NMS and NFMS medium (Fig. 1E). At pH 11 in NMS, 80.6 ± 0.8% of PHB was depolymerized and R3HBA secretion reached 205.8 ± 1.2 mg L^{-1}, a higher concentration compared with the assay in NFMS, where 25.7 ± 7.9% of PHB was depolymerized and a R3HBA titer of 60.1 ± 12.9 mg L^{-1} was measured after 48 h. The mechanisms by which nitrogen influences the depolymerization extent and rate seem to be related to the alleviation of the stringent response. In amino acid starved cells, the alarmone ppGpp accumulates and destabilizes the RNA polymerase σ^{70}, resulting in an induction of genes under the control of alternative sigma σ factors, such as σ^{54} (Brigham et al., 2012). ppGpp has also been implicated in the inhibition of translation (Irving et al., 2021). In *Ralstonia eutropha* H16, PHB mobilization occurs in the absence of the alarmone ppGpp, which in turn requires the presence of a source of nitrogen (Juengert et al., 2017). As further evidence of this mechanism, the genome of *M. parvus* OBBP contains the necessary bifunctional (p)ppGpp synthetase/hydrolase (WP_016921527.1) required for the synthesis and degradation of ppGpp.

PHB depolymerization at pH 4 and pH 7 (with or without O_2) in NMS supported extracellular R3HBA concentrations of 5.42 ± 0.67 mg L^{-1}, 4.83 ± 0.37 mg L^{-1} and 4.01 ± 0.15 mg L^{-1}, respectively. Similarly, extracellular R3HBA concentrations of 4.68 ± 0.37 mg L^{-1}, 6.17 ± 0.22

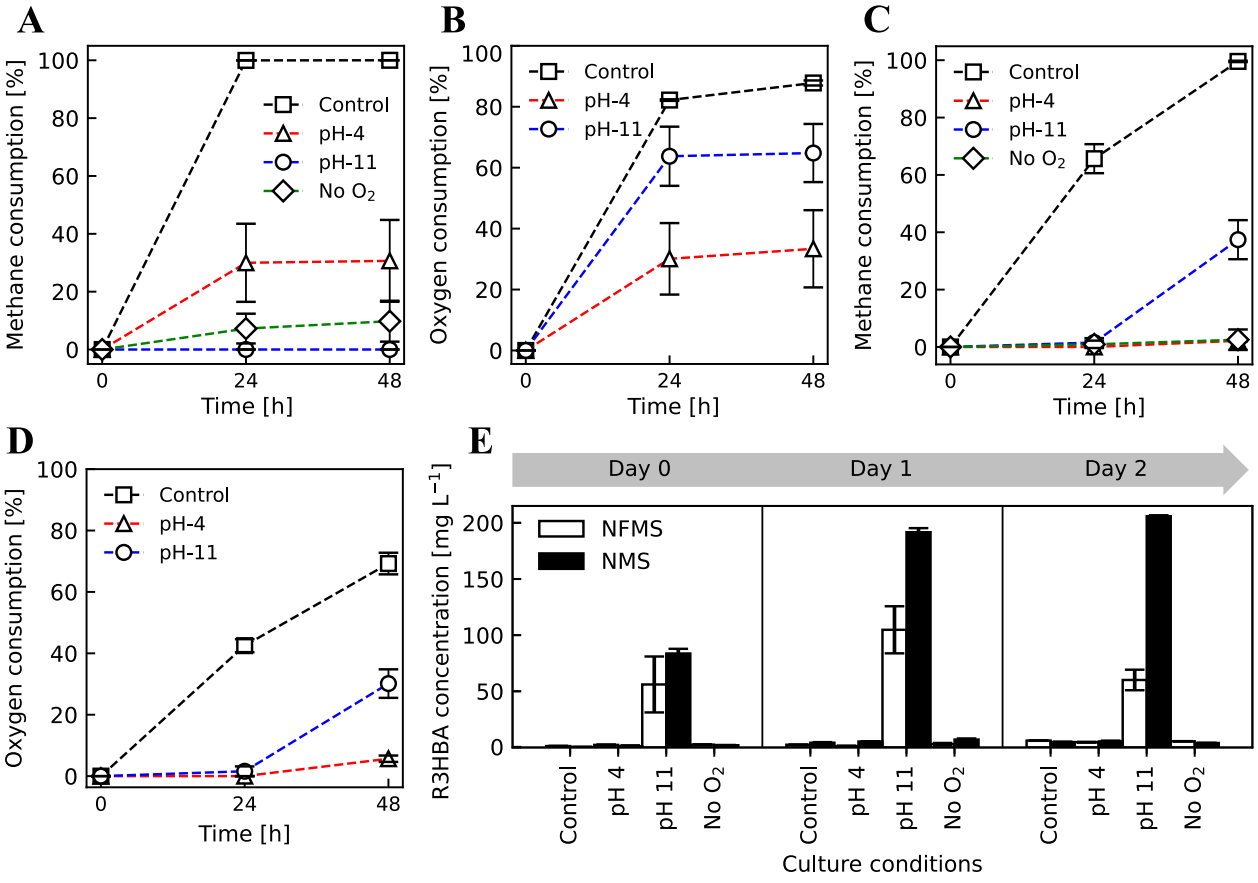

Fig. 1. CH_4 and O_2 consumption during PHB depolymerization in *M. parvus* cultivated in NMS (A, B) and NFMS (C, D) medium at pH 4 (triangles), pH 11 (circles), pH 7 (squares) and without oxygen at pH 7 (diamonds). (E) R3HBA released in *M. parvus* cultures at pH 4, pH 11, pH 7 (with and without oxygen) in NMS (black bars) and NFMS (white bars) medium.

mg L^{-1} and 5.50 ± 0.15 mg L^{-1} were measured after 48 h in NFMS at pH 4 and pH 7 with or without oxygen, respectively. The final pH of the culture broth in the assays initially adjusted to pH 11 in NMS and NFMS media decreased to 8.28 and 6.23, respectively, confirming the secretion of the acidic R3HBA. No significant changes in pH were measured in the rest of the experiments, which agreed with the limited R3HBA release. The estimated Y_{R3HBA} are 31.5 ± 0.08% and 28.9 ± 0.91%, which equates to a PHB to R3HBA conversion of 25.4 ± 0.03% and 7.4 ± 2.1%, for the experiments at initial pH of 11 in NMS and NFMS, respectively.

The *in-vivo* depolymerization of the intracellularly accumulated PHAs to hydroxy acids has been reported in several bacterial strains. For instance, the depolymerization process in *Azohydromonas lata* was carried out in water without shaking to minimize oxygen transfer, at 37 °C and pH 4.0, and achieved a depolymerization efficiency of 96% of the initial PHB to R3HBA in only 30 min (Lee et al., 1999). These author also evaluated PHB depolymerization in *Pseudomonas aeruginosa* PAO1 (DSM 1707), *Pseudomonas oleovorans* (ATCC 29347) and *Cupriavidus necator* (NCIMB 11599) at pH values below 7.0 (Lee et al., 1999). The PHA to hydroxyacids conversion was 20% for *C. necator* and less than 10% for *Pseudomonas* species (Lee et al., 1999).

The conversion of PHA to hydroxyacids in *Pseudomonas putida* GPo1 was improved by changing the depolymerization conditions to an alkaline medium. This strain excreted (*R*)-3-hydroxyoctanaoic (R3HO) acid and (*R*)- 3-hydroxyhexanoic acid (R3HHx) at pH 11 in citrate buffer for 6 h with a PHA degradation efficiency and monomer production yields above 90% (w/w) (Ren et al., 2005). Ruth et al., (2007) engineered a depolymerization strategy at pH 10 in *P. putida* GPo1 under continuous mode with a production of R3HO, R3HHx, (*R*)-3-hydroxy-10 undecenoic acid, (*R*)-3-hydroxy-8-nonenoic acid, (*R*)-3-hydroxy-6-heptenoic acid, (*R*)-3hydroxyundecanoic acid, (*R*)-3-hydroxynonanoic acid, and (*R*)-3 hydroxyheptanoic acid. The study herein presented confirmed the key role of high pH on PHA depolymerization, which is a common feature in *Pseudomonas* species. Hence, *P. putida* GPo1 released 3-hydroxyoctanoic acid and 3-hydroxyhexanoic acid from intracellular

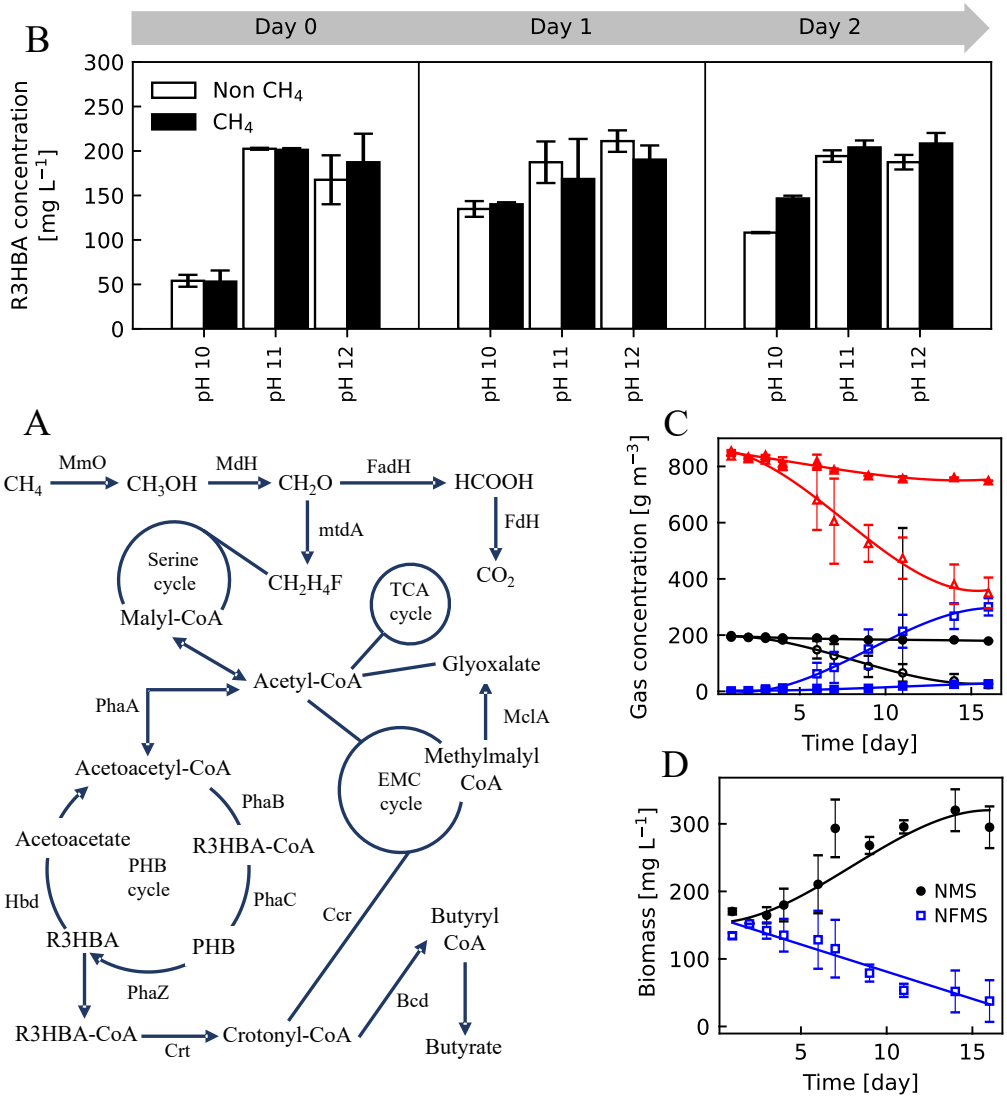

Fig. 2. Schematic representation of the metabolic pathways involved in the polymerization and depolymerization of PHB in *M. parvus* OBBP. MmO, methane monooxygenase; MdH, methanol dehydrogenase; FadH, formaldehyde dehydrogenase; FdH, formate dehydrogenase; MtdA, methylene tetrahydromethanopterin dehydrogenase; PhaA, β-ketothiolase; PhaB, acetoacetyl-CoA reductase; PhaC, PHB polymerase; Hbd, (R)-3-hydroxybutyrate dehydrogenase, Crt, 3-hydroxybutyryl-CoA dehydratase; Ccr, crotonyl-CoA carboxylase/reductase; MclA, malyl-CoA lyase; Bcd, butyryl-CoA dehydrogenase (A). R3HBA concentration in *M. parvus* at pH 10, 11 and 12 in NMS with (black bars) or without (white bars) CH_4 (B). Concentrations of biomass (C) and CH_4 (circles), O_2 (triangles) and CO_2 (square) (D) during the viability assays of *M. parvus* cells previously subjected to a 3 h depolymerization phase at pH 11. Filled and empty symbols correspond to the experiments carried out in NMS and NFMS media, respectively.

PHA at pH 11 with conversions of 76% (0.356 g L^{-1}) and 21% (0.015 g L^{-1}) in 6 h, respectively (Ren et al., 2005). Similarly, *P. putida* Bet001 can depolymerize PHAs up to 98% in 0.2 Tris-HCl buffer at pH 9.1 within 48 h (Anis et al., 2018). In Type II methanotrophs, the production of hydroxyacids has only been described in a genetically engineered *Methylosinus trichosporum* OB3b strain able to synthesize R4HBA from CH_4 via the TCA cycle and the overexpression phosphoenolpyruvate carboxylase (Ppc), isocitrate dehydrogenase (Icd) and 2-oxoglutarate dehydrogenase (SucAB). The highest 4-HB titer obtained was 10.5 mg/L after 6 culture days (Nguyen and Lee, 2021).

PHB synthesis and degradation in methanotrophic bacteria seem to be similar to the metabolic processes carried out by most heterotrophic PHB producers (Vecherskaya et al., 2001). However, there is a limited understanding of the mechanisms that bring about the intracellular PHB depolymerization and the formation of its monomer acids such as R3HBA and crotonic acid in Type II methanotrophs. Vecherskaya et al. (2001) demonstrated how products from the anaerobic fermentation of PHB in methanotrophs can be bioconverted in R3HBA, butyrate, acetate, succinate, and other reduced compounds. Fig. 2A shows the pathways of PHB depolymerization and formation of different metabolites in *M. parvus OBBP* based on a genome-scale metabolic model (Bordel et al., 2019) that has been recently reported. This model shows the fluxes of the PHB degradation from crotonyl-CoA to methylmalyl-CoA, which is dissociated into glyoxylate and propionyl-CoA. The glyoxylate originated from methylmalyl-CoA is incorporated into the serine cycle, and the propionyl-CoA is carboxylated into succinyl-CoA by the ethylmalonyl-CoA cycle (EMC) and then incorporated into the TCA cycle (Bordel et al., 2019). Another parallel pathway involves the enzymatic conversion of crotonyl-CoA to butyryl-CoA and finally to butyrate (Vecherskaya et al., 2001).

4. Optimization of pH during PHB depolymerization

The results shown in Fig. 1B indicate that PHB depolymerization at pH 11 in NMS was superior to that at low pHs in NFMS. However, these results do not clarify if pHs closer to 11 could result in higher R3HBA titers, if pH control could improve R3HBA yields or if methane plays a role in the depolymerization of PHB. In this context, *M. parvus* cells containing 18.1% of PHB were resuspended in NMS medium at 1.32 ± 0.02 gTSS $L^{-1}$and depolymerization was assessed at pHs of 10, 11 and 12 as above described. Unlike previous experiments, the pH of the cultivation broth was periodically monitored and controlled with NaOH during the course of the depolymerization.

M. parvus cells rapidly released R3HBA in the pH range of 10–12 following pH adjustment. Thus, the final extracellular monomer concentration reached 146.6 ± 3.11 mg L^{-1} and 108.2 ± 0.66 mg L^{-1} with or without methane at pH 10 (Fig. 2B). On the other hand, the influence of methane was negligible at pH 11 and pH 12, reaching a PHB depolymerization efficiency of 96.6 ± 2.22% and 92.9 ± 1.5%, respectively, (corresponding to 204 ± 7.8 mg L^{-1} and 208.44 ± 11.81 mg L^{-1} of R3HBA) in the presence of CH_4. Similar PHB depolymerization efficiencies of 98.2 ± 1.10% and 93.6 ± 1.33%, respectively, (corresponding to 194.3 ± 6.5 mg L^{-1} and 187.4 ± 8.2 mg L^{-1} of R3HBA) were recorded in the absence of CH_4 at the end of the experiment at pH 11 and 12, respectively. These data suggested that methane did not play a significant role on PHB depolymerization and that pHs beyond 11.0 exerted little influence on R3HBA release. Based on these results, pH 11 in NMS and in the absence of CH_4 was selected for further experiments. Under this condition, a PHB to R3HBA conversion of 68.0 ± 3.2% was calculated.

The fine-tuning of pH played a key role in R3HBA release and PHB depolymerization in other bacteria species. For instance, Ren et al. (2005) demonstrated that PHA depolymerization in *Pseudomonas* Gpo1 produced the highest titer of monomers (360 mg L^{-1} of 3-OH-C8) at an initial pH of 11, while a significantly smaller concentration of monomers (50 mg L^{-1}) was measured at pH 12. Similarly, depolymerization and R3HBA release in *Azohydromonas lata* peaked at a pH of 4.0 with a PHB to R3HBA conversion of 96% in 30 min, and decreased to 31% at a pH 5.0 (Lee et al., 1999). The production of R3HBA *in vivo* requires a concomitant high PHB depolymerization activity and a low enzymatic activity of Bdh. While intracellular depolymerases have an optimum pH range of 8–10 (Jendrossek and Handrick, 2002), Bdh activity is reported to be pH-dependent, with an activity range of 5–10 and an optimal pH range of 7.5–8.5, decreasing abruptly above pH 10 (Mountassif et al., 2010; Takanashi and Saito, 2006) In this context, this study suggests that the phaZ enzyme, responsible of the depolymerization of PHB towards R3HBA, of *M. parvus* exhibits a high activity at pH 11.

5. Influence of temperature on the kinetic of PHB depolymerization

Since the optimal temperature for both growth and PHB accumulation in *M. parvus* is 30 °C and no growth occurs at temperatures greater than 40 °C (Soni et al., 1998), the kinetics of PHB depolymerization and R3HBA released were investigated at 25 and 35 °C, and pH 11 (manually adjusted to compensate for the release of R3HBA). The R3HBA titers quantified at 25 °C and 35 °C were 240 ± 3.81 mg L^{-1} and 282 ± 20.04 mg L^{-1}, respectively, after 3 h of depolymerization in a cell suspension with an initial PHB concentration of 1.86 ± 0.006 g L^{-1}. The R3HBA production rates per mg of initial PHB were 48.6 ± 6.0 mg R3HBA $(mgPHBi)^{-1}h^{-1}$ at 25 °C and 52.7 ± 2.3 mg R3HBA $(mgPHBi)^{-1}h^{-1}$ at 35 °C, while PHB depolymerization reached 16.5% (Y_{3HBA} = 64.5%) and 24.8% (Y_{3HBA} = 50.5%) at 25 and 35 °C, respectively. These results were similar to those obtained by Lee et al. (1999) during the depolymerization of PHB accumulated in *Azohydromonas lata* at 30, 37 and 45 °C. A moderate increase in R3HBA production rate was found when the temperature increased from 30 to 37 °C, while PHB depolymerization suddenly stopped at 45 °C likely due to enzymatic denaturation. Since R3HBA production rate slightly increased with temperature, but R3HBA yields severely decreased, the following experiments were performed at 30 °C.

After 3 h at 25 °C and pH 10.8, cells were harvested and cultured in NMS (to assess cell growth) and NFMS (to assess PHB accumulation) media in the presence of CH_4 to analyze the viability of the cells post-depolymerization. Cells incubated in NMS medium started to consume methane and oxygen by day 4, being these gases fully depleted after 16 days (Fig. 2C). Biomass concentration increased from 170 mg L^{-1} to 295 mg L^{-1} (Fig. 2D). However, the specific growth rate (μ) of post-depolymerization cells was lower (0.058 h^{-1}) than the specific growth rate of 0.107 h^{-1} reported for fresh *M. parvus* cultures (Bordel et al., 2019). On the other hand, the culture incubated in NFMS medium experienced cell death during the cell viability experiment due to nitrogen limitation.

6. Influence of the initial R3HBA concentration and aeration rate on PHB depolymerization

To assess the effect of oxygen availability on PHB depolymerization in *M. parvus,* three tests with different liquid to air surface ratios were carried out at a constant pH of 11. Fig. 3A shows the kinetics of R3HBA release for the 72 h experiment and the depolymerization, crotonic acid and R3HBA yields in Fig. 3B. The final R3HBA concentration was similar regardless of the O_2 supply, while the largest differences were obtained for the R3HBA yield. Indeed, the lowest R3HBA yield (73.6 ± 4.9%) occurred under the condition restricting O_2 mass transfer (100 mL of broth in a 100 mL E-flask) while under less restrictive O_2 supply rates, R3HBA yields reached 84.3 ± 1.0% and 83.7 ± 2.8% at 50 mL/100 mL and 50 mL/250 mL filling ratios, respectively. In terms of PHB to R3HBA conversion, these values equate to 77.2 ± 0.9% and 75.1 ± 3.3%. Literature suggests that the oxygen content during the depolymerization process could influence the fate of the monomers produced in rather unpredictable manners. In this regard, the PHB accumulated with

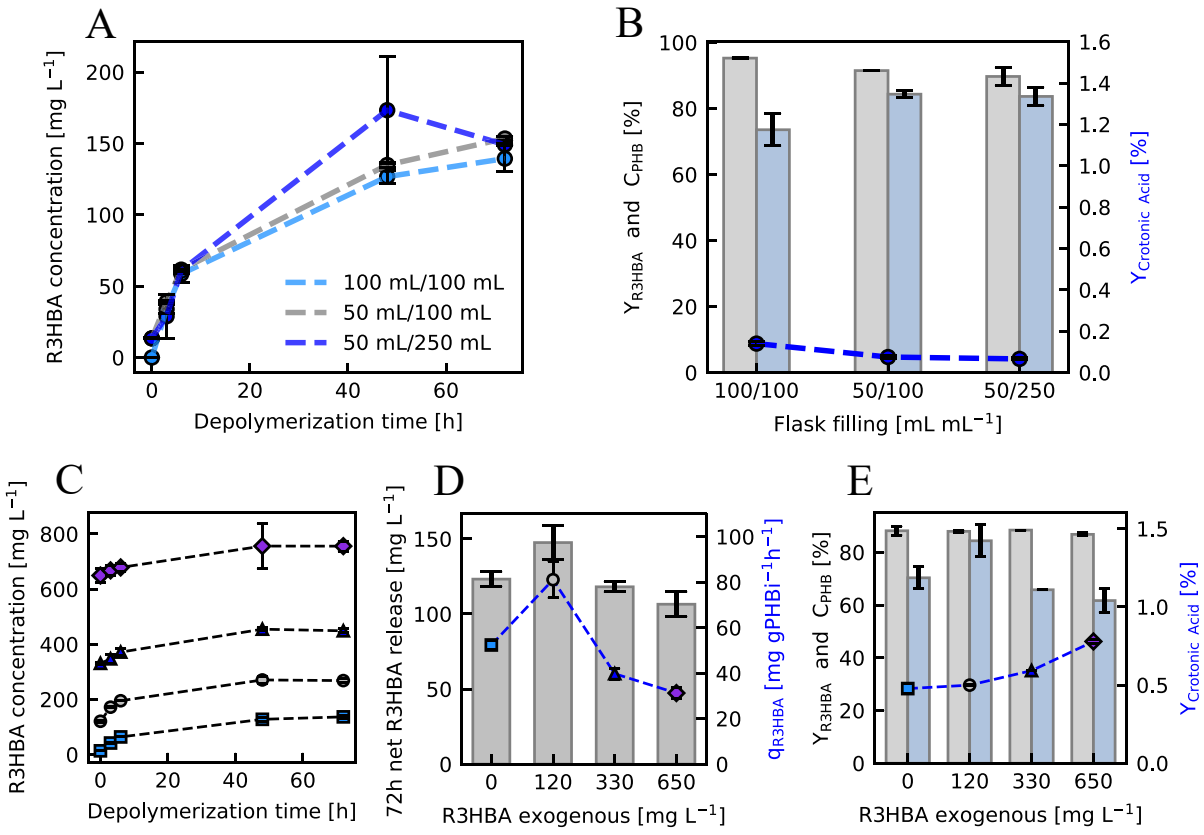

Fig. 3. Influence of the oxygen mass transfer rate on the kinetics of R3HBA excretion (A), depolymerization (grey bars) and R3HBA yields (blue bars) (B). Time course of R3HBA concentration at 0 (square), 120 (circle), 330 (triangle) and 650 (diamond) mg L^{-1} of initial R3HBA (C), net release (bars) and initial production rate of R3HBA (scatter plot) (D) and R3HBA yield (blue bars), depolymerization yield (gray bars) and crotonic acid yields (scatter plot) (E) at pH 11 and NMS medium in *M. parvus* after 72 h.

glycerol as substrate can be depolymerized to R3HBA in *Halomonas sp*. KM-1 under microaerobic conditions (25 mL of broth in 200 mL E-flasks agitated at 50 rpm) in the presence of a nitrogen source. Indeed, 15.2 g L^{-1} of R3HBA were produced in 66 h with a 76.6% PHB to R3HBA conversion under these conditions (Kawata et al., 2012). On the other hand, *Halomonas* sp. OITC1261 behaves differently despite its taxonomic closeness with *Halomonas sp*. KM-1, synthesizing R3HBA concomitantly with PHB under aerobic conditions without extra nitrogen supplementation (Yokaryo et al., 2018).

HPLC analysis of the depolymerization broth at 72 h showed that citric acid (ranging between 1 and 3 mg L^{-1} depending on the O_2 supply rate), malate (20–45 mg L^{-1}), succinate (5–20 mg L^{-1}) and crotonate (less than 0.2 mg L^{-1}) were present along with R3HBA and two unidentified compounds at 18.5 and 19.5 min in the incubation broth drawn after 72 h of depolymerization assay. In addition, a peak at 14.6 min was resolved, presumably corresponding to R3HBA dimers based on previous reports (Lu et al., 2014).

The oxygen consumption during the PHB depolymerization process at pH 11 (Fig. 1B) and the fact that the yield of R3HBA decreased as the supply of oxygen decreased below a certain threshold, suggests that part of the electrons released from the conversion of the depolymerized PHB towards acetyl-CoA are aerobically oxidized for the provision of maintenance energy. This follows from the subsequent findings: (i) the production of acetoacetate from R3HBA produces a molecule of NADH that could be used for ATP production if O_2 is available, (ii) a negligible nitrate consumption was measured at pH 11 during the depolymerization experiment, thus growth can be disregarded, (iii) a limited supply of O_2, achieved by carrying out the depolymerization process in an almost filled E-flask, decreased the R3HBA yield, suggesting that R3HBA was routed towards other metabolites to provide energy for maintenance. The latter finding can be considered as a less extreme version of the experiments by Vecherskaya et al. (2001) under anaerobic conditions, where products characteristics of a fermentative metabolism for energy production were obtained.

R3HBA, as the direct product of PHB depolymerization, might act as an inhibitor of the enzymatic depolymerization activity. To test this hypothesis in *M. parvus*, depolymerization assays were carried out adding exogenous R3HBA before the onset of the depolymerization at concentrations ranging from 0 to 650 mg L^{-1}. The higher limit was higher than the R3HBA titers achieved in previous experiments, where values slightly above 200 mg L^{-1} were found after 48 h of depolymerization at pH 11 with or without methane. Fig. 3C shows the total R3HBA concentration during the 72 h depolymerization experiment, while the net R3HBA released at the end of the experiment (72 h) is shown in Fig. 3D. No significant differences were found between R3HBA concentration released after 72 h with no added R3HBA and any of the experiments with addition of exogenous R3HBA. Fig. 3D also shows the specific initial rate of R3HBA release calculated during the first six hours. This parameter increased from 52.4 ± 1.8 mg of R3HBA per gram of initial PHB (PHBi) per hour in the absence of exogenous R3HBA to 81.1 ± 8.0 mg (g PHBi)$^{-1}$h^{-1} in the presence of 120 mg R3HBA L^{-1}. This increase could be related to impurities in the *in-house* produced R3HBA, although this was not further investigated. Additional increases in the initial R3HBA concentration led to a decrease in the specific initial rate of R3HBA release. Finally, Fig. 3E shows no differences on the depolymerization yield regardless of the initial R3HBA concentration. Interestingly, the Y_{3HBA} was reduced at 330 and 650 mg L^{-1} (65.8 ± 0 and 61.7 ± 4.40%) compared to non R3HBA addition or to 120 mg R3HBA L^{-1}

[1] added, while an increment of the crotonic acid yield to 0.78 ± 0.014% was evidenced at the highest initial R3HBA concentration.

Surprisingly, literature is scarce regarding the effect of R3HBA on the depolymerization kinetics, although R3HBA is the main reaction product. Scherer et al. (1999) found that an extracellular PHB depolymerase from *Aspergillus fumigatus* was reversibly inhibited by trimers of 3-hydroxybutyrate, but no data was presented concerning inhibition by R3HBA.

To further understand the effects of high R3HBA concentration on the depolymerization kinetics, future work will include depolymerization experiments carried out at high initial PHB concentrations. Indeed, PHB concentrations between 1 and 100 g L^{-1} could be attained by biomass concentration to test the possibility of achieving high R3HBA titers without sacrificing yield or increasing the depolymerization time.

7. Conclusion

This work showed for the first time the production of the chiral molecule (*R*)-3-hydroxybutyrate (R3HBA) from methane as a proof of concept to convert this greenhouse gas into a multicarbon value-added product. The process involves the accumulation of PHB in *Methylocystis parvus* OBBP and its in-vivo depolymerization by intracellular enzymes. A PHB to R3HBA conversion of 77.2 ± 0.9% was obtained after 72 h of depolymerization at pH 11 in a mineral medium containing nitrate under aerobic conditions. A reduced O_2 supply and increasing concentrations of exogenous R3HBA negatively affected the R3HBA yield and the initial R3HBA release rate.

CRediT authorship contribution statement

Luz Yañez: Conceptualization, Investigation, Methodology, Writing – original draft. **Yadira Rodriguez:** Conceptualization, Investigation, Methodology, Writing – original draft. **Felipe Scott:** Conceptualization, Formal analysis, Funding acquisition, Supervision, Writing – review & editing. **Alberto Vergara-Fernández:** Funding acquisition, Supervision, Writing – review & editing. **Raúl Muñoz:** Conceptualization, Funding acquisition, Project administration, Supervision, Resources, Writing – review & editing.

Declaration of Competing Interest

The authors declare that they have no known competing financial interests or personal relationships that could have appeared to influence the work reported in this paper.

Acknowledgments

This work was supported by the regional government of Castile and Leon and the EU-FEDER program (CLU 2017-09, UIC 315). The present work was also financially supported by the National Agency for Research and Development (ANID Chile), projects ANID/CONICYT Fondecyt Regular 1211434 and ANID/CONICYT Fondecyt Regular 1190521. Support from grant Apoyo a la Formación de Redes Internacionales entre Centros de Investigación REDES190137 (CONICYT-PCI) is also gratefully acknowledged.

References

Anis, S.N.S., Annuar, M.S.M., Simarani, K., 2018. Microbial biosynthesis and in vivo depolymerization of intracellular medium-chain-length poly-3-hydroxyalkanoates as potential route to platform chemicals. Biotechnol. Appl. Biochem. 65, 784–796. https://doi.org/10.1002/bab.1666.

Bordel, S., Rojas, A., Muñoz, R., 2019. Reconstruction of a Genome Scale Metabolic Model of the polyhydroxybutyrate producing methanotroph *Methylocystis parvus* OBBP. Microb. Cell Fact. 18, 1–11. https://doi.org/10.1186/s12934-019-1154-5.

Brigham, C.J., Speth, D.R., Rha, C., Sinskey, A.J., 2012. Whole-Genome Microarray and Gene Deletion Studies Reveal Regulation of the Polyhydroxyalkanoate Production Cycle by the Stringent Response in *Ralstonia eutropha* H16. Appl. Environ. Microbiol. 78, 8033–8044. https://doi.org/10.1128/AEM.01693-12.

Cao, Q., Zhang, J., Liu, H., Wu, Q., Chen, J., Chen, G.Q., 2014. The mechanism of anti-osteoporosis effects of 3-hydroxybutyrate and derivatives under simulated microgravity. Biomaterials 35, 8273–8283. https://doi.org/10.1016/j.biomaterials.2014.06.020.

Donoso, R.A., Pérez-Pantoja, D., González, B., 2011. Strict and direct transcriptional repression of the pobA gene by benzoate avoids 4-hydroxybenzoate degradation in the pollutant degrader bacterium *Cupriavidus necator* JMP134. Environ. Microbiol. 13, 1590–1600. https://doi.org/10.1111/j.1462-2920.2011.02470.x.

Edenhofer, O., 2014. IPCC 2014 Mitigation of Climate Change. Contribution of Working Group III to the Fifth Assessment Report of the Intergovernmental Panel on Climate. Cambridge University Press, Change, Cambridge.

Etminan, M., Myhre, G., Highwood, E.J., Shine, K.P., 2016. Radiative forcing of carbon dioxide, methane, and nitrous oxide: A significant revision of the methane radiative forcing. Geophys. Res. Lett. 43, 12614–12623. https://doi.org/10.1002/2016GL071930.

Fruggo. Last accessed: January 28,2022. https://www.fruugo.co.uk/contact 2021.

Irving, S.E., Choudhury, N.R., Corrigan, R.M., 2021. The stringent response and physiological roles of (pp)pGpp in bacteria. Nat. Rev. Microbiol. 19, 256–271. https://doi.org/10.1038/s41579-020-00470-y.

Jackson, R.B., Saunois, M., Bousquet, P., Canadell, J.G., Poulter, B., Stavert, A.R., Bergamaschi, P., Niwa, Y., Segers, A., Tsuruta, A., 2020. Increasing anthropogenic methane emissions arise equally from agricultural and fossil fuel sources. Environ. Res. Lett. 15 (7), 071002.

Jawaharraj, K., Shrestha, N., Chilkoor, G., Dhiman, S.S., Islam, J., Gadhamshetty, V., 2020. Valorization of methane from environmental engineering applications: A critical review. Water Res 187, 116400. https://doi.org/10.1016/j.watres.2020.116400.

Jendrossek, D., Handrick, R., 2002. Microbial degradation of polyhydroxyalkanoates. Annu. Rev. Microbiol. 56 (1), 403–432. https://doi.org/10.1146/annurev.micro.56.012302.160838.

Juengert, J.R., Borisova, M., Mayer, C., Wolz, C., Brigham, C.J., Sinskey, A.J., Jendrossek, D., Kivisaar, M., 2017. Absence of ppGpp Leads to Increased Mobilization of Intermediately Accumulated Poly(3-Hydroxybutyrate) in *Ralstonia eutropha* H16. Appl. Environ. Microbiol. 83 (13) https://doi.org/10.1128/AEM.00755-17.

Kawata, Y., Kawasaki, K., Shigeri, Y., 2012. Efficient secreted production of (*R*)-3-hydroxybutyric acid from living *Halomonas* sp. KM-1 under successive aerobic and microaerobic conditions. Appl. Microbiol. Biotechnol. 96, 913–920. https://doi.org/10.1007/s00253-012-4218-6.

Kirschke, S., Bousquet, P., Ciais, P., Saunois, M., Canadell, J.G., Dlugokencky, E.J., Bergamaschi, P., Bergmann, D., Blake, D.R., Bruhwiler, L., Cameron-Smith, P., Castaldi, S., Chevallier, F., Feng, L., Fraser, A., Heimann, M., Hodson, E.L., Houweling, S., Josse, B., Fraser, P.J., Krummel, P.B., Lamarque, J.-F., Langenfelds, R. L., Le Quéré, C., Naik, V., O'Doherty, S., Palmer, P.I., Pison, I., Plummer, D., Poulter, B., Prinn, R.G., Rigby, M., Ringeval, B., Santini, M., Schmidt, M., Shindell, D. T., Simpson, I.J., Spahni, R., Steele, L.P., Strode, S.A., Sudo, K., Szopa, S., van der Werf, G.R., Voulgarakis, A., van Weele, M., Weiss, R.F., Williams, J.E., Zeng, G., 2013. Three decades of global methane sources and sinks. Nat. Geosci. 6 (10), 813–823.

Latimer, A.A., Kakekhani, A., Kulkarni, A.R., Nørskov, J.K., 2018. Direct Methane to Methanol: The Selectivity-Conversion Limit and Design Strategies. ACS Catal. 8, 6894–6907. https://doi.org/10.1021/acscatal.8b00220.

Lee, S.Y., Lee, Y., Wang, F., 1999. Chiral compounds from bacterial polyesters: Sugars to plastics to fine chemicals. Biotechnol. Bioeng. 65, 363–368. https://doi.org/10.1002/(SICI)1097-0290(19991105)65:3<363::AID-BIT15>3.0.CO;2-1.

Liu, H., Kumar, V., Jia, L., Sarsaiya, S., Kumar, D., Juneja, A., Zhang, Z., Sindhu, R., Binod, P., Bhatia, S.K., Awasthi, M.K., 2021. Biopolymer poly-hydroxyalkanoates (PHA) production from apple industrial waste residues: A review. Chemosphere 284, 131427. https://doi.org/10.1016/j.chemosphere.2021.131427.

Lu, J., Takahashi, A., Ueda, S., 2014. 3-Hydroxybutyrate Oligomer Hydrolase and 3-Hydroxybutyrate Dehydrogenase Participate in Intracellular Polyhydroxybutyrate and Polyhydroxyvalerate Degradation in *Paracoccus denitrificans*. Appl. Environ. Microbiol. 80, 986–993. https://doi.org/10.1128/AEM.03396-13.

Matsuyama, A., Yamamoto, H., Kawada, N., Kobayashi, Y., 2001. Industrial production of (*R*)-1,3-butanediol by new biocatalysts. J. Mol. Catal. - B Enzym. 11, 513–521. https://doi.org/10.1016/S1381-1177(00)00032-1.

McAdam, B., Fournet, M.B., McDonald, P., Mojicevic, M., 2020. Production of polyhydroxybutyrate (PHB) and factors impacting its chemical and mechanical characteristics. Polymers (Basel). 12, 1–20. https://doi.org/10.3390/polym12122908.

Mountassif, D., Andreoletti, P., Cherkaoui-Malki, M., Latruffe, N., Kebbaj, M.S.E., 2010. Structural and catalytic properties of the D-3-hydroxybutyrate dehydrogenase from *Pseudomonas aeruginosa*. Curr. Microbiol. 61, 7–12. https://doi.org/10.1007/s00284-009-9568-7.

Müller-Santos, M., Koskimäki, J.J., Alves, L.P.S., de Souza, E.M., Jendrossek, D., Pirttilä, A.M., 2021. The protective role of PHB and its degradation products against stress situations in bacteria. FEMS Microbiol. Rev. 45 (3) https://doi.org/10.1093/femsre/fuaa058.

Nguyen, D.T.N., Lee, O.K., Nguyen, T.T., Lee, E.Y., 2021. Type II methanotrophs: A promising microbial cell-factory platform for bioconversion of methane to chemicals. Biotechnol. Adv. 47, 107700 https://doi.org/10.1016/j.biotechadv.2021.107700.

Nguyen, T.T., Lee, E.Y., 2021. Methane-based biosynthesis of 4-hydroxybutyrate and P (3-hydroxybutyrate-co-4-hydroxybutyrate) using engineered *Methylosinus*

trichosporium OB3b. Bioresour. Technol. 335, 125263 https://doi.org/10.1016/j.biortech.2021.125263.

Nielsen, R., Møller, N., Gormsen, L.C., Tolbod, L.P., Hansson, N.H., Sorensen, J., Harms, H.J., Frøkiær, J., Eiskjaer, H., Jespersen, N.R., Mellemkjaer, S., Lassen, T.R., Pryds, K., Bøtker, H.E., Wiggers, H., 2019. Cardiovascular Effects of Treatment With the Ketone Body 3-Hydroxybutyrate in Chronic Heart Failure Patients. Circulation 139 (18), 2129–2141. https://doi.org/10.1161/CIRCULATIONAHA.118.036459.

Pérez-Rivero, C., López-Gómez, J.P., Roy, I., 2019. A sustainable approach for the downstream processing of bacterial polyhydroxyalkanoates: State-of-the-art and latest developments. Biochem. Eng. J. 150, 107283 https://doi.org/10.1016/j.bej.2019.107283.

Pieja, A.J., Sundstrom, E.R., Criddle, C.S., 2011. Poly-3-hydroxybutyrate metabolism in the type II Methanotroph *Methylocystis parvus* OBBP. Appl. Environ. Microbiol. 77, 6012–6019. https://doi.org/10.1128/AEM.00509-11.

Ravishankara, A.R., Kulenstierna, J., Michalopoulou, E., Höglund- Isaksson, L., et al. 2021. Benefits and Costs of Mitigating Methane Emissions.

Ren, Q., Grubelnik, A., Hoerler, M., Ruth, K., Hartmann, R., Felber, H., Zinn, M., 2005. Bacterial Poly(hydroxyalkanoates) as a Source of Chiral Hydroxyalkanoic Acids. Biomacromolecules 6 (4), 2290–2298. https://doi.org/10.1021/bm050187s.

Ren, Q., Ruth, K., Thöny-Meyer, L., Zinn, M., 2007. Process engineering for production of chiral hydroxycarboxylic acids from bacterial polyhydroxyalkanoates. Macromol. Rapid Commun. 28, 2131–2136. https://doi.org/10.1002/marc.200700389.

Rodríguez, Y., Firmino, P.I.M., Arnáiz, E., Lebrero, R., Muñoz, R., 2020. Elucidating the influence of environmental factors on biogas-based polyhydroxybutyrate production by *Methylocystis hirsuta* CSC1. Sci. Total Environ. 706, 135136. https://doi.org/10.1016/j.scitotenv.2019.135136.

Rostkowski, K.H., Pfluger, A.R., Criddle, C.S., 2013. Stoichiometry and kinetics of the PHB-producing Type II methanotrophs *Methylosinus trichosporium* OB3b and Methylocystis parvus OBBP. Bioresour. Technol. 132, 71–77. https://doi.org/10.1016/j.biortech.2012.12.129.

Ruth, K., Grubelnik, A., Hartmann, R., et al., 2007. Efficient production of (*R*)-3-hydroxycarboxylic acids by biotechnological conversion of polyhydroxyalkonoates and their purification. Biomacromolecules 8, 279–286. https://doi.org/10.1021/bm060585a.

Saunois, M., Bousquet, P., Poulter, B., Peregon, A., et al., 2016. The global methane budget 2000–2012. Earth Syst. Sci. Data 8 (2), 697–751.

Scherer, T.M., Fuller, R.C., Lenz, R.W., Goodwin, S., 1999. Production, purification and activity of an extracellular depolymerase from *Aspergillus fumigatus*. J. Environ. Polym. Degrad. 7, 117–125. https://doi.org/10.1023/A:1022881204565.

Scott, F., Yañez, L., Conejeros, R., Araya, B., Vergara-Fernández, A., 2021. Two internal bottlenecks cause the overflow metabolism leading to poly(3-hydroxybutyrate) production in *Azohydromonas lata* DSM1123. J. Environ. Chem. Eng. 9 (4), 105665. https://doi.org/10.1016/j.jece.2021.105665.

Sirohi, R., Prakash Pandey, J., Kumar Gaur, V., Gnansounou, E., Sindhu, R., 2020. Critical overview of biomass feedstocks as sustainable substrates for the production of polyhydroxybutyrate (PHB). Bioresour. Technol. 311, 123536. https://doi.org/10.1016/j.biortech.2020.123536.

Soni, B.K., Conrad, J., Kelley, R.L., Srivastava, V.J., 1998. Effect of temperature and pressure on growth and methane utilization by several methanotrophic cultures. Appl. Biochem. Biotechnol. - Part A Enzym. Eng. Biotechnol. 70–72, 729–738. https://doi.org/10.1007/BF02920184.

Strong, P.J., Xie, S., Clarke, W.P., 2015. Methane as a resource: Can the methanotrophs add value? Environ. Sci. Technol. 49, 4001–4018. https://doi.org/10.1021/es504242n.

Takanashi, M., Saito, T., 2006. Characterization of two 3-hydroxybutyrate dehydrogenases in poly(3-hydroxybutyrate)-degradable bacterium, *Ralstonia pickettii* T1. J. Biosci. Bioeng. 101, 501–507. https://doi.org/10.1263/jbb.101.501.

Tieu, K., Perier, C., Caspersen, C., Teismann, P., Wu, D.-C., Yan, S.-D., Naini, A., Vila, M., Jackson-Lewis, V., Ramasamy, R., Przedborski, S., 2003. D-β-Hydroxybutyrate rescues mitochondrial respiration and mitigates features of Parkinson disease. J. Clin. Invest. 112 (6), 892–901. https://doi.org/10.1172/JCI18797.

Tokiwa, Y., Ugwu, C.U., 2007. Biotechnological production of (*R*)-3-hydroxybutyric acid monomer. J. Biotechnol. 132, 264–272. https://doi.org/10.1016/j.jbiotec.2007.03.015.

Vecherskaya, M., Dijkema, C., Stams, A.J.M., 2001. Intracellular PHB conversion in a Type II methanotroph studied by 13C NMR. J. Ind. Microbiol. Biotechnol. 26, 15–21. https://doi.org/10.1038/sj.jim.7000086.

Wang, F., Lee, S.Y., 1997. Poly(3-Hydroxybutyrate) Production with High Productivity and High Polymer Content by a Fed-Batch Culture of *Alcaligenes latus* under Nitrogen Limitation. Appl. Envir. Microbiol. 63 (9), 3703–3706. https://doi.org/10.1128/aem.63.9.3703-3706.1997.

Wendlandt, K.D., Jechorek, M., Helm, J., Stottmeister, U., 2001. Producing poly-3-hydroxybutyrate with a high molecular mass from methane. J. Biotechnol. 86, 127–133. https://doi.org/10.1016/S0168-1656(00)00408-9.

Yamanashi, T., Iwata, M., Kamiya, N., Tsunetomi, K., Kajitani, N., Wada, N., Iitsuka, T., Yamauchi, T., Miura, A., Pu, S., Shirayama, Y., Watanabe, K., Duman, R.S., Kaneko, K., 2017. Beta-hydroxybutyrate, an endogenic NLRP3 inflammasome inhibitor, attenuates stress-induced behavioral and inflammatory responses. Sci. Rep. 7 (1) https://doi.org/10.1038/s41598-017-08055-1.

Yañez, L., Conejeros, R., Vergara-Fernández, A., Scott, F., 2020. Beyond Intracellular Accumulation of Polyhydroxyalkanoates: Chiral Hydroxyalkanoic Acids and Polymer Secretion. Front. Bioeng. Biotechnol. 8 https://doi.org/10.3389/fbioe.2020.00248.

Yokaryo, H., Teruya, M., Hanashiro, R., Goda, M., Tokiwa, Y., 2018. Direct Production of (R)-3-Hydroxybutyric Acid of High Optical Purity by *Halomonas* sp. OITC1261 Under Aerobic conditions. Biotechnol. J. 13, 1–23. https://doi.org/10.1002/biot.201700343.

Zhang, J., Cao, Q., Li, S., Lu, X., Zhao, Y., Guan, J.-S., Chen, J.-C., Wu, Q., Chen, G.-Q., 2013. 3-Hydroxybutyrate methyl ester as a potential drug against Alzheimer's disease via mitochondria protection mechanism. Biomaterials 34 (30), 7552–7562. https://doi.org/10.1016/j.biomaterials.2013.06.043.